8-2011

ROLE OF IL-17 AND TH17 CELLS IN HSV INDUCED OCULAR IMMUNOPATHOLOGY

Amol Sahebrao Suryawanshi
asuryawa@utk.edu

To the Graduate Council:

I am submitting herewith a dissertation written by Amol Sahebrao Suryawanshi entitled "ROLE OF IL-17 AND TH17 CELLS IN HSV INDUCED OCULAR IMMUNOPATHOLOGY." I have examined the final electronic copy of this dissertation for form and content and recommend that it be accepted in partial fulfillment of the requirements for the degree of Doctor of Philosophy, with a major in Comparative and Experimental Medicine.

Barry T. Rouse, Major Professor

We have read this dissertation and recommend its acceptance:

Stephen J. Kennel, Michael F. McEntee, Seung J. Baek

Accepted for the Council:

Carolyn R. Hodges

Vice Provost and Dean of the Graduate School

(Original signatures are on file with official student records.)

ROLE OF IL-17 AND T_H17 CELLS IN HSV INDUCED OCULAR IMMUNOPATHOLOGY

A Dissertation
Presented for the
Doctor of Philosophy Degree
The University of Tennessee, Knoxville

Amol Sahebrao Suryawanshi
August 2011

DEDICATION

This dissertation is dedicated to my **MOTHER, SISTER** and **FRIENDS,** without whose help and selfless devotion to me, I could have never achieved my goals.

ACKNOWLEDGEMENTS

My sincere appreciation goes to my PhD mentor, Dr. Barry T. Rouse, who over last four years has helped and supported me in achieving my short-term scientific goals. In the course of time, he honed my abilities to identify unresolved problems in the field of immunology and solve them with a great zeal and zest. Additionally, I would like to extend my profound thanks to the members of my committee, Dr. Michael McEntee, Dr. Stephen Kennel, Dr. Seung J. Baek, and Dr. Mark Y. Sangster, for all their time and needful guidance.

I express my thanks to all the members of lab for providing a stimulating and fun environment to learn and grow. Specially, I would like to thank Naveen K. Rajasagi, Tamara Veiga-Parga, Sharvan Sehrawat, Pradeep BJ Reddy, Shalini Sharma, Seng Ryong Woo and Sachin Mulik for their help and time in my projects. It has been a great pleasure to interact with the other lab members, Susmit Suvas, Pranita Sarangi, Fernanda Gimenez, Jason A. Burchett, Stacey Grimshaw and Greg Spencer.

Finally I express my deepest gratitude to my Mother, Sister, Tau, Om, Krishna and all my friends who were always besides me and motivated to come this far. I am eternally grateful for their everlasting support and faith in my strength and capability.

ABSTRACT

Herpes simplex virus (HSV) infection of the cornea leads to a blinding immuno-inflammatory condition of the eye also called stromal keratitis (SK). SK immunopathology is characterized by the infiltration of $CD4^+$ T cells of Th1 phenotype as well as the development of new blood vessels into the normally avascular cornea. Studies in mouse models of SK have firmly established the role of $CD4^+$ T cells, and particularly of Th1 phenotype, as the principal mediators of SK immunopathology. However, with the recent discovery of IL-17A and Th17 cells, the role of this cytokine as well as Th17 cells remains to be further defined. Recently it was shown that the normal cornea expresses VEGF-A, however its biological activity is impeded by its binding to a soluble form of VEGF-A receptor-1 (sVEGFR-1). Past studies have implicated the role of vascular endothelial growth factor-A (VEGF-A) in HSV induced corneal angiogenesis, however the source of VEGF-A as well as molecular mechanisms, particularly in the context of VEGF-A/sVEGFR-1 balance during HSV infection, are poorly understood.

The first part of this dissertation (I) reviews past literature on HSV induced corneal SK immunopathology. It focuses on the understanding of HSV-1 induced events that particularly results in corneal angiogenesis as well as tissue damage mediated by different type of cells as well as their secreted products. The next three parts (II-IV) focus on the mechanisms of HSV induced corneal angiogenesis as well as the relative role of Th1 and Th17 cells in SK immunopathology. Results in part II focuses on the relative role of IFN-γ/IL-17 as well as Th1/Th17 cells in HSV induced corneal immunopathology. The third section evaluate the significance of VEGF-A/sVEGFR-1

balance in HSV induced corneal neovascularization. Results in part IV focus on the role of IL-17A in altering the balance between VEGF-A and sVEGFR-1 post ocular HSV infection and subsequent corneal angiogenesis.

Collectively these studies identified novel mechanisms by which HSV infection of the cornea leads to the development of angiogenesis as well as corneal tissue damage and subsequent SK immunopathology, the most common cause of infectious blindness in the Western World.

TABLE OF CONTENTS

TABLE OF FIGURES

ABBREVIATIONS

bFGF	Basic Fibroblast Growth Factor
CCL	Chemokine (C-C motif) ligand
CD	Cluster of differentiation
COX-2	Cyclooxygenase
CSF	Colony stimulating factor
CXCL	CXC chemokine ligand
DCs	Dendritic Cells
E-L-R motif	Glutamate (E)-Leucine (L)-Arginine (R) tri-peptide motif
GM-CSF	Granulocyte-monocye colony stimulating factor
HSV	Herpes simplex virus-1
ICAM-1	Intercellular adhesion molecule 1
IFN-α, β, γ	Interferon alpha, beta, gamma
IL	Interleukin
IP-10	Interferon inducible protein 10
MIP-2	Macrophage inflammatory protein 2
MMP	Matrix metalloproteinase
MMPi	Matrix metalloproteinase inhibitor
NFκB	Nuclear Factor – kappa B
NK	Natural Killer
PAMP	Pathogen associated molecular pattern

PECAM	Platelet endothelial cell adhesion molecule
PFU	Plaque forming unit
PMN	Polymorphonuclear leukocytes
SK	Stromal keratitis
sVEGFR-1	Soluble form of VEGF receptor-1
TG	Trigeminal Ganglion
TGF-β	Transforming growth factor beta
Th1	T helper 1 cells (IFN-γ producing $CD4^+$ T cells)
Th17	T helper 17 cells (IL-17 producing $CD4^+$ T cells)
TLR	Toll like receptor
TNF-α	Tumor necrosis factor alpha
VEGF-A	Vascular endothelial growth factor A
VEGFR-1	VEGF-A receptor 1

PART-I

BACKGROUND AND OVERVIEW

HERPES SIMPLEX VIRUS-1 (HSV) and Ocular Immunopathology

Herpes viruses are highly successful pathogens owing to some of the mechanisms to resist removal from host once they have caused infection (1-4). The transmission of HSV infection occurs through intimate contact with mucosal surfaces or abraded skin and oropharyngeal mucosa is the most common site for HSV-1 infection (5). HSV-1 initially replicates at the site of primary infection in the epithelial layer, followed by retrograde migration of intact virions to the trigeminal ganglion (TG) where infection is maintained in a latent state (5-7). During latency, the production of new replication competent virus is usually absent, however, immune suppression of the host can result in reactivation of the virus from latently infected TG (2, 3). After reactivation, the virus generally migrates to the initial site of infection and can lead to development of a variety of immuno-inflammatory reactions depending upon the site of recurrent infection (6, 7). When corneal epithelial cells are the site of infection, a chronic immuno-inflammatory condition may result, which is termed as herpetic stromal keratitis (SK) that can cause damage to normal vision (8).

SK is the commonest cause of infectious blindness in the Western World. According to a recent study it is estimated that in the USA 400,000 persons are affected with 20,000 new cases of SK occurring annually (4). In humans, SK usually occurs following the reactivation of the virus from TG (8). The human SK pathogenesis is very complex, but thought to represent a $CD4^+$ T cell orchestrated inflammatory reaction (8). Most of our knowledge of various events of SK pathogenesis is based on studies on experimental SK in animal models, particularly using the immunocompetent mouse as a

host for primary infection (Fig 1.1) (9-11). In this model, $CD4^+$ T cells primarily orchestrate the SK lesions, however the exact nature of epitopes for these cells is still unidentified (9-11). Characteristically, SK lesions are also marked by the development of pathological angiogenic responses in the cornea that can be extensive and further impair normal vision (4, 12). Thus the clinical phase of SK pathogenesis involves at least two significant events, the migration of $CD4^+$ T cells in the corneal stroma and the development of new blood vessels in the normally avascular cornea (Fig 1.1, 1.2)

Currently, therapeutic intervention of SK usually involves a combination of anti-viral and anti-inflammatory drugs (13-15). However, to control the perpetuating inflammatory reaction, long periods of anti-inflammatory drugs, particularly corticosteroids, are administered which can have serious side effects such as risk of cataract formation and glaucoma (13-15). Additionally, in some patients corticosteroids may promote HSV replication thereby worsening the SK lesion severity (16). Thus there is a need for the development of new and alternative therapeutic strategies to control SK. Understanding various molecular mechanisms responsible for development of complex SK lesion could shed light on possible targets for better control of SK pathology.

Pathogenesis of SK

In the mouse model, primary ocular infection with HSV is followed by initial replication of virus in the corneal epithelium for up to 5-6 days (Fig 2) (4). Live viral particles, as well as transcribed mRNA copies of viral genes were detected from the corneal swabs during early time points up to day 7 post infection (pi). However, viral DNA was detected in the cornea up to day 21 pi when SK lesions were fully evident (4).

Early after HSV infection, a prominent infiltration of innate inflammatory cells, particularly neutrophils, occured in corneal stromal layer adjacent to infected corneal epithelial cells (17). Neutrophils primarily migrated from the limbal blood vessels conceivably in response to various chemokine signals released after initial virus infection (4, 17). Neutrophil influx was characterized by a biphasic response in which initial infiltration started around 18 hrs pi, peaked at day 2 pi followed by a decline reaching to undetectable levels around day 5 pi. A second wave of neutrophil infiltration started from day 7 pi that persisted throughout the course of the clinical phase of SK (4, 17, 18). Although, neutrophils initially played a protective role in the virus clearance (19), subsequently during the clinical phase of SK they contributed to the corneal tissue damage and angiogenesis (17, 18). Thus depletion of neutrophils during early stages of HSV infection with specific monoclonal antibody mAb led to higher viral titers as well as delayed clearance of virus from the cornea (19). However, depletion of neutrophils during the clinical phase of SK resulted in significantly diminished angiogenesis as well as reduced SK lesion severity (18). This reduced inflammatory condition post neutrophil depletion was the result of reduced levels of various molecules secreted by neutrophils, which contribute to the tissue damage. Neutrophils through their degranulation and release of various factors such as nitirci oxide (NO), matrix metalloproteinases (MMPs), VEGF-A, IL-1β, IL-8, IL-12 and TNF-α contributed to the ongoing inflammation and further tissue destruction which may unmask corneal auto-antigens (4, 20-24). VEGF-A and MMP-9 play an important role in HSV induced corneal neovascularization (described later) (18, 23).

In addition to neutrophils, other innate immune cells such as DCs, NK cells, γδ-T cells and macrophages also participate in viral clearance and the subsequent inflammation by secreting various effector molecules such as type I IFNs, cytokines and chemokines (IL-17, IL-1β, IL-12, MIP-2 TNF-α, IFN-γ, IL-23) (4). Among these various cytokines, IL-1β and IL-6 were demonstrated to have a critical and central role in orchestrating the early inflammatory reaction (25-27). Although, after productive HSV infection of epithelial cells, most host gene expression is turned off (27), expression of pro-inflammatory cytokines such as IL-6 and IL-1β is increased at least for an initial period (day 1-2 post infection) and may represent a significant initial source of these cytokines (4, 27-29). Furthermore, uninfected corneal epithelial cells become the significant producers of IL-6 and IL-1β (4). However, it is still poorly understood how the uninfected corneal epithelial cells are programmed to produce these cytokines. One possible explanation for this is that pathogen associated molecular patterns (PAMPs) expressed by virus-infected cells or perhaps extracellular virus itself could activate various pattern recognition receptors. These include Toll-like receptors (TLR)-2, 4, and 9 with subsequent activation of NFκB pathway causing them to synthesize and secrete cytokines (4, 30, 31). Evidence for this is that CpG motifs derived from viral DNA in the cornea could stimulate TLR-9 and induce IL-1β and IL-6 that act in a paracrine fashion on other cells and induce them to secrete various inflammatory mediators that contribute to the immunopathological lesion as well as induction of adaptive immune response (30, 32, 33). Furthermore, IL-1β acts in a paracrine fashion on un-infected corneal epithelial cells and stimulates the production of IL-6 (34, 35). IL-6 triggers the synthesis of MIP-2 (CXCL8), which is involved in neutrophil influx at the site of inflammation. In addition

to IL-1β and IL-6, TNF-α also plays an important role in SK pathogenesis, as indicated by studying SK pathogenesis in mice lacking TNF-α. These results showed that such mice were unable to control virus replication in the cornea and as a consequence exhibited an enhanced SK lesion severity (4, 34-37). Thus early events after HSV infection trigger the production of various cytokines and chemokines, which initiate the innate immune response and set the stage for further adaptive immune response as well as immunopathology.

Is SK Immunopathology: Th1 or Th17 mediated?

Early events of the innate immune response drive various critical events that ultimately result in the adaptive immune response. IL-12 is another critical cytokine that is produced by neutrophils, macrophages and Langerhans DCs and plays an important role in SK pathogenesis (4, 38-40). IL-12 stimulates the production of IFN-γ by macrophages, NK cells, neutrophils as well as $CD4^+$ T cells (40, 41). IFN-γ has been shown to exert both pro-inflammatory and anti-inflammatory activity (4). It promotes neutrophil infiltration at the site of inflammation through upregulation of PECAM-1 and ICAM-1 on corneal epithelial cells (42, 43). Studies in an animal model of SK have revealed a critical contribution of $CD4^+$ T cells of the Th1 subset as principal orchestrators of SK lesions (44, 45). However, the identity of target antigens that drive SK Th1 cells generation during SK immunopathology is poorly understood (4, 44, 45). It is anticipated that initial corneal infiltrating Th1 cells are HSV specific, however later on SK lesion would be dominated by bystander cell population (Ref).

Recent work has revealed the critical pro-inflammatory role of IL-17A in pathogenesis of many inflammatory and autoimmune diseases (46-48). IL-17 mediates the local inflammatory response by stimulating epithelial, endothelial and fibroblastic cells and inducing the release of various inflammatory cytokines (49). IL-17A drives increased influx as well as survival of neutrophils at the site of inflammation by induction of neutrophil chemoattractant as well as GM-CSF mediated granulopoeisis (50, 51). IL-17A signals through a homodimeric IL-17A receptor A (IL-17RA), which is expressed ubiquitously, with higher levels in hematopoietic tissues (52, 53). Signaling through IL-17RA activates both NFκB and Jnk kinase pathway, resulting in an increased expression as well as an improved mRNA stability of various pro-inflammatory cytokines (52, 53).

In the beginning, IL-17A was thought to be primarily produce by activated CD4+ memory T cells (49), however, subsequent studies showed that CD8+ memory T cells can also produce IL-17A upon activation (54). More recently, pioneering studies have revealed a new subset of $CD4^+$ T cells as IL-17 producers and referred as T helper 17 (Th17). 55, 56). Naïve CD4+ T cells differentiate into Th17 cells under optimum antigenic stimulation in the presence of TGF-β and IL-6. This drives the subsequent activation of signal transducer and activator of transcription 3 (STAT3) followed by expression of retinoic acid related orphan receptor γt (RORγt) (57-60).

Th17 cells play a critical role in defense against fungi and extracellular bacteria (60). Additional studies implicated the crucial role of Th17 cells in chronic inflammatory as well as autoimmune pathologies (60). However, slower development of adaptive Th17 responses indicated the possibility of an innate source of IL-17, which contributed to the early defense mechanism against certain microorganisms (61-63). In addition to Th17

cells, IL-17A is also produced by γδ T cells, NK cells, NKT cells, alveolar macrophages as well as neutrophils (63). These studies collectively indicate an important role of IL-17 in innate as well as adaptive immune responses.

Although, Th1 cells constitute a significant proportion of cells during the development of SK lesions, the actual tissue damage appears to be the consequence of inflammatory events that derive primarily from neutrophils. The later cell represents the major cellular component of lesions at all phases of SK pathogenesis (18). The prominence of neutrophils in SK lesions as well as the role of IL-17A in neutrophil migration could indicate that the recently identified proinflammatory cytokine IL-17A may participate in the pathogenesis of lesion development. The role of IFN-γ producing Th1 cells is well studied in HSV induced corneal immunopathology, but the role of IL-17 and Th17 cells is poorly understood. In human SK, the presence of IL-17 has been reported (64). Additionally, the Lausch group showed that the severity of early SK lesions was diminished in mice unable to respond to IL-17 because they lacked the IL-17 receptor (65). However, the cellular source of IL-17 as well as the role this cytokine plays compared to other inflammatory mediators remains to be further defined. Since, Th17 cells have less stringent requirements for antigenic stimulation (66), it is possible that Th17 cells may play an important role in SK pathogenesis during later stages when viral antigen availability is limited. Thus, it could be possible that during the acute phase of SK pathogenesis HSV specific Th1 cells might dominate while HSV non-specific Th17 cells may maintain the later chronic phase. This was a driving issue that was evaluated in our studies with the results described in chapter II.

HSV Induced Corneal Angiogenesis

Another important feature of SK pathogenesis is the development of new blood vessels or angiogenesis in the normally avascular cornea, which together with increased corneal opacity due to infiltration of inflammatory cells impairs normal vision and may lead to blindness (4, 12, 18, 24, 33). Angiogenesis is the formation of new blood vessels from pre-existing blood vessels through an angiogenic remodeling and sprouting of pre-existing angiogenic structures. Development of vasculature (Vasculogenesis) ceases after complete maturation of the blood vessels and most of the blood vessels remain in quiescent stages. However, the body needs to respond to various physiological stimuli and active angiogenesis can be noted in cycling ovary as well as placental development during pregnancy (67). In addition, various pathological conditions leading to hypoxia such as ischemia, tissue injury or inflammation necessitates the supply of oxygenated blood to the damaged tissue (67, 68). Although, blood vessels in adults are maintained in a quiescent state, various stimuli such as malignancy, tissue injury, ischemia, inflammation etc can break this quiescence leading to angiogenic sprouting from existing vessels. This form of angiogenesis is often referred to as pathological angiogenesis and plays an important role in pathogenesis of various diseases such as cancer, corneal and retinal disorders (4, 67, 68).

Pathological angiogenesis when compared to physiological angiogenesis, is less complex and may involve the action of a single growth factor, VEGF-A and its receptors (68). Additionally, it is not a tightly controlled process and unbalanced growth of vessels often results in extensive proliferation, irregular branching with the lack of a proper and

functional hierarchical pattern as observed during normal angiogenesis (68). Furthermore, due to lack of appropriate remodeling and maturation, these newly formed vessels are often tortuous, abnormally developed with a large diameter, and leaky. This leads to severe edema in affected tissue. Moreover, a recent study revealed a differential gene expression pattern in endothelial cells during physiological and pathological angiogenesis, indicating the differential regulation of these processes (67-71). Apparently the neovascularization process looks simpler, but involves various molecular events similar to those of physiological angiogenesis. The various processes such as angiogenic sprouting from capillary endothelial cells, their proliferation, migration to the desired region, organization into tubular structures along with acquisition of pericytes and smooth muscle cells are essential for the proper development of functional vessels (67, 68, 70, 71). In addition, degradation of the complex extracellular matrix is also essential for the development of luminal structures in solid tissue. All these events are orchestrated and coordinated by VEGF-A, different growth factors, matrix-metalloproteinases (MMPs) with spatial and temporal cues from inflammatory cells. These cells serve as additional sources of VEGF-A, MMPs, different cytokines and growth factors (67, 68, 70, 71). The role of VEGF-A in pathological angiogenesis as well as structural details of various types of blood vessels after ectopic VEGF-A expression are well summarized in the review by Nagy et al (68).

Corneal Neovascularization: An Essential Step in SK pathogenesis

Corneal transparency is an essential requisite for optimal vision (72, 73) . The avascularity of cornea is achieved through a fine balance between pro and anti-angiogenic factors (72, 73). Events that cause angiogenesis are disruptive to vision such as occurs after HSV infection of the cornea (4, 12, 24). In mice, HSV infection of the cornea results in sprouting of new blood vessels from limbal vessels as early as day 1 pi and reaches the central cornea by day 20 pi (12, 24). The newly formed vascular bed is often leaky and abnormal releasing inflammatory cells and cytokines into the corneal stroma giving rise to corneal opacity and haze and subsequent vision impairment (4, 12, 24, 37). Although numerous studies in the past have shed light on several events responsible for corneal angiogenesis post HSV infection, the exact molecular mechanisms for this outcome are still poorly understood (4, 12, 24, 33, 37). Interestingly, HSV replication in corneal epithelium results in angiogenesis in the underlying stroma (4). Additionally, HSV does not encode any proteins, that is directly angiogenic as does occurs with some other viruses such as human herpes virus 8 and Orf virus (4, 74-77). Therefore, the mechanisms by which HSV infection drives corneal angiogenesis could involve a cascade of indirect events driven by different pro-angiogenic cytokines and factors (4). Numerous studies from our lab as well as other's have indicated the several angiogenic factors can be involved. These include VEGF-A, basic Fibroblast growth factor (bFGF), bioactive CpG motifs, pro-inflammatory cytokines (IL-6, IL-1β) as well as E-L-R motif containing chemokines in HSV induced corneal neovascularization (12, 23, 37). Although all these molecules may participate in pathological neovascularization,

the VEGF family of proteins, especially VEGF-A signaling through the VEGFR-2 receptor, is likely to be the most consequential (12, 78). In support of this, inhibiting VEGF or interfering with its receptor function, have been shown to be effective therapeutic strategies in mice models of SK (4, 12, 24, 78).

Source of VEGF-A During HSV Induced Ocular Neovascularization

After ocular HSV infection of mice, VEGF-A mRNA transcripts are detectable by 12 h pi and VEGF-A protein by 24 h pi (4, 12). However, one unresolved issue with regard to VEGF and pathological angiogenesis in SK, is the source of the VEGF A that induces the neovascularization as a consequence of the infection. Earlier studies from our lab demonstrated that the primary source of VEGF-A was corneal uninfected epithelial cells exposed to stimulating products such as IL-6 and CpG nucleotides released from infected and dying cells (4, 12). However, more recently, it was observed that VEGF-A can be produced directly by corneal epithelial cells in response to HSV infection (79). Additionally, infiltrating inflammatory cells, especially neutrophils, could also contribute to the source of VEGF-A (4, 18, 22). Interestingly, it was observed that VEGF-A is continuously produced in biologically functional amounts by normal uninfected corneal epithelial cells (73). However, this source of VEGF-A fails to induce abnormal angiogenesis because it is bound to a soluble form of the VEGF receptor 1 (sVEGFR-1) (73). This inhibitory interaction between VEGF-A and sVEGFR-1 was suggested to explain corneal avascularity, which is an essential feature of uninterrupted vision (72, 73). Furthermore, an angiogenic response was observed in the normal eyes when the

bond between VEGF-A and sVEGFR-1 was disrupted using anti-sVEGFR-1 mAb (73). Also, some species fail to express sVEGFR-1 and in one genetic disease of humans, synthesis of the sVEGFR-1 molecule is defective (80). In light of the existence of the VEGF-A trap in normal eyes it could be that pathological angiogenesis, as for example can occur after HSV infection, could also be influenced by the balance between VEGF-A and the sVEGFR-1 molecules. We analyzed this possibility as one of the possible mechanism employed by HSV infection for corneal angiogenesis. Our results indicated that HSV infection of the cornea leads to an imbalance between VEGF-A and sVEGFR-1 in favor of increased free VEGF-A thus leading to the development of angiogenesis (Discussed in Part III).

Role of other pro-angiogenic factors in HSV induced corneal neovascularization

a. CpG Motifs

In addition to the direct production of VEGF-A by HSV infected or uninfected corneal epithelial cells, other factors such as CpG motifs derived from viral DNA can stimulate paracrine production of VEGF-A by corneal epithelial and stromal cells (4, 33). However, it is poorly understood how CpG motifs stimulate VEGF-A production. It is possible that HSV DNA, a rich source of bioactive CpG motifs, can stimulate VEGF-A production through TLR-9 mediated signaling that leads to induction of MyD88 adaptor protein and subsequent induction of NFκB pathways (4, 33). Additionally, CpG repeats induced by HSV infection could stimulate VEGF-A induction through increased

production of IL-1 and IL-6, which promote paracrine expression of VEGF-A by corneal epithelial cells (4).

b. Matrix Metalloproteinases (MMPs)

Different MMPs play an important role in the breakdown of solid extracellular matrix and facilitates migration of endothelial cells, an essential step for the development of new blood vessel in solid tissue (4, 72, 81). MMPs are zinc-containing proteinases, secreted as pro-peptides that are activated in the extracellular milieu. They contribute to extracellular matrix remodeling (81). Several MMPs are expressed and localized to the different sites in the cornea, and they have been shown to play a role in neovascularization (72, 81). MMP-2, -7, -9, -14 were considered to be pro-angiogenic in corneal neovascularization and wound healing (72, 81). Among different MMPs, MMP-9 was shown to play an important role in HSV induced corneal angiogenesis (23). Innate cells, particularly neutrophils were shown to contribute to the early source of MMP-9, since depletion of neutrophils with specific mAb after HSV infection resulted in reduced levels of MMP-9 compared to isotype control antibody treated mice (23). Although, inhibition of MMP-9 activity using siRNA resulted in diminished angiogenesis severity in HSV infected mice, the exact molecular mechanism underlying the MMP-9 mediated neovascularization is poorly understood (4).

c. E-L-R motif containing chemokines

It has been documented that chemokines with E-L-R (tri-peptide sequence Glutamate-Leucine-Arignine) motifs possess angiogenic activity (4, 82, 83). HSV

infection of epithelial cells has been shown to up-regulate the expression of one such chemokine, MIP-2 (36, 84, 85). MIP-2 induced during HSV infection promotes the neutrophil migration at the site of inflammation thus contributing indirectly to the source of VEGF-A (36). Neutrophils, further contribute to the angiogenic response as they act as a source of preformed VEGF-A (22) as well as MMP-9 (23). Thus various chemokines promoting the migration of neutrophils could contribute indirectly the source of pro-angiogenic factors and subsequent angiogenesis after corneal HSV infection.

d. Pro-inflammatory cytokines: IL-1β, IL-6 and IL-17

It is known that productive HSV infection of corneal epithelial cells shuts host protein synthesis (86), but evidence suggests that some pro-inflammatory cytokine genes such as IL-1β and IL-6 are upregulated by HSV infected cells (27-29). After HSV infection of mouse corneal epithelial cells, both IL-1β and IL-6 expression is increased at day 1 pi followed by peak expression at day 10 pi (4, 27-29). Both IL-1β and IL-6 can be potent inducers of VEGF-A expression (87-90). Furthermore, studies from our lab have confirmed the role of IL-1β and IL-6 in the induction of VEGF-A by corneal epithelial as well as stromal fibroblast cells (4, 36, 91). In addition, intrastromal injection of IL-1β and IL-6 results in corneal angiogenesis in a VEGF-A dependent manner indicating their critical role in the induction of VEGF-A (4, 36, 91). Accordingly, blocking of IL-1β with the IL-1 receptor antagonist or neutralization of IL-6 with specific anti-IL-6 mAb showed diminished corneal angiogenic responses as compared to control treated mice post HSV infection (36, 37, 91).

In addition to IL-1β and IL-6, IL-17 has been shown to exhibit pro-angiogenic activity in different angiogenesis models (48, 49, 52). IL-17A signaling through the IL-17 receptor A induces the expression of a wide range of molecules such as VEGF-A, nitric oxide, prostaglandins, colony stimulating factor (CSF) - 2, CSF-3, MIP-2, CXCL1 (KC), CXCL2, CXCL-5, CXCL6, ICAM-1 and CCL2 by stromal fibroblast cells (48, 49, 52). Additionally, IL-17 also increases the expression of IL-1β, IL-6 and TNF-α by fibroblasts as well as monocytes (92, 93). Moreover, IL-17 was shown to play a direct role in angiogenesis through increased migration and cord formation of vascular endothelial cells in vitro as well as to increase the in vivo angiogenic response in a rat cornea assay (94). Since, IL-17A expression is upregulated after HSV-1 infection (64, 65), it is possible that IL-17A may contribute to HSV induced corneal angiogenesis. We analyzed this possibility for the role of IL-17A in corneal angiogenesis post HSV infection and results are described in chapter IV show that IL-17A promotes and orchestrates several events critical for angioggeneis after HSV infection.

Conclusions

In summary, HSV infection of the cornea leads to the development of a complex immunopathological reaction in cornea, termed as stromal keratitis. Clinically, SK lesions are characterized by severe keratitis, necrosis, corneal opacity, as well as development of new blood vessels in the normally avascular cornea. Pathogenesis of SK involves several events such as viral replication, migration of cells of innate and adaptive immune responses, increased expression of various cytokines and chemokines as well as

angiogenic factors. Although, numerous past studies have elucidated the various molecular events responsible for the development of complex immuno-inflammatory lesions, mechanisms responsible for corneal angiogenesis, as well as the relative involvement of different subsets of $CD4^+$ T Cells in SK pathogenesis are poorly understood.

The work described in this dissertation evaluated three important aspects of HSV immunopathology that includes:

1) Relative role of IL-17/IFN-γ and Th1/Th17 cells in HSV induced corneal immunopathology. In this study we showed that SK immunopathology was the outcome of a combined and sequential role of both Th1 and Th17 cells. Th1 cells were HSV specific migrated initially during the early stages of clinical SK followed by the migration of Th17 cells mostly of which were HSV non-specific. IL-17A contributed to the SK immunopathology by promoting HSV induced angiogenesis as well as increased infiltration of neutrophils. In contrast IFN-γ was found protective during early the stages of SK pathogenesis, but was pathogenic during the later stages when SK lesions were fully evident.

2) Understanding the molecular mechanisms responsible for an imbalance between VEGF-A and sVEGFR-1 and subsequent corneal angiogenesis post HSV infection. We found that HSV infection of the cornea lead to an increased expression of VEGF-A, but reduced sVEGFR-1 expression. In addition to decreased expression of sVEGFR-1, we observed the degradation of sVEGFR-1, which was primarily catalyzed by MMP-2, -7 and -9. Finally, we confirmed that

neutrophils act as a source of additional VEGF-A as well as various sVEGFR-1 degrading MMPs.

3) Role of IL-17A mediated effects on the balance between VEGF-A and sVEGFR-1 in HSV induced corneal neovascularization. In this study, we showed that IL-17A expression was increased after HSV infection. IL-17A through multiple mechanisms contributed to the disruption of the inhibitory interaction between VEGF-A and sVEGFR-1. IL-17A also promoted the expression of VEGF-A, sVEGFR-1 degrading MMPs and CXCL1/KC a chemoattractant for neutrophils. The net effect was increased VEGF-A levels along with a decrease of sVEGFR-1 with the outcome of corneal angiogenesis post HSV infection.

Collectively, data presented here have identified important aspects of HSV induced corneal immunopathology, which can be exploited for better therapeutic management of SK, an important cause of infectious blindness in the Western World.

LIST OF REFERENCES

1. Bloom, D. C. (2004) HSV LAT and neuronal survival, Int Rev Immunol 23, 187-198.
2. Daheshia, M., Feldman, L. T., and Rouse, B. T. (1998) Herpes simplex virus latency and the immune response, Curr Opin Microbiol 1, 430-435.
3. Jones, C. (1998) Alphaherpesvirus latency: its role in disease and survival of the virus in nature, Adv Virus Res 51, 81-133.
4. Biswas, P. S., and Rouse, B. T. (2005) Early events in HSV keratitis--setting the stage for a blinding disease, Microbes Infect 7, 799-810.
5. Bader, C., Crumpacker, C. S., Schnipper, L. E., Ransil, B., Clark, J. E., Arndt, K., and Freedberg, I. M. (1978) The natural history of recurrent facial-oral infection with herpes simplex virus, J Infect Dis 138, 897-905.
6. Enquist, L. W., Husak, P. J., Banfield, B. W., and Smith, G. A. (1998) Infection and spread of alphaherpesviruses in the nervous system, Adv Virus Res 51, 237-347.
7. Fraser, N. W., and Valyi-Nagy, T. (1993) Viral, neuronal and immune factors which may influence herpes simplex virus (HSV) latency and reactivation, Microb Pathog 15, 83-91.
8. Streilein, J. W., Dana, M. R., and Ksander, B. R. (1997) Immunity causing blindness: five different paths to herpes stromal keratitis, Immunol Today 18, 443-449.
9. Metcalf, J. F., Hamilton, D. S., and Reichert, R. W. (1979) Herpetic keratitis in athymic (nude) mice, Infect Immun 26, 1164-1171.

10. Russell, R. G., Nasisse, M. P., Larsen, H. S., and Rouse, B. T. (1984) Role of T-lymphocytes in the pathogenesis of herpetic stromal keratitis, Invest Ophthalmol Vis Sci 25, 938-944.

11. Mercadal, C. M., Bouley, D. M., DeStephano, D., and Rouse, B. T. (1993) Herpetic stromal keratitis in the reconstituted scid mouse model, J Virol 67, 3404-3408.

12. Zheng, M., Deshpande, S., Lee, S., Ferrara, N., and Rouse, B. T. (2001) Contribution of vascular endothelial growth factor in the neovascularization process during the pathogenesis of herpetic stromal keratitis, J Virol 75, 9828-9835.

13. Deshpande, S., Banerjee, K., Biswas, P. S., and Rouse, B. T. (2004) Herpetic eye disease: immunopathogenesis and therapeutic measures, Expert Rev Mol Med 6, 1-14.

14. Knickelbein, J. E., Hendricks, R. L., and Charukamnoetkanok, P. (2009) Management of herpes simplex virus stromal keratitis: an evidence-based review, Surv Ophthalmol 54, 226-234.

15. McGhee, C. N., Dean, S., and Danesh-Meyer, H. (2002) Locally administered ocular corticosteroids: benefits and risks, Drug Saf 25, 33-55.

16. Weinstein, B. I., Schwartz, J., Gordon, G. G., Dominguez, M. O., Varma, S., Dunn, M. W., and Southren, A. L. (1982) Characterization of a glucocorticoid receptor and the direct effect of dexamethasone on herpes simplex virus infection of rabbit corneal cells in culture, Invest Ophthalmol Vis Sci 23, 651-659.

17. Thomas, J., Gangappa, S., Kanangat, S., and Rouse, B. T. (1997) On the essential involvement of neutrophils in the immunopathologic disease: herpetic stromal keratitis, J Immunol 158, 1383-1391.

18. Suryawanshi, A., Mulik, S., Sharma, S., Reddy, P. B., Sehrawat, S., and Rouse, B. T. (2011) Ocular neovascularization caused by herpes simplex virus type 1 infection results from breakdown of binding between vascular endothelial growth factor A and its soluble receptor, J Immunol 186, 3653-3665.

19. Tumpey, T. M., Chen, S. H., Oakes, J. E., and Lausch, R. N. (1996) Neutrophil-mediated suppression of virus replication after herpes simplex virus type 1 infection of the murine cornea, J Virol 70, 898-904.

20. Daheshia, M., Kanangat, S., and Rouse, B. T. (1998) Production of key molecules by ocular neutrophils early after herpetic infection of the cornea, Exp Eye Res 67, 619-624.

21. Mistry, S. K., Zheng, M., Rouse, B. T., and Morris, S. M., Jr. (2001) Induction of arginases I and II in cornea during herpes simplex virus infection, Virus Res 73, 177-182.

22. Scapini, P., Calzetti, F., and Cassatella, M. A. (1999) On the detection of neutrophil-derived vascular endothelial growth factor (VEGF), J Immunol Methods 232, 121-129.

23. Lee, S., Zheng, M., Kim, B., and Rouse, B. T. (2002) Role of matrix metalloproteinase-9 in angiogenesis caused by ocular infection with herpes simplex virus, J Clin Invest 110, 1105-1111.

24. Zheng, M., Schwarz, M. A., Lee, S., Kumaraguru, U., and Rouse, B. T. (2001) Control of stromal keratitis by inhibition of neovascularization, Am J Pathol 159, 1021-1029.

25. Staats, H. F., and Lausch, R. N. (1993) Cytokine expression in vivo during murine herpetic stromal keratitis. Effect of protective antibody therapy, J Immunol 151, 277-283.

26. Lausch, R. N., Chen, S. H., Tumpey, T. M., Su, Y. H., and Oakes, J. E. (1996) Early cytokine synthesis in the excised mouse cornea, J Interferon Cytokine Res 16, 35-40.

27. Kanangat, S., Babu, J. S., Knipe, D. M., and Rouse, B. T. (1996) HSV-1-mediated modulation of cytokine gene expression in a permissive cell line: selective upregulation of IL-6 gene expression, Virology 219, 295-300.

28. Tran, M. T., Dean, D. A., Lausch, R. N., and Oakes, J. E. (1998) Membranes of herpes simplex virus type-1-infected human corneal epithelial cells are not permeabilized to macromolecules and therefore do not release IL-1alpha, Virology 244, 74-78.

29. Paludan, S. R. (2001) Requirements for the induction of interleukin-6 by herpes simplex virus-infected leukocytes, J Virol 75, 8008-8015.

30. Lund, J., Sato, A., Akira, S., Medzhitov, R., and Iwasaki, A. (2003) Toll-like receptor 9-mediated recognition of Herpes simplex virus-2 by plasmacytoid dendritic cells, J Exp Med 198, 513-520.

31. Kurt-Jones, E. A., Chan, M., Zhou, S., Wang, J., Reed, G., Bronson, R., Arnold, M. M., Knipe, D. M., and Finberg, R. W. (2004) Herpes simplex virus 1

interaction with Toll-like receptor 2 contributes to lethal encephalitis, Proc Natl Acad Sci U S A 101, 1315-1320.

32. Klinman, D. M., Zheng, M., Gierynska, M., and Rouse, B. T. (2002) DNA Containing Bioactive CpG Motifs Promote Angiogenesis, Drug News Perspect 15, 358-363.

33. Zheng, M., Klinman, D. M., Gierynska, M., and Rouse, B. T. (2002) DNA containing CpG motifs induces angiogenesis, Proc Natl Acad Sci U S A 99, 8944-8949.

34. Yan, X. T., Tumpey, T. M., Kunkel, S. L., Oakes, J. E., and Lausch, R. N. (1998) Role of MIP-2 in neutrophil migration and tissue injury in the herpes simplex virus-1-infected cornea, Invest Ophthalmol Vis Sci 39, 1854-1862.

35. Fenton, R. R., Molesworth-Kenyon, S., Oakes, J. E., and Lausch, R. N. (2002) Linkage of IL-6 with neutrophil chemoattractant expression in virus-induced ocular inflammation, Invest Ophthalmol Vis Sci 43, 737-743.

36. Banerjee, K., Biswas, P. S., Kim, B., Lee, S., and Rouse, B. T. (2004) CXCR2-/- mice show enhanced susceptibility to herpetic stromal keratitis: a role for IL-6-induced neovascularization, J Immunol 172, 1237-1245.

37. Biswas, P. S., Banerjee, K., Zheng, M., and Rouse, B. T. (2004) Counteracting corneal immunoinflammatory lesion with interleukin-1 receptor antagonist protein, J Leukoc Biol 76, 868-875.

38. Kanangat, S., Thomas, J., Gangappa, S., Babu, J. S., and Rouse, B. T. (1996) Herpes simplex virus type 1-mediated up-regulation of IL-12 (p40) mRNA

expression. Implications in immunopathogenesis and protection, J Immunol 156, 1110-1116.

39. Osorio, Y., Wechsler, S. L., Nesburn, A. B., and Ghiasi, H. (2002) Reduced severity of HSV-1-induced corneal scarring in IL-12-deficient mice, Virus Res 90, 317-326.

40. Kumaraguru, U., and Rouse, B. T. (2002) The IL-12 response to herpes simplex virus is mainly a paracrine response of reactive inflammatory cells, J Leukoc Biol 72, 564-570.

41. Lund, R. J., Chen, Z., Scheinin, J., and Lahesmaa, R. (2004) Early target genes of IL-12 and STAT4 signaling in th cells, J Immunol 172, 6775-6782.

42. Tang, Q., and Hendricks, R. L. (1996) Interferon gamma regulates platelet endothelial cell adhesion molecule 1 expression and neutrophil infiltration into herpes simplex virus-infected mouse corneas, J Exp Med 184, 1435-1447.

43. Yannariello-brown, J., Hallberg, C. K., Haberle, H., Brysk, M. M., Jiang, Z., Patel, J. A., Ernst, P. B., and Trocme, S. D. (1998) Cytokine modulation of human corneal epithelial cell ICAM-1 (CD54) expression, Exp Eye Res 67, 383-393.

44. Niemialtowski, M. G., and Rouse, B. T. (1992) Phenotypic and functional studies on ocular T cells during herpetic infections of the eye, J Immunol 148, 1864-1870.

45. Niemialtowski, M. G., and Rouse, B. T. (1992) Predominance of Th1 cells in ocular tissues during herpetic stromal keratitis, J Immunol 149, 3035-3039.

46. Aggarwal, S., and Gurney, A. L. (2002) IL-17: prototype member of an emerging cytokine family, J Leukoc Biol 71, 1-8.

47. Moseley, T. A., Haudenschild, D. R., Rose, L., and Reddi, A. H. (2003) Interleukin-17 family and IL-17 receptors, Cytokine Growth Factor Rev 14, 155-174.

48. Kolls, J. K., and Linden, A. (2004) Interleukin-17 family members and inflammation, Immunity 21, 467-476.

49. Fossiez, F., Djossou, O., Chomarat, P., Flores-Romo, L., Ait-Yahia, S., Maat, C., Pin, J. J., Garrone, P., Garcia, E., Saeland, S., Blanchard, D., Gaillard, C., Das Mahapatra, B., Rouvier, E., Golstein, P., Banchereau, J., and Lebecque, S. (1996) T cell interleukin-17 induces stromal cells to produce proinflammatory and hematopoietic cytokines, J Exp Med 183, 2593-2603.

50. Laan, M., Prause, O., Miyamoto, M., Sjostrand, M., Hytonen, A. M., Kaneko, T., Lotvall, J., and Linden, A. (2003) A role of GM-CSF in the accumulation of neutrophils in the airways caused by IL-17 and TNF-alpha, Eur Respir J 21, 387-393.

51. Laan, M., Cui, Z. H., Hoshino, H., Lotvall, J., Sjostrand, M., Gruenert, D. C., Skoogh, B. E., and Linden, A. (1999) Neutrophil recruitment by human IL-17 via C-X-C chemokine release in the airways, J Immunol 162, 2347-2352.

52. Gaffen, S. L. (2009) Structure and signalling in the IL-17 receptor family, Nat Rev Immunol 9, 556-567.

53. Shen, F., and Gaffen, S. L. (2008) Structure-function relationships in the IL-17 receptor: implications for signal transduction and therapy, Cytokine 41, 92-104.

54. He, D., Wu, L., Kim, H. K., Li, H., Elmets, C. A., and Xu, H. (2006) CD8+ IL-17-producing T cells are important in effector functions for the elicitation of contact hypersensitivity responses, J Immunol 177, 6852-6858.

55. Park, H., Li, Z., Yang, X. O., Chang, S. H., Nurieva, R., Wang, Y. H., Wang, Y., Hood, L., Zhu, Z., Tian, Q., and Dong, C. (2005) A distinct lineage of CD4 T cells regulates tissue inflammation by producing interleukin 17, Nat Immunol 6, 1133-1141.

56. Harrington, L. E., Hatton, R. D., Mangan, P. R., Turner, H., Murphy, T. L., Murphy, K. M., and Weaver, C. T. (2005) Interleukin 17-producing CD4+ effector T cells develop via a lineage distinct from the T helper type 1 and 2 lineages, Nat Immunol 6, 1123-1132.

57. Bettelli, E., Carrier, Y., Gao, W., Korn, T., Strom, T. B., Oukka, M., Weiner, H. L., and Kuchroo, V. K. (2006) Reciprocal developmental pathways for the generation of pathogenic effector TH17 and regulatory T cells, Nature 441, 235-238.

58. Mangan, P. R., Harrington, L. E., O'Quinn, D. B., Helms, W. S., Bullard, D. C., Elson, C. O., Hatton, R. D., Wahl, S. M., Schoeb, T. R., and Weaver, C. T. (2006) Transforming growth factor-beta induces development of the T(H)17 lineage, Nature 441, 231-234.

59. Veldhoen, M., Hocking, R. J., Atkins, C. J., Locksley, R. M., and Stockinger, B. (2006) TGFbeta in the context of an inflammatory cytokine milieu supports de novo differentiation of IL-17-producing T cells, Immunity 24, 179-189.

60. Korn, T., Bettelli, E., Oukka, M., and Kuchroo, V. K. (2009) IL-17 and Th17 Cells, Annu Rev Immunol 27, 485-517.

61. Martin, B., Hirota, K., Cua, D. J., Stockinger, B., and Veldhoen, M. (2009) Interleukin-17-producing gammadelta T cells selectively expand in response to pathogen products and environmental signals, Immunity 31, 321-330.

62. Sutton, C. E., Lalor, S. J., Sweeney, C. M., Brereton, C. F., Lavelle, E. C., and Mills, K. H. (2009) Interleukin-1 and IL-23 induce innate IL-17 production from gammadelta T cells, amplifying Th17 responses and autoimmunity, Immunity 31, 331-341.

63. Cua, D. J., and Tato, C. M. (2010) Innate IL-17-producing cells: the sentinels of the immune system, Nat Rev Immunol 10, 479-489.

64. Maertzdorf, J., Osterhaus, A. D., and Verjans, G. M. (2002) IL-17 expression in human herpetic stromal keratitis: modulatory effects on chemokine production by corneal fibroblasts, J Immunol 169, 5897-5903.

65. Molesworth-Kenyon, S. J., Yin, R., Oakes, J. E., and Lausch, R. N. (2008) IL-17 receptor signaling influences virus-induced corneal inflammation, J Leukoc Biol 83, 401-408.

66. Weaver, C. T., Hatton, R. D., Mangan, P. R., and Harrington, L. E. (2007) IL-17 family cytokines and the expanding diversity of effector T cell lineages, Annu Rev Immunol 25, 821-852.

67. Carmeliet, P. (2005) Angiogenesis in life, disease and medicine, Nature 438, 932-936.

68. Nagy, J. A., Dvorak, A. M., and Dvorak, H. F. (2007) VEGF-A and the induction of pathological angiogenesis, Annu Rev Pathol 2, 251-275.

69. Seaman, S., Stevens, J., Yang, M. Y., Logsdon, D., Graff-Cherry, C., and St Croix, B. (2007) Genes that distinguish physiological and pathological angiogenesis, Cancer Cell 11, 539-554.

70. Carmeliet, P. (2000) Mechanisms of angiogenesis and arteriogenesis, Nat Med 6, 389-395.

71. Folkman, J., and D'Amore, P. A. (1996) Blood vessel formation: what is its molecular basis?, Cell 87, 1153-1155.

72. Azar, D. T. (2006) Corneal angiogenic privilege: angiogenic and antiangiogenic factors in corneal avascularity, vasculogenesis, and wound healing (an American Ophthalmological Society thesis), Trans Am Ophthalmol Soc 104, 264-302.

73. Ambati, B. K., Nozaki, M., Singh, N., Takeda, A., Jani, P. D., Suthar, T., Albuquerque, R. J., Richter, E., Sakurai, E., Newcomb, M. T., Kleinman, M. E., Caldwell, R. B., Lin, Q., Ogura, Y., Orecchia, A., Samuelson, D. A., Agnew, D. W., St Leger, J., Green, W. R., Mahasreshti, P. J., Curiel, D. T., Kwan, D., Marsh, H., Ikeda, S., Leiper, L. J., Collinson, J. M., Bogdanovich, S., Khurana, T. S., Shibuya, M., Baldwin, M. E., Ferrara, N., Gerber, H. P., De Falco, S., Witta, J., Baffi, J. Z., Raisler, B. J., and Ambati, J. (2006) Corneal avascularity is due to soluble VEGF receptor-1, Nature 443, 993-997.

74. Boshoff, C. (1998) Kaposi's sarcoma. Coupling herpesvirus to angiogenesis, Nature 391, 24-25.

75. Bais, C., Santomasso, B., Coso, O., Arvanitakis, L., Raaka, E. G., Gutkind, J. S., Asch, A. S., Cesarman, E., Gershengorn, M. C., and Mesri, E. A. (1998) G-protein-coupled receptor of Kaposi's sarcoma-associated herpesvirus is a viral oncogene and angiogenesis activator, Nature 391, 86-89.

76. Haque, N. S., Fallon, J. T., Taubman, M. B., and Harpel, P. C. (2001) The chemokine receptor CCR8 mediates human endothelial cell chemotaxis induced by I-309 and Kaposi sarcoma herpesvirus-encoded vMIP-I and by lipoprotein(a)-stimulated endothelial cell conditioned medium, Blood 97, 39-45.

77. Sun, R., Lin, S. F., Staskus, K., Gradoville, L., Grogan, E., Haase, A., and Miller, G. (1999) Kinetics of Kaposi's sarcoma-associated herpesvirus gene expression, J Virol 73, 2232-2242.

78. Kim, B., Tang, Q., Biswas, P. S., Xu, J., Schiffelers, R. M., Xie, F. Y., Ansari, A. M., Scaria, P. V., Woodle, M. C., Lu, P., and Rouse, B. T. (2004) Inhibition of ocular angiogenesis by siRNA targeting vascular endothelial growth factor pathway genes: therapeutic strategy for herpetic stromal keratitis, Am J Pathol 165, 2177-2185.

79. Wuest, T. R., and Carr, D. J. (2010) VEGF-A expression by HSV-1-infected cells drives corneal lymphangiogenesis, J Exp Med 207, 101-115.

80. Jordan, T., Hanson, I., Zaletayev, D., Hodgson, S., Prosser, J., Seawright, A., Hastie, N., and van Heyningen, V. (1992) The human PAX6 gene is mutated in two patients with aniridia, Nat Genet 1, 328-332.

81. Sivak, J. M., and Fini, M. E. (2002) MMPs in the eye: emerging roles for matrix metalloproteinases in ocular physiology, Prog Retin Eye Res 21, 1-14.

82. Arenberg, D. A., Polverini, P. J., Kunkel, S. L., Shanafelt, A., Hesselgesser, J., Horuk, R., and Strieter, R. M. (1997) The role of CXC chemokines in the regulation of angiogenesis in non-small cell lung cancer, J Leukoc Biol 62, 554-562.

83. Arenberg, D. A., Polverini, P. J., Kunkel, S. L., Shanafelt, A., and Strieter, R. M. (1997) In vitro and in vivo systems to assess role of C-X-C chemokines in regulation of angiogenesis, Methods Enzymol 288, 190-220.

84. Su, Y. H., Yan, X. T., Oakes, J. E., and Lausch, R. N. (1996) Protective antibody therapy is associated with reduced chemokine transcripts in herpes simplex virus type 1 corneal infection, J Virol 70, 1277-1281.

85. Tumpey, T. M., Cheng, H., Yan, X. T., Oakes, J. E., and Lausch, R. N. (1998) Chemokine synthesis in the HSV-1-infected cornea and its suppression by interleukin-10, J Leukoc Biol 63, 486-492.

86. Kwong, A. D., and Frenkel, N. (1989) The herpes simplex virus virion host shutoff function, J Virol 63, 4834-4839.

87. Nakahara, H., Song, J., Sugimoto, M., Hagihara, K., Kishimoto, T., Yoshizaki, K., and Nishimoto, N. (2003) Anti-interleukin-6 receptor antibody therapy reduces vascular endothelial growth factor production in rheumatoid arthritis, Arthritis Rheum 48, 1521-1529.

88. Saijo, Y., Tanaka, M., Miki, M., Usui, K., Suzuki, T., Maemondo, M., Hong, X., Tazawa, R., Kikuchi, T., Matsushima, K., and Nukiwa, T. (2002) Proinflammatory cytokine IL-1 beta promotes tumor growth of Lewis lung

carcinoma by induction of angiogenic factors: in vivo analysis of tumor-stromal interaction, J Immunol 169, 469-475.

89. Salven, P., Hattori, K., Heissig, B., and Rafii, S. (2002) Interleukin-1alpha promotes angiogenesis in vivo via VEGFR-2 pathway by inducing inflammatory cell VEGF synthesis and secretion, FASEB J 16, 1471-1473.

90. Wei, L. H., Kuo, M. L., Chen, C. A., Chou, C. H., Lai, K. B., Lee, C. N., and Hsieh, C. Y. (2003) Interleukin-6 promotes cervical tumor growth by VEGF-dependent angiogenesis via a STAT3 pathway, Oncogene 22, 1517-1527.

91. Biswas, P. S., Banerjee, K., Kim, B., and Rouse, B. T. (2004) Mice transgenic for IL-1 receptor antagonist protein are resistant to herpetic stromal keratitis: possible role for IL-1 in herpetic stromal keratitis pathogenesis, J Immunol 172, 3736-3744.

92. Takahashi, H., Numasaki, M., Lotze, M. T., and Sasaki, H. (2005) Interleukin-17 enhances bFGF-, HGF- and VEGF-induced growth of vascular endothelial cells, Immunol Lett 98, 189-193.

93. Numasaki, M., Lotze, M. T., and Sasaki, H. (2004) Interleukin-17 augments tumor necrosis factor-alpha-induced elaboration of proangiogenic factors from fibroblasts, Immunol Lett 93, 39-43.

94. Numasaki, M., Fukushi, J., Ono, M., Narula, S. K., Zavodny, P. J., Kudo, T., Robbins, P. D., Tahara, H., and Lotze, M. T. (2003) Interleukin-17 promotes angiogenesis and tumor growth, Blood 101, 2620-2627.

APPENDIX

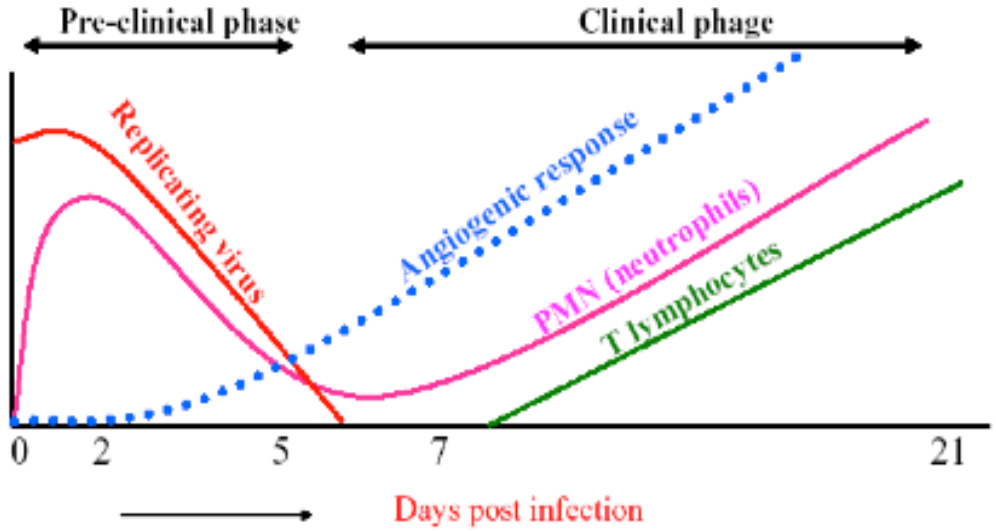

FIGURE 1.1 PRINCIPAL EVENTS IN HSV INDUCED CORNEAL SK PATHOGENESIS

Post HSV infection of the cornea, replicating virus is detectable in the cornea till day 7 pi. Early after HSV infection, PMN, particularly neutrophils infiltrate the stromal layer of cornea, and play an important role in virus clearance. Development of new blood vessels from existing limbal vessels can be noted as early as day 1 pi. During clinical phase SK lesions become evident which are characterized by the infiltration of lymphocyte, particularly Th1 cells, neutrophils and the development of blood vessels.

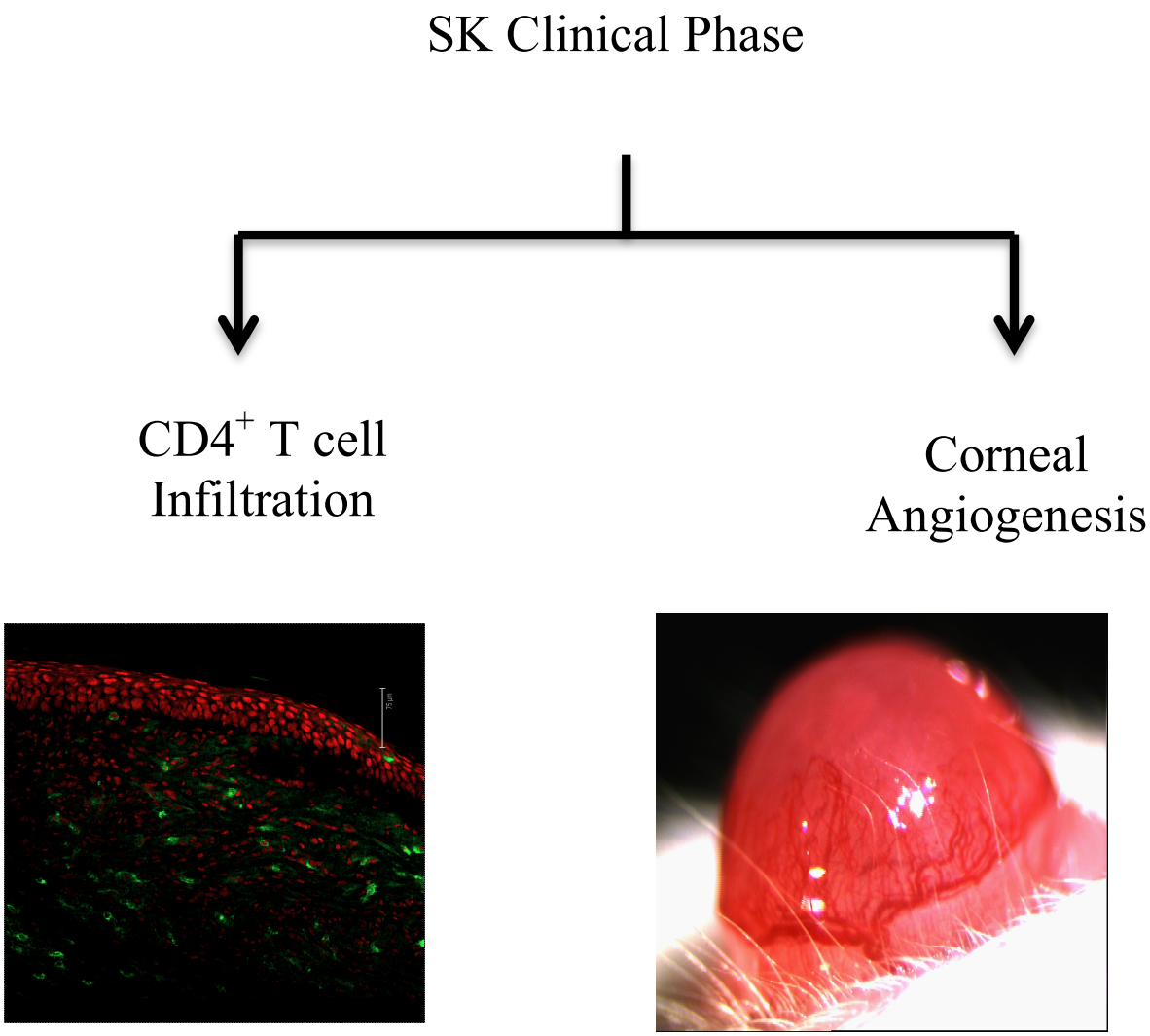

FIGURE 1.2 CLINICAL PHASE OF SK

Clinical phase of SK is marked by corneal infiltration of the T lymphocytes, particularly $CD4^+$ T lymphocytes and the development of new blood vessels in normally avascular cornea.

PART-II

ROLE OF IL-17 AND TH17 CELLS IN HSV INDUCED CORNEAL IMMUNOPATHOLOGY

Research described in this chapter is a slightly modified version of an article that is accepted for publication in *Journal of Immunology* by Amol Suryawanshi, Sachin Mulik, Shalini Sharma, Pradeep BJ Reddy, Sharvan Sehrawat and Barry T Rouse.

Suryawanshi A, Veiga-Parga, Rajasagi N, Reddy PB, Sehrawat S and Rouse BT. Role of IL-17 and Th17 Cells in HSV Induced Corneal Immunopathology. *J. Immunol.* 2011. 187 (4).

In this chapter "our" and "we" refers to me and co-authors. My contribution in the paper includes (1) Selection of the topic (2) Compiling and interpretation of the literature (3) Designing experiments (4) Understanding the literature and interpretation of the results (5) Providing comprehensible structure to the paper (6) Preparation of graphs and figures (7) Writing and editing.

Abstract

Herpes Simplex Virus-1 (HSV) infection of the cornea leads to a blinding immuno-inflammatory lesion of the eye termed stromal keratitis (SK). Recently, IL-17 producing $CD4^+$ T cells (Th17) were shown to play a prominent role in many autoimmune conditions, but the role of IL-17 and/or of Th17 cells in virus immunopathology is unclear. Here we show that, after HSV infection of the cornea, IL-17 is upregulated in a biphasic manner with an initial peak production around day 2 pi and a second wave starting from day 7 pi with a steady increase until day 21 pi, a time

point when clinical lesions are fully evident. Further studies demonstrated that innate cells particularly, γδ T cells, were major producers of IL-17 early after HSV infection. However, during the clinical phase of SK, the predominant source of IL-17 was Th17 cells which infiltrated the cornea only after the entry of Th1 cells. By ex-vivo stimulation, the half fraction of IFN-γ producing $CD4^+$ T (Th1) cells were HSV specific, whereas very few Th17 cells responded to HSV stimulation. The delayed influx of Th17 cells in the cornea was attributed to the local chemokine and cytokine milieu. Finally, HSV infection of IL-17 receptor knockout mice, as well as IL-17 neutralization in WT mice showed diminished SK severity. In conclusion, our results show that IL-17 and Th17 cells contribute to the pathogenesis of SK, the most common cause of infectious blindness in the western world.

Introduction

Ocular infection with herpes simplex virus (HSV) can cause a chronic inflammatory reaction in the corneal stroma that may culminate in blindness (*1, 2*). This stromal keratitis (SK) lesion in humans is suspected to represent an immunopathological reaction, a notion well supported by studies with animal models of SK (*2-5*). An inevitable consequence of ocular HSV infection is life long latency in neuronal cells of the trigeminal ganglion (*6*). In humans, periodic reactivation from some latently infected cells give rise to replicating virus that acts as the most common stimulus for SK lesion development (*2-5*). A major objective of SK research is to identify the role of cellular and molecular events involved in tissue damage and its resolution with a view to improving

current means of management of this often distressing disease. Studies in the mouse models of SK have firmly established an essential role for T cells as the principal orchestrators of SK lesions (*7, 8*). However, the actual tissue damage appearance to be the consequence of inflammatory events that derive primarily from neutrophils that represent the major cellular component of lesions at all phases of SK pathogenesis (*9, 10*). The prominence of neutrophils in SK lesions could indicate that the recently identified proinflammatory cytokine IL-17 is a significant participant in the pathogenesis of lesion development. Accordingly, IL-17 functions indirectly to cause tissue infiltration by neutrophils, acts as a neutrophil survival factor and also may drive the cells to produce and release tissue damaging molecules such as MMPs and oxyradicals (*11-15*).

In human SK, the presence of IL-17 has been reported (*16*). Additionally, the Lausch group showed that the severity of early SK lesions were diminished in mice unable to respond to IL-17 because they lacked the IL-17 receptor (*17*). However, the cellular source of IL-17 as well as the role this cytokine plays compared to other inflammatory mediators remains to be further defined. This is the topic of the present communication.

We show that HSV infection of the cornea leads to the biphasic upregulation of IL-17. Initially its source was innate cells that included γδ T cells, whereas later during the clinical phase Th17 cells were the predominant producer. The $CD4^+$ T cell subset responsible for orchestrating SK appeared to be mainly Th1 cells at all stages of SK. On the other hand, very few Th17 cells infiltrated into the cornea during early stages of SK (day 8 and 15 pi) but became more prominent during very late stage of SK (day 21 pi), when SK lesions were fully evident. The late entry of Th17 cells was partly explained by the delayed

upregulation of IL-6 and TGF-β, cytokines responsible for Th17 generation, as well as CCL20 expression in the cornea, a chemokine responsible for the migration of Th17 cells at the site of inflammation. On the basis of anti-cytokine suppression and comparison of lesion severity between WT and IL-17 receptor knock out (IL-17RKO) mice, our result show that IL-17 contributes to inflammatory events during the pathogenesis of SK. Future therapies targeting the IL-17 response could be useful to alleviate the SK lesion severity, an important cause of infectious blindness in humans.

Material and Methods

Mice, Virus and cell lines. IL-17RA -/- mice on C57B1/6 background were obtained from Amgen Inc. (Thousand Oaks, CA, USA). C57BL/6 mice were purchased from Harlan Sprague Dawley, Indianapolis, IN. Animals were housed in the animal facilities approved by the Association for Assessment and Accreditation of Laboratory Animal Care (AAALAC) at The University of Tennessee and all experimental procedures were in complete agreement with the Association for research in Vision and Ophthalmology resolution on the use of animals in research. HSV-1 RE Tumpey and HSV-KOS viruses were grown in Vero Cell monolayers (ATCC no. CCL81, American Type Culture Collection). The virus was concentrated, titrated, and stored in aliquots at -80^0 C until use.

Corneal HSV Infection and Clinical Scoring. Corneal infections of mice were conducted under deep anaesthesia induced by i.p. injection of avertin as previously described (*18*). Mice were scarified on their corneas with 27-gauge needle, and a 3-µl

drop containing 1×10^4 PFU of virus was applied to the eye. The eyes were examined on different days pi for the development and progression of clinical lesion by slit-lamp biomicroscope (Kowa Company, Nagoya, Japan). The progression of SK lesion severity and angiogenesis of individually scored mice was recorded. The scoring system was as follows: 0, normal cornea; +1, mild corneal haze; +2, moderate corneal opacity or scarring; +3, severe corneal opacity but iris visible; +4, opaque cornea and corneal ulcer; +5, corneal rupture and necrotizing keratitis. The severity of angiogenesis was recorded as described previously (*19*). According to this system, a grade of 4 for a given quadrant of the circle represents a centripetal growth of 1.5 mm towards the corneal center. The score of the four quadrants of the eye were then summed to derive the neo vessel index (range 0-16) for each eye at a given time point.

Reagents and Antibodies. CD4-allophycocyanin (RM4-5), IL-17-PE (TC11-18H10), IFN- γ-FITC (XMG1.2), γδ TCR-FITC (GL3), anti-CD3 (145.2C11), anti-CD28 (37.51), purified anti-IL-17, purified anti-IFN- γ and GolgiStop (Brefeldin A) were purchased from BD Bioscience. Foxp3-PE, IL-17 and IFN- γ ELISA kit were purchased from eBioscience. Anti γδ TCR (UC3-10A6) and Hamster IgG isotype control Ab were purchased from Bio-X-Cell. PMA and ionomycin were purchased from Sigma-Aldrich.

γδ T cell Depletion. C57BL/6 mice were injected on day 2 before infection with 500 μg/mouse anti-mouse γδ TCR (clone UC3-10A6) followed by 250 μg/mouse on day of infection.

Sub-conjunctival Injection. Subconjunctival injections of anti-IL-17 were performed as described previously (*20*). Briefly, subconjunctival injections were done using a 2 cm, 32 gauge needle and syringe (Hamilton, Reno, NV) to penetrate the perivascular region

of conjunctiva, and the required dose of anti-IL-17 mAb was delivered into subconjunctival space. Control mice received isotype mAb.

IL-17 and IFN-γ Neutralization. C57BL/6 mice were ocularly infected and 0.05 mg of anti-IL-17 or anti-IFN- γ was given intraperitoneally (i.p.) starting from day -1 followed by day 2 and day 5 pi or starting from day 7 followed by day 10 and 13 pi. For local depletion, 5 μg anti-IL-17 mAb was administered by sub-conjunctival injection following same regimes as described above.

Isolation of corneal-infiltrating cells and flow cytometry. HSV infected corneas were harvested from different group of mice at indicated time point pi. Six to eighth corneas per group were excised, pooled group wise, and digested with 60 U/ml Liberase for 35 minutes at 37^0C in a humified atmosphere of 5% CO_2. After incubation, the corneas were disrupted by grinding with a syringe plunger on a cell strainer and single-cell suspensions were made in complete RPMI 1640 medium. The single cell suspensions obtained from corneas, DLNs and spleen were stained for different cell surface molecules for FACS. All steps performed at 4^0C. Briefly, cell suspension were first blocked with an unconjugated anti-CD32/CD16 mAb for 30 min in FACS buffer. After washing with FACS buffer, samples were incubated with CD4-APC (RM4-5) for 30 min on ice. Finally, the cells were washed three times and re-suspended in 1% *para*-formaldehyde.

To measure the number of IFN-γ, IL-17 and IL-2 producing $CD4^+$ T cells, intracellular cytokine staining was performed. Briefly, 10^6 freshly isolated cells from DLNs, spleens or corneas were left untreated or stimulated with PMA plus ionomycin along with GolgiStop for 4 hrs at 37^0C in 5% CO_2. To quantify IL-2 producing $CD4^+$ T cells, cells were stimulated with anti-CD3 (1ug/ml) and anti-CD28 (0.5 ug/ml) for 5 hrs

in the presence of GolgiStop at 37^0C in 5% CO_2. To enumerate the HSV-specific Th1 and Th17 cells, cells were stimulated with 2 multiplicity of UV-inactivated HSV and incubated overnight at 37^0C in 5% CO_2. GolgiStop (10mg/ml) was added for the last 5 hrs of the stimulation. At the end of stimulation period, cell surface staining was performed as described above, followed by intracellular cytokine staining using Cytofix/Cytoperm kit (BD Pharmingen) in accordance with the manufacturer's recommendations. FITC labeled IFN-γ and PE labeled IL-17 antibodies were used. After final washing cells were resuspended in 1% *para*-formaldehyde. The stained samples were acquired with a FACS Calibur (BD Biosciences) and the data were analyzed using the FlowJo software.

Quantitative PCR (QPCR). Corneal cells were lysed and total mRNA was extracted using TRIzol LS reagent (Invitrogen). Total cDNA was made with 500 ng of RNA using oligo(dT) primer. Quantitative PCR was performed using SYBR Green PCR Master Mix (Applied Biosystem, Foster City, CA) with iQ5 real-time PCR detection ssystme (Bio Rad, Hercules, CA). The expression levels of different molecules were normalized to β-actin using ΔCt calculation. Relative expression between control and experimental groups were calculated using the $2^{-\Delta\Delta Ct}$ formula. The PCR primers used were as follows

β ACTIN- For 5'-TCCGTAAAGAATCTCATGCC-3', Rev 5'-ATCTTCATCCTCCTAGGAGC-3'; IFN-Y For 5'-GGATGCATTCATGAGTATTGC-3', Rev 5'-GCTTCCTGAGGCTGGATTC-3'; IL17A For 5'-GCTCCAGAAGGCCCTCAG-3', Rev 5'- CTTTCCCTCCGCATTGACA-3'; IL6- For 5'- CGTGGAAATGAGAAAAGAGTTGTGC-3', Rev 5'-ATGCTTAGGCATAACGCACTAGGT-3' TGFβ-For 5'-

TTGCTTCAGCTCCACAGAGA-3', Rev 5'- TGGTTGTAGAGGGCAAGGAC-3'; CCL20 - For 5'-GCCTCTCGTACATACAGACGC-3', Rev5'-CCAGTTCTGCTTTGGATCAGC-3'.

ELISA. The pooled corneal samples were homogenized using a tissue homogenizer and supernatant was used for analysis. The concentrations of IL-17A and IFN-γ were measured by using sandwich ELISA kits (eBioscience) as per the manufacturer's instructions.

Statistics. Student's t test was performed to determine statistical significance and data are expressed as mean ± SEM.

Results

IL-17 is up-regulated in the cornea of mice ocularly infected with HSV-1

Total mRNA isolated from the corneas of HSV infected mice was analyzed for the relative fold changes in IL-17 mRNA expression by RT-PCR. As is evident in Figure 2.1A, the expression profile revealed that IL-17 was upregulated in a biphasic manner. During the early phase, IL-17 expression was elevated at day 2 pi, but returned to near basal levels around day 5 pi. This was followed by a subsequent upregulation of IL-17 starting from day 7 pi with a steady increase until day 21 pi (last observed time point), which corresponds to the chronic phase of the disease. In addition, quantification of IL-17 by ELISA revealed a similar pattern of expression as observed with RT-PCR (Figure 2.1B). Early after HSV-1 infection, innate cells infiltrate the cornea, and $CD4^+$ T cells start infiltrating the infected cornea around day 7p.i. (*1*). Recent studies have implicated

innate cells, particularly γδ T cells as one of the major sources of IL-17 (*21-25*). Therefore to investigate this possibility in our system, IL-17 producing γδ T cells were enumerated by intracellular cytokine staining (ICCS) after stimulation with PMA/ionomycin. Around 16% of total γδ T cells produced IL-17 (Figure 2.1C), and depletion of γδ T cells using a specific monoclonal antibody diminished the levels of IL-17 as measured by ELISA (Figure 2.1D). Collectively, these data show that IL-17 expression is upregulated in a biphasic manner following HSV infection and innate γδ T cells contribute to the early source of IL-17.

Th1 cells predominate during early stages of SK pathogenesis followed by Th17 cells in later stages.

Past studies showed that $CD4^+$ T cell infiltration of the corneal stroma becomes readily apparent by 7 day pi (*1, 7, 8*), but the relative composition of the $CD4^+$ T effectors was not recorded. Using the intracellular cytokine staining approach with cells isolated from collagen digested pooled corneas, the relative frequencies of Th17 and Th1 cells were measured in the HSV infected corneas at day 8, 15 and 21 pi. As shown in Figure 2.2A, stimulation of corneal cells with PMA and ionomycin revealed a large proportion of $CD4^+$ T cells producing either IFN-γ or IL-17 within the corneal infiltrate. However, the ratio of frequencies of Th1 to Th17 were higher at all tested time point pi. Additionally, Th1 cells showed an initial increase at day 15 over day 8 pi followed by reduced frequencies at day 21 pi. In contrast to Th1 cells, Th17 cells were scarcely detectable on day 8 pi and this was followed by a gradual increase in their frequency with the progression of SK (Figure 2.2A). The total cell numbers for each population revealed

similar kinetics (Figure 2.2B, middle column). Furthermore, intracellular staining of corneal cells stimulated with UV inactivated viral antigen preparation revealed a high percentage (≤ 24.4 %) HSV specific Th1 cells as compared to a lower percentage (≤ 0.35 %) of HSV specific Th17 cells (Figure 2.2A right column). In addition, analysis of local draining lymph nodes (DLN) for Th1 and Th17 cells, revealed a similar pattern as observed for the cornea (Figure 2.2 C, D). These results indicate Th1 cells initially infiltrate the site of infection followed by the increased infiltration of Th17 cells during late stages of SK.

Local cytokine/chemokine directs delayed entry and/or differentiation of Th17 cells in the cornea.

The delayed migration of Th17 cells in the cornea could be the result of the early conditions suppressing Th17 cells or conditions such as local cytokine and chemokine milieu favoring Th17 cell generation and/or migration during later stages of SK. To further investigate this issue, studies were carried out for the corneal quantification of different cytokines as well as chemokines, particularly those that are involved in the generation, migration and suppression of Th17 cell responses. Since Th17 cells differentiate from naïve $CD4^+$ T cell in the presence of IL-6 and TGF-β with antigenic stimulation (*26-28*), we quantified the relative fold change of IL-6 and TGF-β at various days pi as compared to mock infected cornea (Figure 2.3 A and 2.3 B). The results showed relatively low levels of IL-6 at day 8 pi followed by a peak at day 15 pi. (Figure 2.3A). TGF-β levels were upregulated from day 8 pi and, peaked at day 15 pi. As compared to day 15 pi, both IL-6 and TGF-β levels were reduced by day 21 pi.

Furthermore, quantification of CCL20 a known ligand for CCR6, which is preferentially, expressed by homeostatically proliferating Th17 cells as well as Treg cells (*29, 30*), was significantly expressed only after day 15 pi (Figure 2.3C). Furthermore, since a recent study has shown the suppressive role of IL-2 in the generation of Th17 cells (*31*), we quantified CD4 T cells producing IL-2 in the local DLN and spleen by ICCS assay. As shown in Figure 2.3D-E, IL-2 producing $CD4^+$ T cells were significantly higher in frequency as well as numbers at day 8 pi followed by a reduction at day 15 and day 21 pi. This early and robust IL-2 production by $CD4^+$ T cells could be responsible for the promotion of Th1 as well as the suppression of Th17 responses in lymphoid organs early after HSV infection. However, during the progression of SK, increased IL-6, TGF-β as well as chemokine CCL20 expression in the cornea could be responsible for either generation or migration of Th17 cells during the later stages of SK.

The Dual Role of IFN-γ in HSV induced immunopathology

Since, IFN- γ suppresses the induction and expansion of Th17 cells (*17, 32-34*), we investigated the role of IFN-γ in relation to IL-17 as well as Th-17 cells. Similar to IL-17, IFN-γ showed biphasic upregulation. However, the second peak expression was observed around day 7 pi followed by a steady decline with the progression of SK (Figure 2.4A). Measurement of IFN-γ cytokine by ELISA revealed similar kinetics of expression as observed with QPCR analysis (Figure 2.4B). To demonstrate the role of IFN-γ in SK, IFN-γ depletion was carried out from day -1 followed by depletion on day 2 and day 5. The severity of SK lesions was scored on day 8 and day 11. As shown in figure 2.4C, early depletion of IFN-γ significantly increased the severity of SK on day 8.

However, on day 11 it reached that of isotype antibody treated control mice group. Furthermore, all mice from IFN- γ depleted group showed signs of severe encephalitis, which necessitated termination of experiments. In contrast, depletion of the second peak of IFN-γ during later stages of SK (on day 7, 10 and 13) showed significantly diminished SK lesion severity on day 11 and day 15 pi (Figure 2.4D). The analysis of various cell types from the corneas showed reduced frequencies of total $CD4^+$ T cells, the Th1 subset, but increased percentage of the Th17 subset (Figure 2.4E-F). However, the total numbers of total $CD4^+$ T cells, Th1 and Th17 cells were reduced in IFN-γ depleted mice as compared to isotype treated antibody treated mice. These results demonstrate an early protective role of IFN-γ likely acting by controlling virus replication in cornea. However, IFN-γ exerts a pathologic role once virus is cleared from the cornea as occurs during the later stages of SK. Taken together, our data indicates that Th1 cells are the initial main orchestrators of SK lesions followed later on in the chronic phase by the contribution of both Th1 and Th17 cells. Early infiltration of Th1 cells initiates the inflammatory condition particularly cytokines and chemokine environment that promotes generation and/or migration of highly pathogenic Th17 cells. This late migration of Th17 cells maintains the SK pathology via their secretion of IL-17, which acts as a pro-inflammatory cytokine through various mechanisms.

IL-17 neutralization diminishes SK lesion severity.

To further investigate the role of IL-17 in SK pathogenesis, the effects of neutralizing IL-17 with monoclonal Ab was studied over a 15 day observation period. Intraperitoneal Treatment was began on 1 day before infection followed by injections on

day 2 and day 5 pi. The early neutralization of IL-17 reduced the SK lesion severity on day 11 pi (Fig 2.5A). To further confirm the role of IL-17 during later stages of SK, IL-17 neutralization was started from day 7 pi when SK lesions become evident, followed by depletion on day 10 and 13 pi. This therapeutic neutralization of IL-17 also reduced the severity of SK lesions further confirming the pathogenic role of IL-17 during the later stages of SK (Fig 2.5B). In addition, therapeutic local depletion of IL-17 by subconjunctival administration of anti-IL-17 antibody also resulted in significantly diminished SK lesion scores (Fig 2.5C). Examination of corneal sections by histopathological analysis revealed reduced inflammatory response in the IL-17 depleted corneas, with less fibrosis of corneal stroma, no or minimal hypertrophy of epithelial layers as well as diminished infiltration of leukocytes, particularly neutrophils (Fig 2.5D). Moreover, the frequencies as well as total numbers of $CD4^+$ T cells, Th1 and Th17 cells were also reduced in the anti-IL-17 treated group (Fig 2.5E-F). The reduced numbers of Th1 cells could be the result of reduced infiltration of neutrophils, which may act as a source of CXC chemokines essential for Th1 infiltration (*35*). Taken together, these data indicated the pathogenic role of IL-17 during early as well as late phases of SK.

IL-17R KO mice show reduced SK lesion severity.

To further confirm the role of IL-17 in SK pathogenesis, mice lacking IL-17 receptor signaling were ocularly infected with HSV and SK lesion severity was monitored and compared with WT mice. The disease severity differed significantly at all tested time point pi between WT and IL-17R KO mice (Fig 2.6A). The onset of SK was delayed and SK lesions were less severe in IL-17R KO, as compared to their WT

counterparts. The severity of SK lesions (scores of ≥3) was reduced in mice in the IL-17R KO group (3 of 8 eyes at day 21) compared to WT counterparts (7 of 8 eyes at day 21) (Fig 2.6A right panel). Furthermore, histopathological analysis of WT corneas at day 15 pi showed loss of the corneal epithelial layer, extensive stromal fibrosis, infiltration of large number of leukocytes in the stromal layers with the resultant thickening of corneal stroma (Fig 2.6B, upper panels). In contrast to WT corneas, section from IL-17R KO corneas showed no damage to the epithelial layer with minimal fibrosis as well as infiltration by inflammatory leukocytes at day 15 pi (Fig 2.6B lower panels). Moreover, immunofluorescence staining of corneal sections for $CD4^+$ T cells at day 15 pi showed diminished infiltration of $CD4^+$ T cells in IL-17R KO mice as compared to WT mice (Figure 2.6C). To further quantify the different cell types infiltrating the cornea, experiments were terminated on day 15 to study cellular parameters. As shown, the frequencies (Fig 2.6D-F) and absolute numbers (Fig 2.6G) of total $CD4^+$ T cells, Th1 and Th17 cells were decreased in the IL-17R KO compared to WT mice. Additionally, the expression of pro-inflammatory cytokines such as IL-6, IL-17, IL-1β were diminished in IL-17R KO mice corneas as compared to the WT samples (data not shown). Analysis of DLN and spleen of WT and IL-17R KO, mice showed reduced frequencies, but not total cell numbers of each population (Fig 2.7). As shown in Figure 7A-D, the frequencies of Th1 and Th17 cells showed two fold reduction in DLNs and spleen from IL-17R KO mice as compared to WT mice. However, the total numbers of each subpopulation were equal in both IL-17R KO and WT mice DLNs and spleen (Fig 2.7E and F). These observations revealed that although, the total cell numbers were equal in DLNs and spleens from IL-17R KO and WT mice, the frequencies and total cell numbers were

reduced at the inflammatory site (cornea) in IL-17R KO mice as compared to WT counterparts. Taken together, these results indicated the pro-inflammatory role of IL-17 in SK pathogenesis

Discussion

In this study we show that HSV infection of the cornea leads to a biphasic increase in corneal expression of IL-17. Moreover, the subsequent HSV induced SK immunopathology is the outcome of the effector functions mediated by both Th1 and Th17 cells. The pro-inflammatory cytokine IL-17 drives initial as well as late events in SK pathogenesis and also contributes significantly to the pathology of SK. However, the sources of IL-17 during early and late stages of SK were different. Initially, innate cells such as γδ T cells were the main producers and later on in the chronic phase Th17 cells were the producers. Additionally, IFN-γ was shown important for the early protection from HSV infection, but cells producing IFN-γ also contributes to the pathology once the virus is absent. Furthermore, HSV induced immunopathological lesions involve both Th1 and Th17 cells with their respective importance changing with time. Accordingly, in line with previous published reports, our data demonstrates that Th1 cells mainly initiate and orchestrate SK lesions at least during the early stages followed by the entry of Th17 cells when the disease is at peak. Interestingly, significant proportion of Th1 cells secreted IFN- γ upon stimulation with UV inactivated HSV virus, but most Th17 cells failed to produce IL-17 under similar conditions, indicating that Th17 cells could be

involved in a bystander fashion in SK pathogenesis. Furthermore, depletion of IL-17 during both early as well as during the chronic phase of SK pathogenesis and infection of IL-17R KO mice showed reduced SK lesion severity. The findings indicate an important role for IL-17 at all stages of SK pathogenesis. Accordingly targeting IL-17 production represents a logical target to control SK, an important cause of human blindness.

Innate cells such as γδ T cells act as one of the major early sources of IL-17, as shown in some other systems (*21-25*). Thus our data is in line with the previously published reports where γδ T cells were shown to be main source of innate IL-17 (*21-25*). IL-17 orchestrates the local inflammatory response by stimulating epithelial, endothelial and fibroblastic cells to produce and release various inflammatory cytokines (*12, 36-39*). Furthermore, IL-17 drives increased influx, as well as survival, of neutrophils at the site of inflammation by the induction of neutrophil chemoattracts, as well as GM-CSF mediated granulopoeisis (*12, 39-41*). In ocular HSV infection, an initial influx of neutrophils plays an important role in virus clearance (*42*). The diminished expression of neutrophil chemoattractants for neutrophils and subsequent reduced infiltration of neutrophils occurs in IL-17R KO mice post HSV infection (*17*). Similarly, we found a reduced infiltration of neutrophils in HSV infected IL-17R KO mice as well as post IL-17 neutralization during early as well as during late stages of SK pathogenesis (data not shown). Taken together, the data show that during HSV infection of the cornea, IL-17 contributes to the early innate cell response by promoting the migration of neutrophils.

Recent work has discovered a critical role of Th17 cells in various chronic and autoimmune inflammatory conditions (*33, 34, 43-45*), and our data show that Th17 cells do participate in SK pathogenesis. However, in contrast to autoimmune as well as some

chronic inflammatory conditions, where Th17 cells may play a dominant role, HSV induced immunopathology results from the participation of both Th1 and Th17 cells with the relative importance changing as disease progresses. Accordingly, our data from IFN-γ and IL-17 neutralization as well as IL-17R KO mice shows that both Th1 and Th17 mediated immune response contributes to SK pathogenesis. Th1 cells were the first to infiltrate the cornea, and significant proportions of them were HSV-specific. They set the stage for the development of complex SK lesions that additionally involves Th7 cells. However, the Th17 cells could migrate only after the entry of Th1 cells, indicating their role in the later stages of SK. Our data accord with a recent study showing that only Th1 cells could gain entry in the non-inflamed tissue and initiate inflammatory response followed by entry of Th17 cells in the inflamed CNS (*46*). Furthermore, almost none of the Th17 cells responded to HSV specific antigen when stimulated ex-vivo which may indicate their bystander role in SK pathogenesis. However, diminished SK severity in the absence of IL-17 receptor signaling, as well as post IL-17 neutralization during early as well as late stages of SK, indicated that IL-17 does play a pro-inflammatory role in SK pathogenesis.

Although, presently we cannot detect the antigen specificity of these Th17 cells, they could be reactive against yet unidentified unmasked self-corneal antigens or be functioning in a bystander fashion. A recent study on an autoimmune condition of the retina using experimental autoimmune uveitis model, showed that both the retinal antigen specific Th1 and Th17 cells could drive autoimmunity depending upon the local conditions at the time of antigen exposure as well as type of T effector cell present (*47*). However, our data show that during viral immunopathology, higher levels of IFN-γ occur

early after HSV infection could promote Th1 and suppress Th17 immune responses. During autoimmune conditions exposure of self-unmasked antigens occur that provides constant stimulation to the T effector cells at the site of inflammation (*48*). The body might sense this chronic persistence of antigen as the need arises for stronger and more pathogenic immune response for the removal of such persistent antigen. The highly pathogenic nature of IL-17 and or Th17 cells meets this criterion and might be the outcome of such persistent antigenic stimulation as observed in many autoimmune conditions. However, during acute infections, effective Th1 and Th2 responses could clear the antigen from the site of infection, avoiding the Th17 mediated immunopathology. In contrast, chronic persistence of antigen could be sensed by the body, with a resultant robust T effector response such as a Th17 cell mediated immune response, which can cause damage and subsequent immunopathology. SK, being a chronic disorder could mimic this condition, where initial acute viral infection is controlled by the Th1 cell response that initiates inflammatory milieu in the cornea. This initial damage to the corneal tissue could uncover self-antigens that help drive the subsequent Th17 mediated highly inflammatory reaction. Alternatively, one recent study showed that Th17 cells can be activated in the context of the local microenvironment and could cause tissue specific damage in an antigen non-specific way that depended upon the presence of IL-6 (*49*). Thus, it might be possible that these Th17 cells during late stages of SK could be non-specific to the corneal Ag and acting in a bystander fashion stimulated in the presence of the complex inflammatory cytokine milieu. However, this issue needs to be addressed further using adoptive transfer of non-specific Th17 cells in

the context of HSV induced SK immunopathology. Such studies are currently undergoing in our laboratory.

Our data also demonstrates a dual role of IFN-γ during HSV mediated immunopathology. Innate cells contribute to the early source of IFN-γ after HSV infection and Th1 cells from day 7 pi (*1, 50*). Thus, IFN-γ neutralization during the pre-clinical phase when replication virus is still present in cornea (1), lead to the transient increased tissue damage presumably driven by virus. Furthermore, this early depletion caused severe encephalitis, possibly an effect of higher viral titers indicating the early protective role of IFN-γ as previously documented (*1, 49, 51*). Interestingly, neutralization of IFN-γ after day 7 pi resulted in significantly reduced SK severity indicating a crucial role of IFN-γ and/or Th1 cells as the initiators and main orchestrators of early immunopathological lesions of SK. Since, IL-2 and IFN-γ suppresses Th17 response (*17, 31-34*), conceivably during HSV induced immunopathology higher levels of IFN-γ in the cornea could be suppressing the early development of Th17 responses. Furthermore the chronic inflammatory situation in the cornea might be creating appropriate conditions for the generation and or migration of Th17 cells. Naïve $CD4^+$ T cells differentiate into Th17 cells under appropriate antigenic stimulation in the presence of IL-6 and TGF-β (*26-28*). Furthermore, Th17 cells express the chemokine receptor, CCR6, and migrate to the site of inflammation through the specific chemokine, CCL20 (*29, 30*). Indeed, our data for the expression levels of IL-6, TGF-β and CCL20 indicated that conditions favored either migration and/or generation of Th17 cells occur only during the very late stage of SK pathogenesis. This might explain the delayed appearance of Th17 cells in the cornea.

Taken together, our results demonstrate the relative contribution of IL-17/Th17 and IFN-γ/Th1 cells in the pathogenesis of SK. Both cell types participate in the pathogenesis of SK depending on the stage of SK. The demonstration of the pathogenic role of IL-17/Th17 cells in later stages of SK is a novel finding and could have implication for future therapeutic intervention for HSV induced immunopathology, an important cause of infectious human blindness.

LIST OF REFERENCES

1. Biswas, P. S., and Rouse, B. T. (2005) Early events in HSV keratitis--setting the stage for a blinding disease, *Microbes Infect 7*, 799-810.
2. Streilein, J. W., Dana, M. R., and Ksander, B. R. (1997) Immunity causing blindness: five different paths to herpes stromal keratitis, *Immunol Today 18*, 443-449.
3. Metcalf, J. F., Hamilton, D. S., and Reichert, R. W. (1979) Herpetic keratitis in athymic (nude) mice, *Infect Immun 26*, 1164-1171.
4. Russell, R. G., Nasisse, M. P., Larsen, H. S., and Rouse, B. T. (1984) Role of T-lymphocytes in the pathogenesis of herpetic stromal keratitis, *Invest Ophthalmol Vis Sci 25*, 938-944.
5. Sarangi, P. S. and B. T. Rouse. 2010. Herpetic Keratitis. In ocular Disease Mechanisms and Management. L. A. Levin and D. M. Alberts, eds., eds. Saunders Elsevier, Philadelphia, PA, p. 91-97.
6. Knotts, F. B., Cook, M. L., and Stevens, J. G. (1974) Pathogenesis of Herpetic Encephalitis in Mice after Ophthalmic Inoculation, *J Infect Dis 130*, 16-27.
7. Niemialtowski, M. G., and Rouse, B. T. (1992) Predominance of Th1 cells in ocular tissues during herpetic stromal keratitis, *J Immunol 149*, 3035-3039.
8. Niemialtowski, M. G., and Rouse, B. T. (1992) Phenotypic and functional studies on ocular T cells during herpetic infections of the eye, *J Immunol 148*, 1864-1870.
9. Suryawanshi, A., Mulik, S., Sharma, S., Reddy, P. B., Sehrawat, S., and Rouse, B. T. (2011) Ocular neovascularization caused by herpes simplex virus type 1 infection results from breakdown of binding between vascular endothelial growth factor A and its soluble receptor, *J Immunol 186*, 3653-3665.

10. Rajasagi, N. K., Reddy, P. B., Suryawanshi, A., Mulik, S., Gjorstrup, P., and Rouse, B. T. (2011) Controlling herpes simplex virus-induced ocular inflammatory lesions with the lipid-derived mediator resolvin E1, *J Immunol 186*, 1735-1746.

11. Chabaud, M., Garnero, P., Dayer, J. M., Guerne, P. A., Fossiez, F., and Miossec, P. (2000) Contribution of interleukin 17 to synovium matrix destruction in rheumatoid arthritis, *Cytokine 12*, 1092-1099.

12. Fossiez, F., Djossou, O., Chomarat, P., Flores-Romo, L., Ait-Yahia, S., Maat, C., Pin, J. J., Garrone, P., Garcia, E., Saeland, S., Blanchard, D., Gaillard, C., Das Mahapatra, B., Rouvier, E., Golstein, P., Banchereau, J., and Lebecque, S. (1996) T cell interleukin-17 induces stromal cells to produce proinflammatory and hematopoietic cytokines, *J Exp Med 183*, 2593-2603.

13. Jovanovic, D. V., Martel-Pelletier, J., Di Battista, J. A., Mineau, F., Jolicoeur, F. C., Benderdour, M., and Pelletier, J. P. (2000) Stimulation of 92-kd gelatinase (matrix metalloproteinase 9) production by interleukin-17 in human monocyte/macrophages: a possible role in rheumatoid arthritis, *Arthritis Rheum 43*, 1134-1144.

14. Koenders, M. I., Kolls, J. K., Oppers-Walgreen, B., van den Bersselaar, L., Joosten, L. A., Schurr, J. R., Schwarzenberger, P., van den Berg, W. B., and Lubberts, E. (2005) Interleukin-17 receptor deficiency results in impaired synovial expression of interleukin-1 and matrix metalloproteinases 3, 9, and 13 and prevents cartilage destruction during chronic reactivated streptococcal cell wall-induced arthritis, *Arthritis Rheum 52*, 3239-3247.

15. Shalom-Barak, T., Quach, J., and Lotz, M. (1998) Interleukin-17-induced gene expression in articular chondrocytes is associated with activation of mitogen-activated protein kinases and NF-kappaB, *J Biol Chem 273*, 27467-27473.

16. Maertzdorf, J., Osterhaus, A. D., and Verjans, G. M. (2002) IL-17 expression in human herpetic stromal keratitis: modulatory effects on chemokine production by corneal fibroblasts, *J Immunol 169*, 5897-5903.

17. Molesworth-Kenyon, S. J., Yin, R., Oakes, J. E., and Lausch, R. N. (2008) IL-17 receptor signaling influences virus-induced corneal inflammation, *J Leukoc Biol 83*, 401-408.

18. Deshpande, S. P., Lee, S., Zheng, M., Song, B., Knipe, D., Kapp, J. A., and Rouse, B. T. (2001) Herpes simplex virus-induced keratitis: evaluation of the role of molecular mimicry in lesion pathogenesis, *J Virol 75*, 3077-3088.

19. Dana, M. R., Zhu, S. N., and Yamada, J. (1998) Topical modulation of interleukin-1 activity in corneal neovascularization, *Cornea 17*, 403-409.

20. Fenton, R. R., Molesworth-Kenyon, S., Oakes, J. E., and Lausch, R. N. (2002) Linkage of IL-6 with neutrophil chemoattractant expression in virus-induced ocular inflammation, *Invest Ophthalmol Vis Sci 43*, 737-743.

21. Cua, D. J., and Tato, C. M. (2010) Innate IL-17-producing cells: the sentinels of the immune system, *Nat Rev Immunol 10*, 479-489.

22. Hamada, S., Umemura, M., Shiono, T., Tanaka, K., Yahagi, A., Begum, M. D., Oshiro, K., Okamoto, Y., Watanabe, H., Kawakami, K., Roark, C., Born, W. K., O'Brien, R., Ikuta, K., Ishikawa, H., Nakae, S., Iwakura, Y., Ohta, T., and Matsuzaki, G. (2008) IL-17A produced by gammadelta T cells plays a critical role

in innate immunity against listeria monocytogenes infection in the liver, *J Immunol 181*, 3456-3463.

23. Lockhart, E., Green, A. M., and Flynn, J. L. (2006) IL-17 production is dominated by gammadelta T cells rather than CD4 T cells during Mycobacterium tuberculosis infection, *J Immunol 177*, 4662-4669.

24. Shibata, K., Yamada, H., Hara, H., Kishihara, K., and Yoshikai, Y. (2007) Resident Vdelta1+ gammadelta T cells control early infiltration of neutrophils after Escherichia coli infection via IL-17 production, *J Immunol 178*, 4466-4472.

25. Umemura, M., Yahagi, A., Hamada, S., Begum, M. D., Watanabe, H., Kawakami, K., Suda, T., Sudo, K., Nakae, S., Iwakura, Y., and Matsuzaki, G. (2007) IL-17-mediated regulation of innate and acquired immune response against pulmonary Mycobacterium bovis bacille Calmette-Guerin infection, *J Immunol 178*, 3786-3796.

26. Bettelli, E., Carrier, Y., Gao, W., Korn, T., Strom, T. B., Oukka, M., Weiner, H. L., and Kuchroo, V. K. (2006) Reciprocal developmental pathways for the generation of pathogenic effector TH17 and regulatory T cells, *Nature 441*, 235-238.

27. Mangan, P. R., Harrington, L. E., O'Quinn, D. B., Helms, W. S., Bullard, D. C., Elson, C. O., Hatton, R. D., Wahl, S. M., Schoeb, T. R., and Weaver, C. T. (2006) Transforming growth factor-beta induces development of the T(H)17 lineage, *Nature 441*, 231-234.

28. Veldhoen, M., Hocking, R. J., Atkins, C. J., Locksley, R. M., and Stockinger, B. (2006) TGFbeta in the context of an inflammatory cytokine milieu supports de novo differentiation of IL-17-producing T cells, *Immunity 24*, 179-189.

29. Hirota, K., Yoshitomi, H., Hashimoto, M., Maeda, S., Teradaira, S., Sugimoto, N., Yamaguchi, T., Nomura, T., Ito, H., Nakamura, T., Sakaguchi, N., and Sakaguchi, S. (2007) Preferential recruitment of CCR6-expressing Th17 cells to inflamed joints via CCL20 in rheumatoid arthritis and its animal model, *J Exp Med 204*, 2803-2812.

30. Yamazaki, T., Yang, X. O., Chung, Y., Fukunaga, A., Nurieva, R., Pappu, B., Martin-Orozco, N., Kang, H. S., Ma, L., Panopoulos, A. D., Craig, S., Watowich, S. S., Jetten, A. M., Tian, Q., and Dong, C. (2008) CCR6 regulates the migration of inflammatory and regulatory T cells, *J Immunol 181*, 8391-8401.

31. Laurence, A., Tato, C. M., Davidson, T. S., Kanno, Y., Chen, Z., Yao, Z., Blank, R. B., Meylan, F., Siegel, R., Hennighausen, L., Shevach, E. M., and O'Shea J, J. (2007) Interleukin-2 signaling via STAT5 constrains T helper 17 cell generation, *Immunity 26*, 371-381.

32. Cruz, A., Khader, S. A., Torrado, E., Fraga, A., Pearl, J. E., Pedrosa, J., Cooper, A. M., and Castro, A. G. (2006) Cutting edge: IFN-gamma regulates the induction and expansion of IL-17-producing CD4 T cells during mycobacterial infection, *J Immunol 177*, 1416-1420.

33. Harrington, L. E., Hatton, R. D., Mangan, P. R., Turner, H., Murphy, T. L., Murphy, K. M., and Weaver, C. T. (2005) Interleukin 17-producing CD4+

effector T cells develop via a lineage distinct from the T helper type 1 and 2 lineages, *Nat Immunol 6*, 1123-1132.

34. Park, H., Li, Z., Yang, X. O., Chang, S. H., Nurieva, R., Wang, Y. H., Wang, Y., Hood, L., Zhu, Z., Tian, Q., and Dong, C. (2005) A distinct lineage of CD4 T cells regulates tissue inflammation by producing interleukin 17, *Nat Immunol 6*, 1133-1141.

35. Scapini, P., Lapinet-Vera, J. A., Gasperini, S., Calzetti, F., Bazzoni, F., and Cassatella, M. A. (2000) The neutrophil as a cellular source of chemokines, *Immunol Rev 177*, 195-203.

36. Numasaki, M., Fukushi, J., Ono, M., Narula, S. K., Zavodny, P. J., Kudo, T., Robbins, P. D., Tahara, H., and Lotze, M. T. (2003) Interleukin-17 promotes angiogenesis and tumor growth, *Blood 101*, 2620-2627.

37. Pickens, S. R., Volin, M. V., Mandelin, A. M., 2nd, Kolls, J. K., Pope, R. M., and Shahrara, S. (2010) IL-17 contributes to angiogenesis in rheumatoid arthritis, *J Immunol 184*, 3233-3241.

38. Yao, Z., Painter, S. L., Fanslow, W. C., Ulrich, D., Macduff, B. M., Spriggs, M. K., and Armitage, R. J. (1995) Human IL-17: a novel cytokine derived from T cells, *J Immunol 155*, 5483-5486.

39. Shen, F., and Gaffen, S. L. (2008) Structure-function relationships in the IL-17 receptor: implications for signal transduction and therapy, *Cytokine 41*, 92-104.

40. Laan, M., Cui, Z. H., Hoshino, H., Lotvall, J., Sjostrand, M., Gruenert, D. C., Skoogh, B. E., and Linden, A. (1999) Neutrophil recruitment by human IL-17 via C-X-C chemokine release in the airways, *J Immunol 162*, 2347-2352.

41. Laan, M., Prause, O., Miyamoto, M., Sjostrand, M., Hytonen, A. M., Kaneko, T., Lotvall, J., and Linden, A. (2003) A role of GM-CSF in the accumulation of neutrophils in the airways caused by IL-17 and TNF-alpha, *Eur Respir J 21*, 387-393.

42. Tumpey, T. M., Chen, S. H., Oakes, J. E., and Lausch, R. N. (1996) Neutrophil-mediated suppression of virus replication after herpes simplex virus type 1 infection of the murine cornea, *J Virol 70*, 898-904.

43. Bettelli, E., Oukka, M., and Kuchroo, V. K. (2007) T(H)-17 cells in the circle of immunity and autoimmunity, *Nat Immunol 8*, 345-350.

44. Koenders, M. I., Lubberts, E., Oppers-Walgreen, B., van den Bersselaar, L., Helsen, M. M., Kolls, J. K., Joosten, L. A., and van den Berg, W. B. (2005) Induction of cartilage damage by overexpression of T cell interleukin-17A in experimental arthritis in mice deficient in interleukin-1, *Arthritis Rheum 52*, 975-983.

45. Langrish, C. L., Chen, Y., Blumenschein, W. M., Mattson, J., Basham, B., Sedgwick, J. D., McClanahan, T., Kastelein, R. A., and Cua, D. J. (2005) IL-23 drives a pathogenic T cell population that induces autoimmune inflammation, *J Exp Med 201*, 233-240.

46. O'Connor, R. A., Prendergast, C. T., Sabatos, C. A., Lau, C. W., Leech, M. D., Wraith, D. C., and Anderton, S. M. (2008) Cutting edge: Th1 cells facilitate the entry of Th17 cells to the central nervous system during experimental autoimmune encephalomyelitis, *J Immunol 181*, 3750-3754.

47. Luger, D., Silver, P. B., Tang, J., Cua, D., Chen, Z., Iwakura, Y., Bowman, E. P., Sgambellone, N. M., Chan, C. C., and Caspi, R. R. (2008) Either a Th17 or a Th1 effector response can drive autoimmunity: conditions of disease induction affect dominant effector category, *J Exp Med 205*, 799-810.

48. Steinman, L. (2007) A brief history of T(H)17, the first major revision in the T(H)1/T(H)2 hypothesis of T cell-mediated tissue damage, *Nat Med 13*, 139-145.

49. Siffrin, V., Radbruch, H., Glumm, R., Niesner, R., Paterka, M., Herz, J., Leuenberger, T., Lehmann, S. M., Luenstedt, S., Rinnenthal, J. L., Laube, G., Luche, H., Lehnardt, S., Fehling, H. J., Griesbeck, O., and Zipp, F. (2010) In vivo imaging of partially reversible th17 cell-induced neuronal dysfunction in the course of encephalomyelitis, *Immunity 33*, 424-436.

50. Yu, Z., Manickan, E., and Rouse, B. T. (1996) Role of interferon-gamma in immunity to herpes simplex virus, *J Leukoc Biol 60*, 528-532.

51. Bouley, D. M., Kanangat, S., Wire, W., and Rouse, B. T. (1995) Characterization of herpes simplex virus type-1 infection and herpetic stromal keratitis development in IFN-gamma knockout mice, *J Immunol 155*, 3964-3971.

APPENDIX

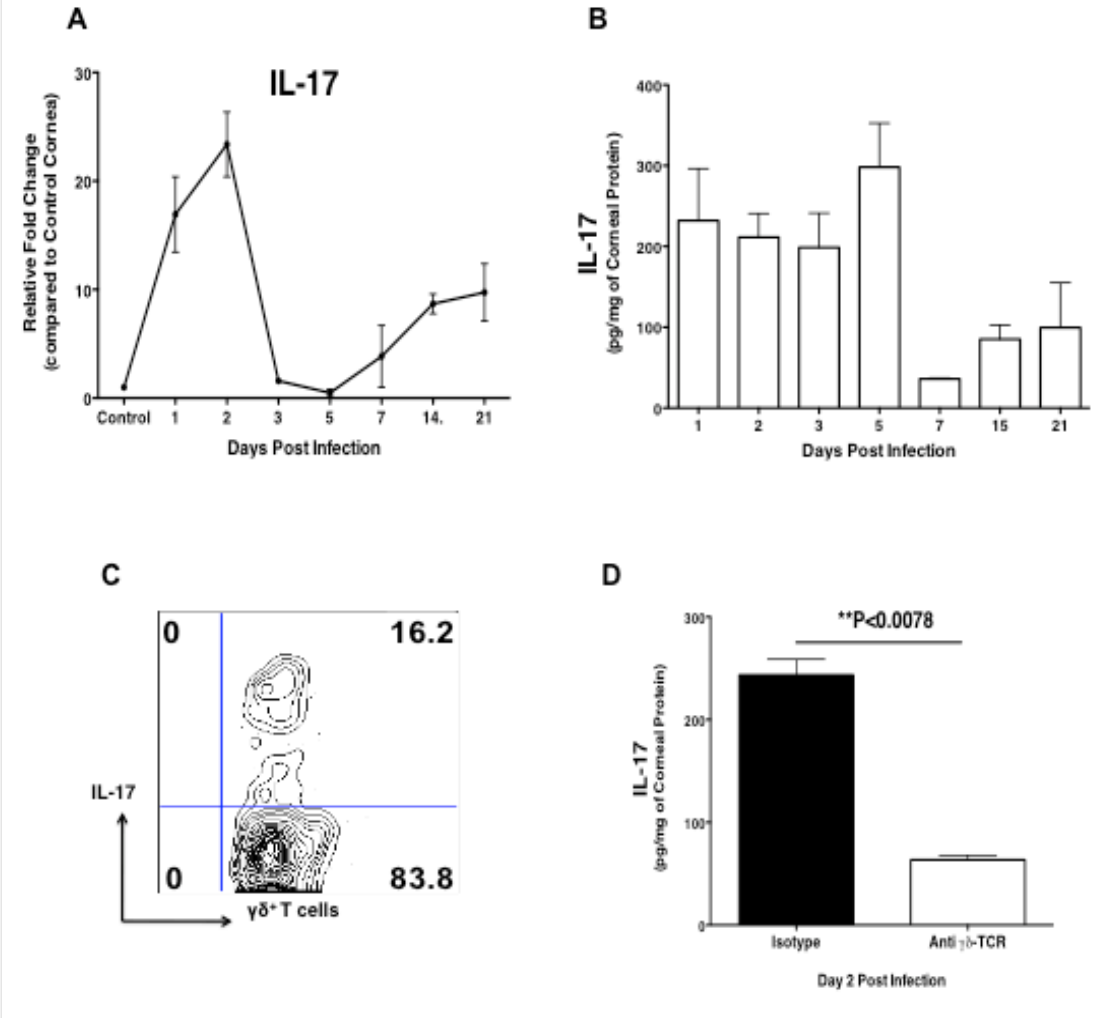
A
IL-17
Relative Fold Change (compared to Control Cornea)
30
20
10
0
Control
1
2
3
5
7
14.
21
Days Post Infection
B
IL-17 (pg/mg of Corneal Protein)
400
300
200
100
0
1
2
3
5
7
15
21
Days Post Infection
C
0
16.2
0
83.8
IL-17
γδ+ T cells
D
**P<0.0078
IL-17 (pg/mg of Corneal Protein)
300
200
100
0
Isotype
Anti γδ-TCR
Day 2 Post Infection

FIGURE 2.1. IL-17 EXPRESSION IS UPREGULATED IN THE HSV INFECTED CORNEA AND INNATE CELLS CONTRIBUTE TO THE EARLY SOURCE OF IL-17.

C57BL/6 mice were ocularly infected with 1X 10^4 PFU of HSV. Control mice were mock infected with PBS. At each time point 6 corneas were collected and pooled for measurement of IL-17 levels by RT-PCR, ELISA or ICCS assay. (A-B) The kinetic analysis for the expression of IL-17 in the HSV infected cornea as determined by RT-PCR (A) and ELISA (B). The expression levels of IL-17 by RT-PCR at various time points were quantified relative to β-actin using $\Delta\Delta C_T$ method. (C) On day 2 pi, corneas were collected and analyzed by ICCS assay for the production of IL-17 by γδ T cells. Cells were stimulated with PMA/Ionomycin for 4 hrs in the presence of Brefeldin A. (D) The IL-17 levels at day 2 pi in γδ T cell depleted C57BL/6 mice as determined by ELISA. Animals in the control group received isotype antibody. Data are shown for one representative experiment out of two with 6 to 8 mice at each indicated time point pi. Statistical levels of significance were analyzed by Student's t test. Error bars ar

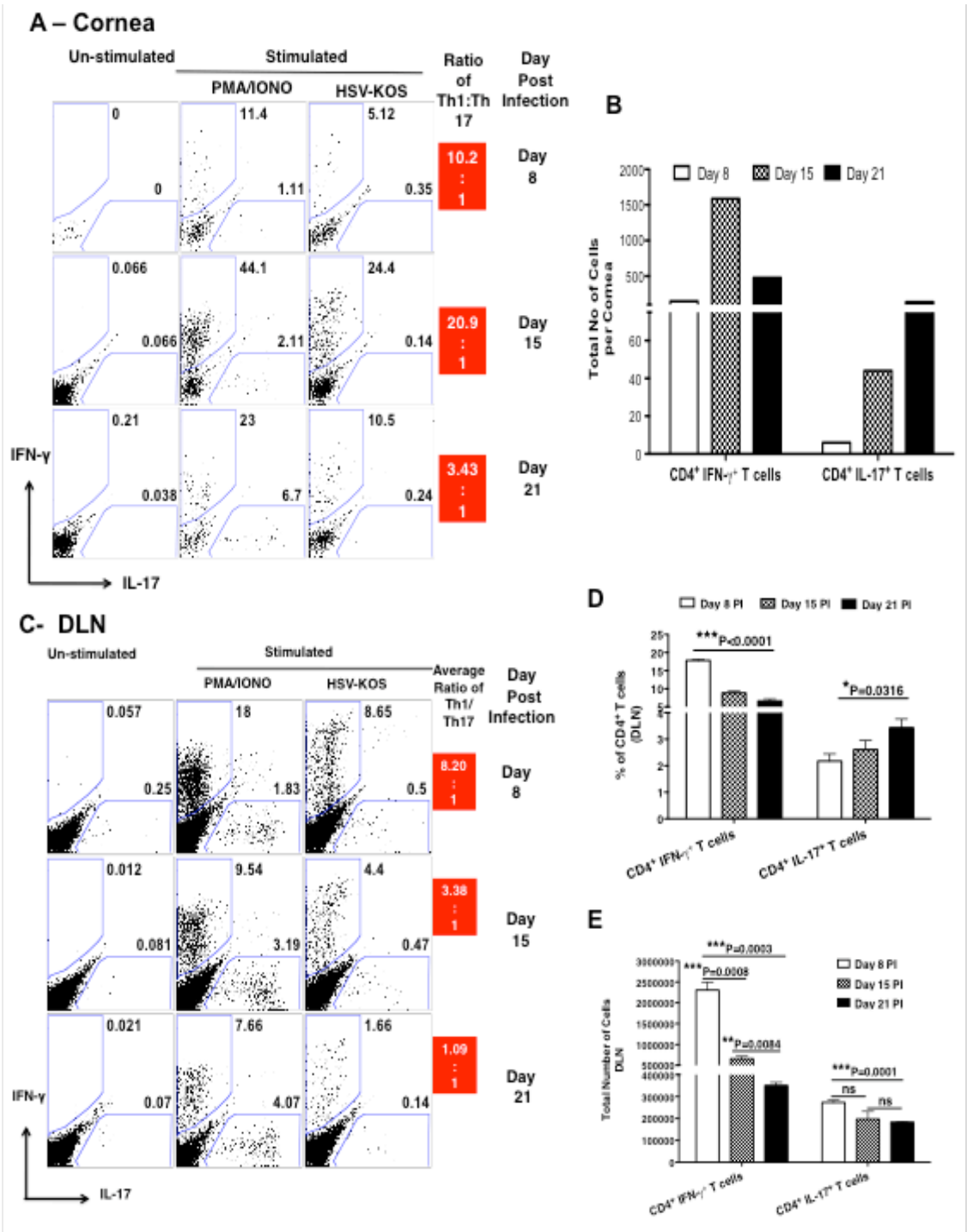
A – Cornea
Un-stimulated
Stimulated
PMA/IONO
HSV-KOS
Ratio of Th1:Th 17
Day Post Infection
0
11.4
5.12
10.2 : 1
Day 8
0
1.11
0.35
0.066
44.1
24.4
20.9 : 1
Day 15
0.066
2.11
0.14
0.21
23
10.5
3.43 : 1
Day 21
0.038
6.7
0.24
IFN-γ
IL-17
B
Day 8
Day 15
Day 21
Total No of Cells per Cornea
2000
1500
1000
500
60
40
20
0
CD4+ IFN-γ+ T cells
CD4+ IL-17+ T cells
C- DLN
Un-stimulated
Stimulated
PMA/IONO
HSV-KOS
Average Ratio of Th1/ Th17
Day Post Infection
0.057
18
8.65
8.20 : 1
Day 8
0.25
1.83
0.5
0.012
9.54
4.4
3.38 : 1
Day 15
0.081
3.19
0.47
0.021
7.66
1.66
1.09 : 1
Day 21
0.07
4.07
0.14
IFN-γ
IL-17
D
Day 8 PI
Day 15 PI
Day 21 PI
***P<0.0001
*P=0.0316
% of CD4+ T cells (DLN)
25
20
15
10
5
4
3
2
1
0
CD4+ IFN-γ+ T cells
CD4+ IL-17+ T cells
E
***P=0.0003
***P=0.0008
**P=0.0084
***P=0.0001
ns
ns
Day 8 PI
Day 15 PI
Day 21 PI
Total Number of Cells DLN
3000000
2500000
2000000
1500000
1000000
500000
400000
300000
200000
100000
0
CD4+ IFN-γ+ T cells
CD4+ IL-17+ T cells

FIGURE 2.2. KINETIC ANALYSIS OF TH1 AND TH17 CELLS IN THE CORNEA AND DLN OF HSV INFECTED MICE.

C57BL/6 mice were ocularly infected with 1X 10^4 PFU of HSV and each time point 6 to 8 corneas were collected, pooled and liberase digested. The corneal single cell suspensions were analyzed for the CD4+ T cell expression of IL-17 and IFN-γ by ICCS assay. (A) Representative FACS plots for the corneal Th1 and Th17 cells at each time point pi. The cells were either un-stimulated (left column) or stimulated with PMA/Ionomycin for 4 hrs (middle column) in the presence of Brefeldin A. For quantification of Ag-specific $CD4^+$ T cells (right panel), cells were stimulated for 16 hrs with UV-inactivated HSV-KOS, with the addition of Brefeldin A for last 5 hrs of stimulation. FACS plots shown are gated on $CD4^+$ T cells. The ratio shown on the right side is a comparison of PMA/Ionomycin stimulated Th1 to Th17 cells on respective day pi. (B) Total number Th1 and Th17 cells per cornea at day 8, 15 and 21 pi by ICCS assay post stimulation with PMA/Ionomycin. (C) Representative FACS plot for Th1 and Th17 cells from the local DLN of HSV infected mice at day 8, 15 and 21 pi. The cells were either un-stimulated or stimulated with PMA/Ionomycin for 4 hrs or with UV-HSV-KOS for 16 hrs. (D) Frequencies and total numbers (E) of Th1 and Th17 cells from DLN at day 8, 15 and 21 pi as determined by ICCS assay post stimulation with PMA/Ionomycin. Data are shown for one representative experiment out of two with 6 to 8 mice at each indicated time point pi. Statistical levels of significance were analyzed by Student's t test. Error bars are SEM.

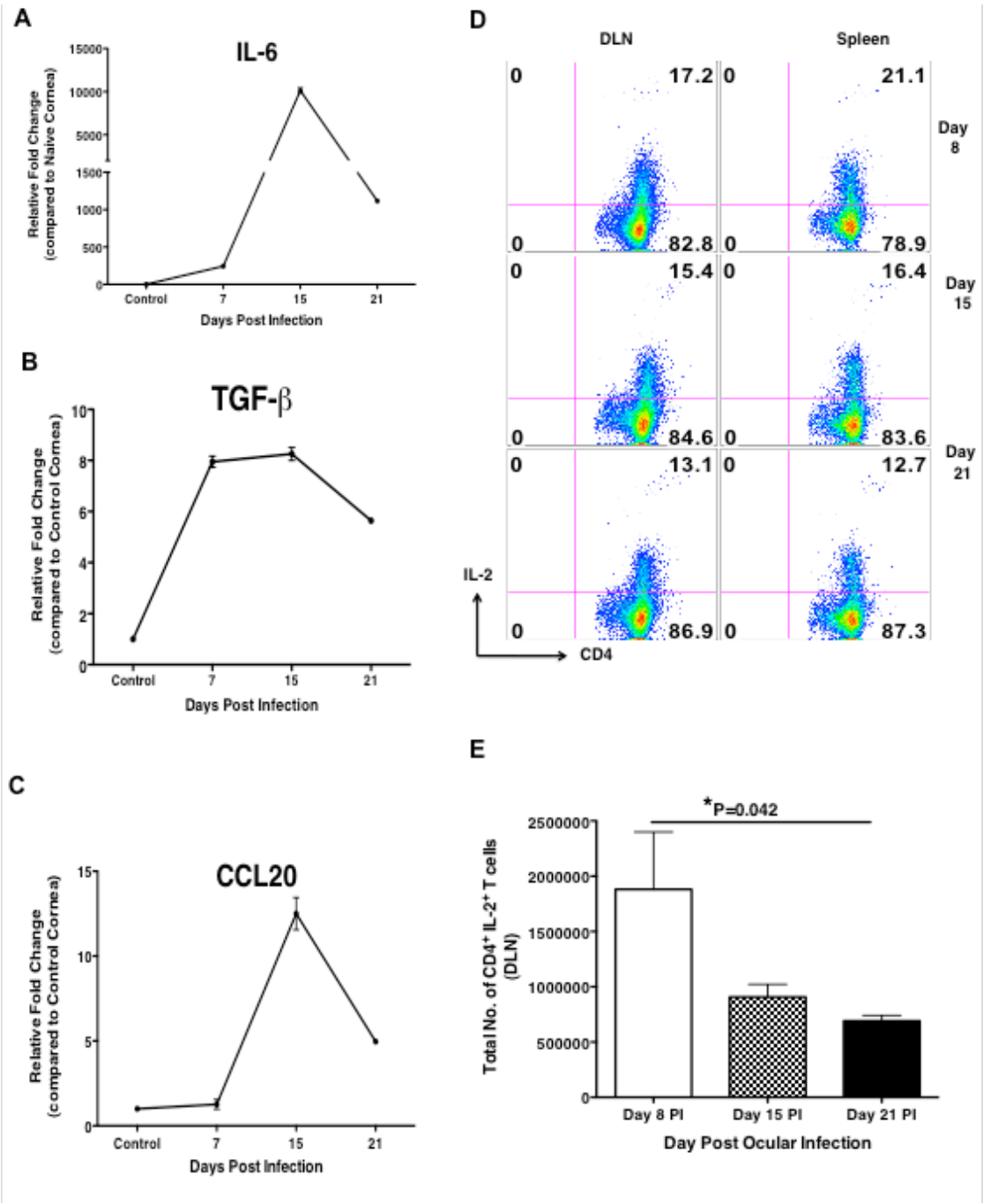
A
IL-6
Relative Fold Change (compared to Naive Cornea)
15000
10000
5000
1500
1000
500
0
Control
7
15
21
Days Post Infection
B
TGF-β
Relative Fold Change (compared to Control Cornea)
10
8
6
4
2
0
Control
7
15
21
Days Post Infection
C
CCL20
Relative Fold Change (compared to Control Cornea)
15
10
5
0
Control
7
15
21
Days Post Infection
D
DLN
Spleen
0
17.2
0
21.1
Day 8
0
82.8
0
78.9
0
15.4
0
16.4
Day 15
0
84.6
0
83.6
0
13.1
0
12.7
Day 21
0
86.9
0
87.3
IL-2
CD4
E
*P=0.042
Total No. of CD4+ IL-2+ T cells (DLN)
2500000
2000000
1500000
1000000
500000
0
Day 8 PI
Day 15 PI
Day 21 PI
Day Post Ocular Infection

FIGURE 2.3. DELAYED EXPRESSION OF IL-6, TGF-B AND CCL20 ALONG WITH REDUCED IL-2 EXPRESSION BY $CD4^+$ T CELLS DIRECTS THE DELAYED GENERATION AND/OR ENTRY OF TH17 CELLS.

C57BL/6 mice were ocularly infected with 1X 10^4 PFU of HSV. Control mice were mock infected with PBS. Mice were sacrificed on day 8, 15 and 21 pi and corneas, local DLN and spleen were collected for the analysis by RT-PCR and ICCS assay. (A-C) At each time point 6 corneas were collected and pooled for the measurement of IL-6 (A), TGF-β (B) and CCL20 (C) levels by RT-PCR. The expression levels of different molecules were quantified relative to β-actin using $\Delta\Delta C_T$ method. The IL-2 producing $CD4^+$ T cells were analyzed by ICCS assay as described in materials and methods. Representative FACS plots (D) and total cell numbers (E) for IL-2 producing $CD4^+$ T cells from the DLN and spleen at day 8, 15 and 21 day pi. Cells are gated on $CD4^+$ T cells. Data are shown for one representative experiment out of two with 6 mice at each indicated time point pi. Statistical levels of significance were analyzed by Student's t test. Error bars are SEM.

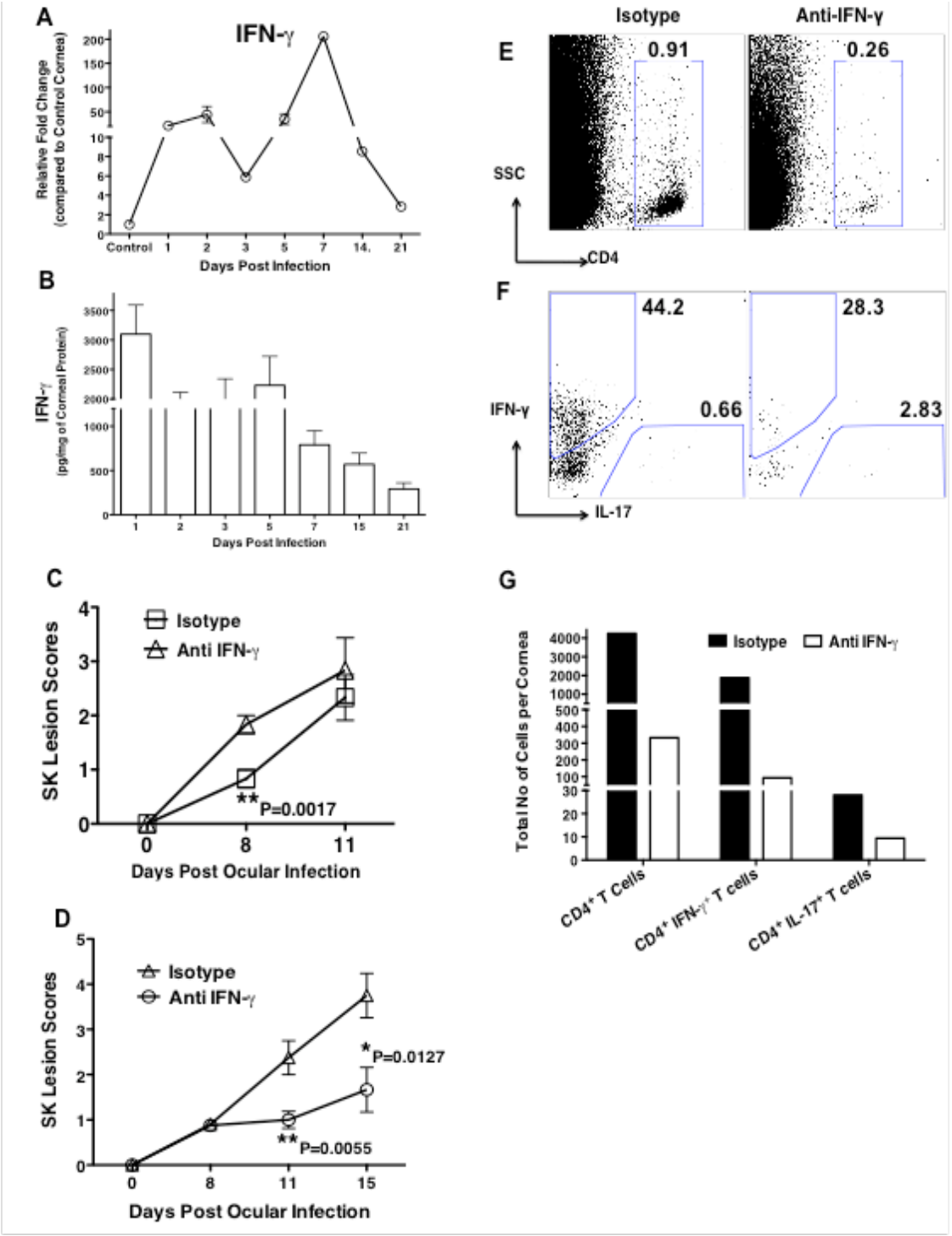
A
IFN-γ
Relative Fold Change (compared to Control Cornea)
Control 1 2 3 5 7 14. 21
Days Post Infection
B
IFN-γ (pg/mg of Corneal Protein)
Days Post Infection
C
Isotype
Anti IFN-γ
SK Lesion Scores
**P=0.0017
Days Post Ocular Infection
D
Isotype
Anti IFN-γ
SK Lesion Scores
*P=0.0127
**P=0.0055
Days Post Ocular Infection
E
Isotype
Anti-IFN-γ
0.91
0.26
SSC
CD4
F
44.2
28.3
0.66
2.83
IFN-γ
IL-17
G
Isotype
Anti IFN-γ
Total No of Cells per Cornea
CD4+ T Cells
CD4+ IFN-γ+ T cells
CD4+ IL-17+ T cells

FIGURE 2.4. EARLY PROTECTIVE AND LATE PATHOLOGIC ROLE OF IFN-Γ IN SK

C57BL/6 mice were ocularly infected with 1X 10^4 PFU of HSV. Control mice were mock infected with PBS. At each time point 6 corneas were collected and pooled for measurement of IFN- γ levels by RT-PCR, ELISA or for analysis by ICCS assay. (A-B) The kinetic analysis for the expression of IFN-γ in the HSV infected cornea as determined by RT-PCR (A) and ELISA (B). The expression levels of IFN-γ by RT-PCR at various time points were quantified relative to β-actin using $\Delta\Delta C_T$ method. (C-D) Diminished SK lesion severity in mice treated with anti-IFN- γ as compared to isotype Ab treated mice. Group of 2 to 4 mice were treated i.p. with anti-IFN- γ on either starting from day -1, followed by treatment on day 2 and day 5 pi (C); or either starting from day 7 pi followed by treatment on day 10 and 13 pi (D). Mice in control group received isotype control Ab. (E-H) Mice from experiment (D) were sacrificed on day 15 pi and corneas were collected for the analysis of different cell population by flow cytometry. Representative FACS plots for total corneal infiltrating $CD4^+$ T cells (E) and Th1 and Th17 cells after stimulation with PMA/Ionomycin (F) from isotype and anti-IFN-γ treated groups. (G) Total cell number per cornea for $CD4^+$ T cells, Th1 and Th17 cells shows reduced infiltration of cells in the cornea after IFN-γ neutralization. Data are a representative summary of two independent experiments. Statistical levels of significance were analyzed by Student's t test. Error bars are SEM.

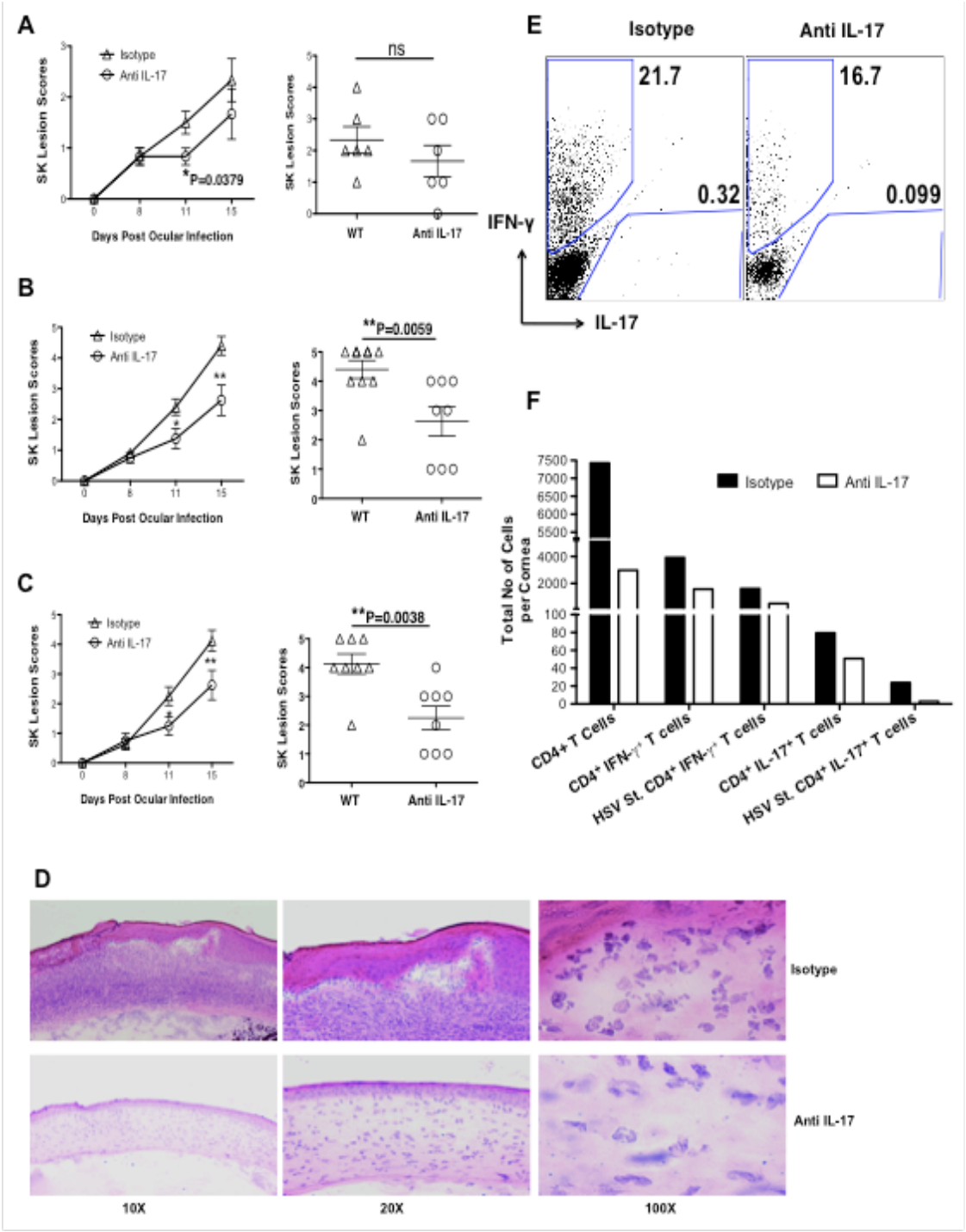
A
Isotype
Anti IL-17
SK Lesion Scores
Days Post Ocular Infection
*P=0.0379
ns
WT
Anti IL-17
B
**P=0.0059
C
**P=0.0038
D
Isotype
Anti IL-17
10X
20X
100X
E
Isotype
Anti IL-17
21.7
16.7
0.32
0.099
IFN-γ
IL-17
F
Total No of Cells per Cornea
CD4+ T Cells
CD4+ IFN-γ+ T cells
HSV St. CD4+ IFN-γ+ T cells
CD4+ IL-17+ T cells
HSV St. CD4+ IL-17+ T cells

FIGURE 2.5. IL-17 NEUTRALIZATION DIMINISHES SK LESION SEVERITY.

C57BL/6 mice ocularly infected with $1X10^4$ PFU of HSV were divided into two groups each with 6 to 8 mice. One group of mice received antibody against IL-17 and mice in control group were administered with isotype antibody. (A-C) Diminished SK lesion severity in mice treated with anti-IL-17 mAb. SK lesion score for individual cornea on day 15 pi (right) are shown. (A) Early neutralization of IL-17 was carried by i.p. injection of anti-IL-17 mAb from day -1 followed by day 2 and 5 pi. (B) Late neutralization of IL-17 was carried by i.p. injection of anti-IL-17 mAb from day 7 followed by day 10 and 13 pi. (C) Local depletion of IL-17 was carried by sub-conjunctival delivery of anti-IL-17 using same strategy as that of late depletion. (D) Representative H&E stained corneal sections of isotype treated (top panel) and IL-17 depleted (bottom panel) mice collected on day 15 pi from experiment B. The figure shows the pictures of the section taken at X 10 (left), X 20 (middle) and X 100 (right) of original magnification. (E-F) Mice from late depleted groups (as shown in B) were sacrificed on day 15 pi and corneas were harvested and pooled group wise for the analysis of various cell types (n = 6-8 per group) by flow cytometry. Representative FACS plot for total corneal infiltrating Th1 and Th17 cells (E) from isotype and anti-IL-17 treated groups. (F) Total cell number per cornea for CD 4+ T cells, Th1, Th17 cells shows reduced infiltration of cells in the cornea after IL-17 neutralization. Data are a representative summary of two independent experiments. Statistical levels of significance were analyzed by Student's t test. Error bars are SEM. Statistical levels of significance were analyzed by Student's t test. Error bars are SEM.

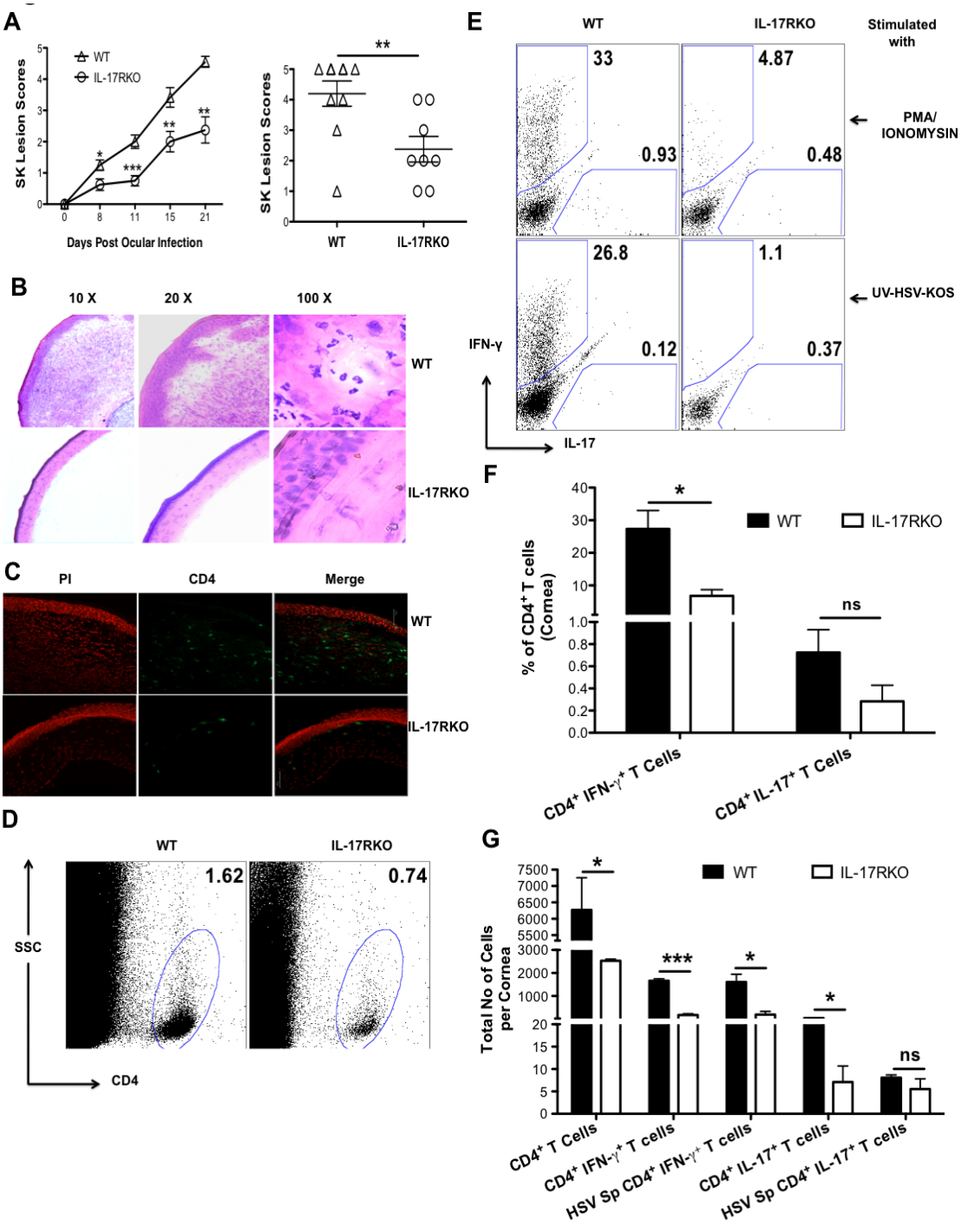
A
WT
IL-17RKO
SK Lesion Scores
Days Post Ocular Infection
SK Lesion Scores
WT
IL-17RKO
B
10 X
20 X
100 X
WT
IL-17RKO
C
PI
CD4
Merge
WT
IL-17RKO
D
WT
IL-17RKO
1.62
0.74
SSC
CD4
E
WT
IL-17RKO
Stimulated with
33
4.87
0.93
0.48
PMA/ IONOMYSIN
26.8
1.1
0.12
0.37
UV-HSV-KOS
IFN-γ
IL-17
F
% of CD4+ T cells (Cornea)
WT
IL-17RKO
ns
CD4+ IFN-γ+ T Cells
CD4+ IL-17+ T Cells
G
Total No of Cells per Cornea
WT
IL-17RKO
ns
CD4+ T Cells
CD4+ IFN-γ+ T cells
HSV Sp CD4+ IFN-γ+ T cells
CD4+ IL-17+ T cells
HSV Sp CD4+ IL-17+ T cells

FIGURE 2.6. IL-17R KO MICE ARE RESISTANT TO SK.

C57BL/6 and IL-17R KO mice were infected with $1X10^4$ PFU of HSV. (A) The disease progression kinetics and SK severity was assessed on day 8, 11, 15 and 21 pi (left panel). Right panel shows the score of individual eye on day 15 pi (B) Representative H&E stained corneal sections from WT (upper row) and IL-17R KO (lower row) mice collected on day 15 pi. The figure shows the pictures of the section taken at X 10 (left), X 20 (middle) and X 100 (right) original magnification. (C) Representative immunofluorescence micrograph of corneas for $CD4^+$ T cells (green) from WT and IL-17R KO mice on day 15 pi. The sections were counterstained with propidium iodide (red). Scale bars, 75μm. Mice were sacrificed on day 15 pi and corneas were harvested and pooled group wise for the analysis of various cell types (n = 6-8 per group). (D) Representative FACS plots for corneal infiltrating total $CD4^+$ T cells. (E) Intracellular staining was conducted to quantify Th1 and Th17 cells by stimulating them with PMA/Ionomycin (top) and HSV-KOS virus (bottom). (F) The bar diagram shows the average frequencies of Th1 and Th17 cells after stimulation with PMA/ionomycin or UV inactivated HSV-KOS from two independent experiments. (G) The bar diagram is a summary for total numbers of corneal infiltrating $CD4^+$ T cells, IFN-γ^+ $CD4^+$ T cells, HSV stimulated IFN- γ^+ $CD4^+$ T cells, IL-17^+ $CD4^+$ T cells, HSV-Stimulated IL-17^+ $CD4^+$ T cells in the corneas of WT and IL-17R KO mice. Data are shown as a summary of two independent experiments with 6 to 8 mice per group. Statistical levels of significance were analyzed by Student's t test. *< 0.05; ***< 0.001. Error bars are SEM.

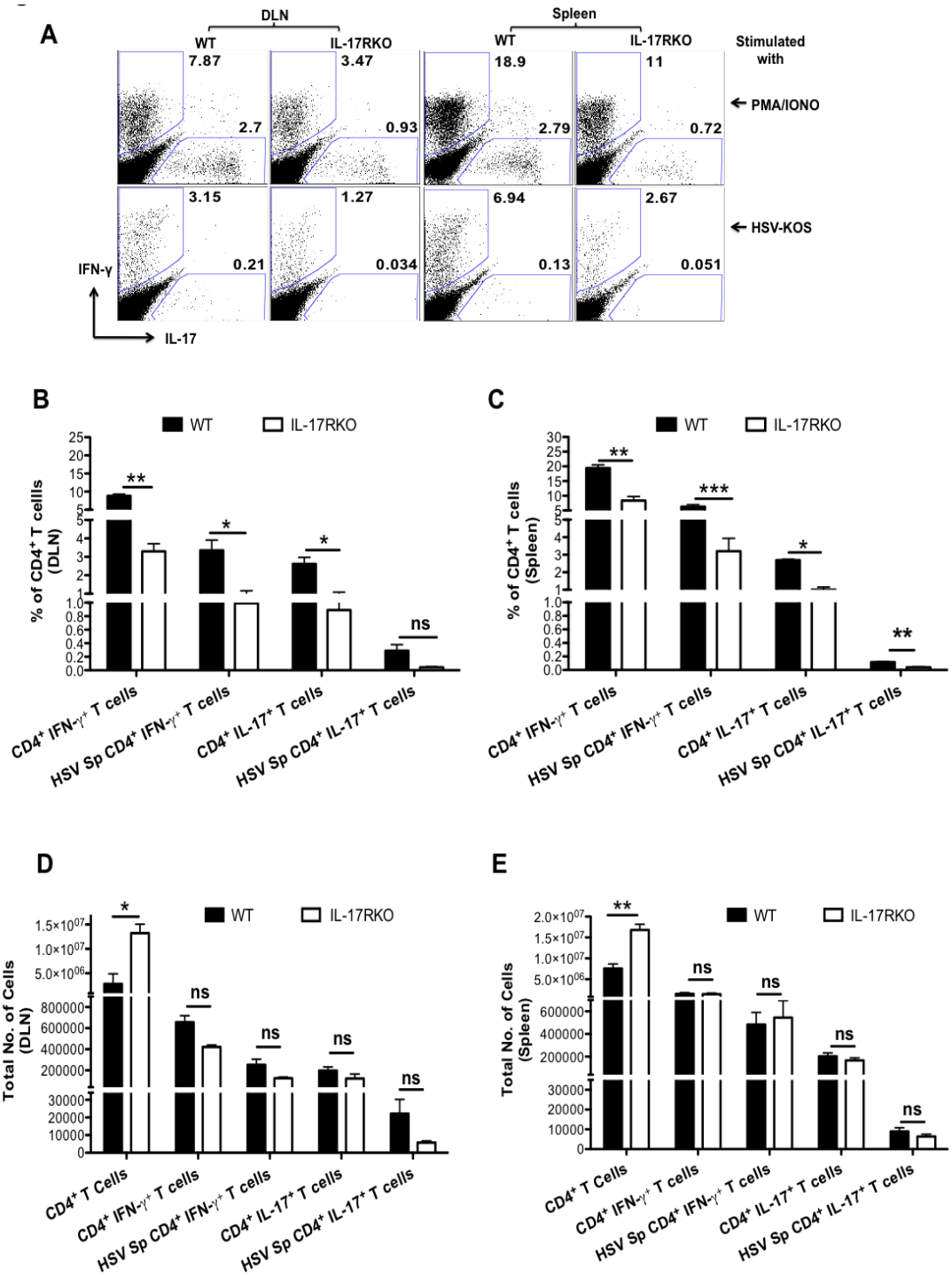
A
DLN
Spleen
WT
IL-17RKO
WT
IL-17RKO
Stimulated with
7.87
2.7
3.47
0.93
18.9
2.79
11
0.72
PMA/IONO
3.15
0.21
1.27
0.034
6.94
0.13
2.67
0.051
HSV-KOS
IFN-γ
IL-17
B
WT
IL-17RKO
% of CD4+ T cells (DLN)
**
*
*
ns
CD4+ IFN-γ+ T cells
HSV Sp CD4+ IFN-γ+ T cells
CD4+ IL-17+ T cells
HSV Sp CD4+ IL-17+ T cells
C
WT
IL-17RKO
% of CD4+ T cells (Spleen)
**
***
*
**
CD4+ IFN-γ+ T cells
HSV Sp CD4+ IFN-γ+ T cells
CD4+ IL-17+ T cells
HSV Sp CD4+ IL-17+ T cells
D
WT
IL-17RKO
Total No. of Cells (DLN)
*
ns
ns
ns
ns
CD4+ T Cells
CD4+ IFN-γ+ T cells
HSV Sp CD4+ IFN-γ+ T cells
CD4+ IL-17+ T cells
HSV Sp CD4+ IL-17+ T cells
E
WT
IL-17RKO
Total No. of Cells (Spleen)
**
ns
ns
ns
ns
CD4+ T Cells
CD4+ IFN-γ+ T cells
HSV Sp CD4+ IFN-γ+ T cells
CD4+ IL-17+ T cells
HSV Sp CD4+ IL-17+ T cells

FIGURE 2.7. IL-17R KO MICE EXHIBIT REDUCED FREQUENCIES BUT NOT NUMBERS OF TH1 AND TH17 CELLS IN DLN AND SPLEEN POST HSV INFECTION.

C57BL/6 and IL-17R KO mice were infected with $1X10^4$ PFU of HSV. Mice were sacrificed on day 15 pi and single cell suspensions of the individual spleen and draining cervical lymph nodes (DLN) were prepared. (n = 4). (A) Representative FACS plots for Th1 and Th17 cells stimulated with PMA/Ionomycin (top) or HSV-KOS virus (bottom). (B, C) Summary for average frequencies of different $CD4^+$ T cell types as depicted in A from DLN (B) and spleen (C). (D, E) The total numbers of IFN-γ^+ $CD4^+$ T cells, HSV stimulated IFN- γ^+ $CD4^+$ T cells, IL-17^+ $CD4^+$ T cells, HSV-Stimulated IL-17^+ $CD4^+$ T cells and $Foxp3^+$ $CD4^+$ T cells from DLN (D) and spleen (E) of WT and IL-17RKO mice.

PART-III

AN IMBLANCE BETWEEN VEGF-A AND sVEGFR-1 MEDIATES CORNEAL NEOVASCULARIZATION AFTER HSV-1 OCULAR INFECTION

Research described in this chapter is a slightly modified version of an article that is accepted for publication in *Journal of Immunology* by Amol Suryawanshi, Sachin Mulik, Shalini Sharma, Pradeep BJ Reddy, Sharvan Sehrawat and Barry T Rouse.

Suryawanshi A, Mulik S. Sharma S, Reddy PB, Sehrawat S and Rouse BT. Ocular neovascularization caused by herpes simplex virus type 1 infection results from breakdown of binding between vascular endothelial growth factor A and its soluble receptor. *J Immunol.* 2011. 186, 3653-3665.

In this chapter "our" and "we" refers to me and co-authors. My contribution in the paper includes (1) Selection of the topic (2) Compiling and interpretation of the literature (3) Designing experiments (4) Understanding the literature and interpretation of the results (5) Providing comprehensible structure to the paper (6) Preparation of graphs and figures (7) Writing and editing.

Abstract

The normal cornea is transparent which is essential for normal vision and although the angiogenic factor VEGF-A is present in the cornea, its angiogenic activity is impeded by being bound to a soluble form of the VEGF receptor-1 (sVEGFR-1 or sVR-1). This report investigates the effect on the balance between VEGF-A and sVEGFR-1 that occurs following ocular infection with HSV, that causes prominent neovascularization, an essential step in the pathogenesis of the vision-impairing lesion,

stromal keratitis (SK). We demonstrate that HSV-1 infection causes increased production of VEGF-A, but reduces sVEGFR-1 levels resulting in an imbalance of VEGF-A and sVEGFR-1 levels in ocular tissues. Moreover, the sVEGFR-1 protein made was degraded by the metalloproteinase (MMP) enzymes MMP-2, MMP-7 and MMP-9 produced by infiltrating inflammatory cells that were principally neutrophils. Inhibition of neutrophils, or inhibition of sVEGFR-1 breakdown with the MMP inhibitor (MMPi) marimostat, or the provision of exogenous recombinant sVEGFR-1 protein all resulted in reduced angiogenesis. Our results make the novel observation that ocular neovascularization resulting from HSV infection involves a change in the balance between VEGF-A and its soluble inhibitory receptor. Future therapies aimed to increase the production and activity of sVEGFR-1 protein could benefit the management of SK, an important cause of human blindness.

Introduction

Normal ocular function requires that photons can passage through ocular tissues anterior to the retina with minimal impedance. In consequence, tissues anterior to the retina are transparent and numerous strategies are used by the normal eye to maintain transparency. These include mechanisms to suppress inflammatory and immune reactions and means to suppress ocular vascularization, both enemies of normal vision (1, 2). Nevertheless, in some circumstances, damage to the eye can result in chronic inflammatory reactions and/or pathological neovascularization and these events may seriously impair vision. This is often the outcome of ocular infection with Herpes Simplex virus 1 (HSV-1) (3,4). Invariably, HSV-1 infection is followed by lifelong viral

persistence and this source of virus can give rise to subsequent infections in the cornea (5, 6). Repeated recurrences often result in significant vision impairing lesions that occur mainly in the corneal stroma (5, 6). Such stromal keratitis (SK) lesions have a complex pathogenesis but result mainly from T cell orchestrated immunopathological reactions to viral or perhaps unmasked ocular antigens (5, 7). Characteristically, SK also includes pathological neovascularization that can be extensive, especially in animal models of SK (8).

The therapeutic management of SK usually targets the inflammatory reaction but controlling pathological angiogenesis also represents a useful approach, as has been demonstrated in experimental situations (9, 10). Although several molecules may be involved in pathological neovascularization, the VEGF family of proteins, especially VEGF-A signaling through the VEGFR-2 receptor, is likely to be the most consequential (11, 12). In support of this, inhibiting VEGF-A, or interfering with its receptor function, were shown to be effective therapeutic strategies in mice models of SK (8-10).

One unsolved issue with regard to VEGF-A and pathological angiogenesis in SK, is the source of the VEGF-A that induces neovascularization. Initial studies indicated that VEGF-A was synthesized de novo in epithelial cells as a consequence of the infection, although it is not clear if the primary source of VEGF-A is virus infected cells themselves or nearby cells exposed to products released from infected and dying cells (13, 14). Another VEGF-A source, especially after the initial event of SK pathogenesis, may be infiltrating inflammatory cells, especially neutrophils that are prominent cells in SK lesions (8). More recently, it was realized that VEGF-A is continuously produced in biologically functional amounts by corneal epithelial cells. However, this source of

VEGF-A fails to mediate angiogenesis because it is bound to a soluble form of the VEGF receptor 1 (sVEGFR-1-1) (15). This so-called VEGF-A trap may be the primary reason the undamaged cornea is not vascularized (15). Curiously, angiogenesis can be elicited in the normal eye if the bond between VEGF-A and sVEGFR-1-1 is disrupted in some way (15). Of interest, some species fail to express sVEGFR-1-1 and in one genetic disease of humans, synthesis of the sVEGFR-1-1 molecule is defective (16). Both situations result in corneal vascularization.

In light of the existence of the VEGF-A trap in normal eyes, pathological angiogenesis, as for example can occur after HSV-1 infection, could also be influenced by the balance between VEGF-A and the sVEGFR-1-1 molecules. We analyze this possibility in the present communication. Our results confirm the previous report that VEFG-A is present and bound to sVEGFR-1-1 in normal ocular tissue (15). We further show that one consequence of HSV-1 infection is the occurrence of an imbalance in the levels of VEGF-A and sVEGFR-1-1 mRNA and proteins. Our results could mean that therapies designed to increase the presence, or retard the breakdown, of sVEGFR-1 may be useful approaches to help manage the severity of SK, an important cause of blindness.

MATERIALS AND METHODS

Mice, Virus and cell lines. Female 6 to 8 week old C57BL/6 mice were purchased from Harlan Sprague Dawley, Indianapolis, IN. Animals were housed in the animal facilities approved by the Association for Assessment and Accreditation of Laboratory Animal Care (AAALAC) at The University of Tennessee and all experimental procedures were in complete agreement with the Association for research in Vision and Ophthalmology

resolution on the use of animals in research. HSV-1 RE Tumpey and HSV-KOS viruses were grown in Vero Cell monolayers (ATCC no. CCL81, American Type Culture Collection). The virus was concentrated, titrated, and stored in aliquots at -80^0 C until use. MK/T-1 cell line (Immortalised keratocytes from C57/BL6 mouse corneal stroma) was kindly gifted by Dr. Reza Dana, Schepens Eye Research Institute and Department of Ophthalmology, Harvard Medical School, Boston MA.

Corneal HSV-1 Infection and Clinical Scoring. Corneal infections of C57BL/6 mice were conducted under deep anaesthesia induced by i.p. injection of avertin as previously described (8). Mice were scarified on their corneas with 27-gauge needle, and a 3-µl drop containing 1×10^4 PFU of virus was applied to the eye. The eyes were examined on different days pi for the development and progression of clinical lesion by slit-lamp biomicroscope (Kowa Company, Nagoya, Japan). The progression of SK lesion severity and angiogenesis of individually scored mice was recorded. The scoring system was as follows: 0, normal cornea; +1, mild corneal haze; +2, moderate corneal opacity or scarring; +3, severe corneal opacity but iris visible; +4, opaque cornea and corneal ulcer; +5, corneal rupture and necrotizing keratitis. The severity of angiogenesis was recorded as described previously (17). According to this system, a grade of 4 for a given quadrant of the circle represents a centripetal growth of 1.5 cm towards the corneal center. The score of the four quadrants of the eye were then summed to derive the neo vessel index (range 0-16) for each eye at a given time point.

Sub-conjunctival Injection. Subconjunctival injections of different drugs were performed as described previously (18). Briefly, subconjunctival injections were done using a 2-cm, 32-gauge needle and syringe (Hamilton, Reno, NV) to penetrate the

perivascular region of conjunctiva, and the required dose of sVEGFR-1 or MMPi was delivered into subconjunctival space. Control mice received isotype fusion protein or solvent used for MMPi.

Treatment of mice with rsVEGFR-1-1 and MMP inhibitor. 6- to 8-wk-old C57/BL6 mice were ocularly infected under deep anesthesia with 1×10^4 PFU of HSV-1 RE Tumpey and divided randomly into groups. One group of mice was administered with 5 μg of rsVEGFR-1-1 (R & D Systems, Minneapolis, MN) in 7 μl PBS subconjunctivally on 36 hours p.i. and then every alternate day from day 5 until day 13 postinfection. In some experiments, rsVEGFR-1-1 was injected subconjunctivally every alternate day starting from day 7 until day 13 postinfection. Animals in the control group were given recombinant human IgG1 Fc protein (R & D Systems) following either of the regimens for respective experiment. The MMPi, marimastat (200 μg /mouse) (Tocris Cookson Inc, Ellisville, MO) was administered subconjunctivally either starting from day 2 or day 5 pi followed by every alternate day until day 13pi. Mice in the control group were given the mock injections. Mice were observed for the development and progression of angiogenesis and SK lesions severity from day 7 until day 15 pi. In some experiments MMPi treatment was started from day 2 and continued every alternate day until day 6 pi. Mice were sacrificed on day 7 pi and corneas were collected for further analysis. All the experiments were repeated at least two times.

Neutrophil Depletion with mAb. 6 to 8 week old C57/BL6 mice were ocularly infected under deep anesthesia with 1×10^4 PFU of HSV-1 RE Tumpey and divided randomly into groups. One group of animals was administered with 100 μg of anti-Gr-1 mAb (RB6-8C5; BioXcell, West Lebanon, NH) intraperitoneally on day 7 and 9 pi. Experiments

were terminated on day 11 pi and corneal samples were collected for further analysis. To study the effect of neutrophil depletion on HSV-1 mediated corneal angiogenesis, antibody treatment was given every alternate day starting from day 7 until day 13 pi. Mice were observed for the development and progression of angiogenesis and SK lesions until day 15 pi. Animals in control group were given isotype control (IgG2b) Ab (LTF-2; BioXcell) following the same regimen. All experiments were repeated at least two times.

Immunofluorescence staining. For immunofluorescence staining, the eyes from naïve uninfected mice were enucleated, and snap frozen in OCT compound. Six-micron thick sections were cut, air dried, and fixed in acetone-methanol (1:1) at room -20 ^{0}C for 10 min. Sections were blocked with 10% goat serum containing 0.05% Tween20 and 1:200 dilution of Fc block (Clone 2.42G2; BD Biosciences Pharmingen, San Diego, CA). Rat anti-sVEGFR-1-1 (141515; R & D Systems) was diluted in 1% BSA containing 0.1% Triton-X and incubated at room temp for 1 hr. After incubations sections were washed several times with PBST and then stained with rabbit anti rat Alexa-488 for 45 min. The corneal sections were repeatedly washed with PBST and mounted with ProLong gold antifade mounting media containing DAPI as a nuclear stain (Molecular Probes, Invitrogen) and visualized under a Immunofluorescence microscope. For Whole mount corneal staining, corneas from rsVEGFR-1-1 and Isotype treated mice were dissected under stereomicroscope. Corneal whole mounts were rinsed in PB for 30 min and flattened on a glass slide under stereomicroscope. Corneal flat mounts were dried and fixed in 100% acetone for 10 min at - 20^{0}C. Nonspecific binding was blocked with 5% BSA containing 1:200 dilution of Fc block for 2 hr at 37^{0}C. CD31-PE (MEC13.3; BD Biosciences-Pharmingen) antibody was used t a concentration of 1:250 in 1% BSA for

overnight followed by subsequent washes in PBS. Corneas were mounted with ProLong Gold antifade and visualized with fluorescence microscope.

Purification of Neutrophils. Ly6G+ neutrophils were purified from the pooled liberase (Roche Diagnostics, Indianapolis, IN) digested corneal single cell suspension obtained from HSV infected mice using anti-Ly6G+ microbeads (Miltenyi Biotec, Auburn, CA). The purity was achieved at the extent of 90%. Purified neutrophils were further analyzed by reverse transcription-PCR and WB for the expression of different MMPs.

Flow Cytometry. Corneas were excised, pooled group wise, and digested with 60 U/ml Liberase for 35 minutes at 37^0C in a humified atmosphere of 5% CO_2. After incubation, the corneas were disrupted by grinding with a syringe plunger on a cell strainer and a single-cell suspension was made in complete RPMI 1640 medium. The single cell suspensions obtained from corneas were stained for different cell surface molecules for FACS. All steps performed at 4^0C. Briefly, cell suspension was first blocked with an unconjugated anti-CD32/CD16 mAb for 30 min in FACS buffer. After washing with FACS buffer, samples were incubated with CD45-allophycocyanin (30-F11), CD11b-PerCP (M1/79), Ly6G-PE (1A8), CD4-allophycocyanin (RM4.5) (All from BD Biosciences-Pharmingen) for 30 min on ice. Finally, the cells were washed three times and re-suspended in 1% *para*-formaldehyde. The stained samples were acquired with a FACS Calibur (BD Biosciences) and the data were analyzed using the FlowJo software.

Quantitative PCR (QPCR). Corneal cells were lysed and total mRNA was extracted using TRIzol LS reagent (Invitrogen). Total cDNA was made with 1 μg of RNA using oligo(dT) primer. Quantitative PCR was performed using SYBR Green PCR Master Mix (Applied Biosystem, Foster City, CA) with iQ5 real-time PCR detection ssystme (Bio

Rad, Hercules, CA). The expression levels of different molecules were normalized to β-actin using ΔCt calculation. Relative expression between control and experimental groups were calculated using the $2^{-\Delta\Delta Ct}$ formula. The PCR primers used are included as table 1 in Supplemental information.

Reverse Transcription Polymerase chain reaction (RT-PCR). RT-PCR was performed to detect the presence of mRNA transcripts of various molecules (VEGF-A, sVEGFR-11, beta actin and different MMPs) according to manufacturers protocol (Promega, Madison, WI). Briefly, cDNA was prepared from total mRNA extracted from different samples. cDNAs were amplified by PCR and were resolved on 1% agarose gel The PCR primers used are included as table 1 in Supplemental information. The PCR primers used are shown in table 2 in Supplemental information.

Western blot analysis. The supernatants from lysed corneal cells were quantified using BCA protein Assay kit (Thermo scientific, Waltham, MA) using BSA as a standard and samples with equal protein concentrations were denatured by boiling in Laemmli buffer. Polypeptides were resolved by SDS-PAGE and transferred onto a PVDF membrane. The membrane was blocked with 5% BSA in Tris-buffered saline with Tween20 (20 mM Tris [pH 7.4], 137 mM NaCl, and 0.1% Tween20) overnight at 4^0C and probed with specific primary and secondary antibodies. Proteins were detected using chemiluminiscent HRP substrate (Millipore, Billerica, MA). The membrane was kept in stripping buffer for 10 min and re-probed using anti-β-actin antibody. The antibodies used were rat anti-sVEGFR-1-1 (141515; R&D Systems), mouse anti-VEGF-A (EE02; Santa Cruz Biotechnology, Santa Cruz, CA), mouse anti MMP-2 (8B4; Santa Cruz Biotechnology, Santa Cruz, CA), goat anti mouse MMP-8 (M-20; Santa Cruz Biotechnology, Santa Cruz,

CA), goat anti mouse MMP-9 (C-20; Santa Cruz Biotechnology, Santa Cruz, CA), goat anti mouse MMP-12 (M-19; Santa Cruz Biotechnology, Santa Cruz, CA), mouse anti-β-actin (AC74; Sigma-Aldrich, St Louis MO), goat anti rat IgG-HRP (R & D Systems), goat anti-mouse IgG-HRP (Santa Cruz Biotechnology) and donkey anti goat IgG-HRP (Santa Cruz Biotechnology).

Coimmunoprecipitation. Coimmunoprecipitation was performed using Pierce Coimmunoprecipitation kit according to manufacturer's protocol (Thermo Scientific). Briefly, 50 µg of anti sVEGFR-1-1 antibody was immobilized to antibody coupling resin by incubating the antibody to resin containing column for 2 hrs at room temperature. Care was taken to keep resin slurry in suspension during incubation. The 200 µl supernatant from lysed corneal cells (800 µg of total protein) was incubated for 2 hrs at 4^{o}C with the above mentioned resin immobilized antibody. Finally, 50 µl of the elution buffer was added and immunoprecipitate was eluted out and analyzed by WB.

ELISA. The pooled corneal samples were homogenized using a tissue homogenizer and supernatant was used for analysis. The concentrations of VEGF-A and sVEGFR-1-1 were measured using Quantikine sandwich ELISA kits (R&D Systems) according to manufacturers protocol.

Quantification of total number of molecules for sVEGFR-1 and VEGF-A. The total number of sVEGFR-1 and VEGF-A molecules from naïve as well as different day pi samples were calculated using following formula.

Total Number of Molecules = Quantity of Protein × Molecular Weight × Avogadro's No.

In vitro assay for VEGF-A and sVEGFR-1-1 production. A mouse stromal fibroblast cell line (MK/T-1) was used to study differential effect of HSV-1 on production of

VEGF-A and sVEGFR-1-1. The cells were cultured and plated onto 6-well tissue culture plates in 10% DMEM. The cells around >90% confluents were infected with HSV-KOS at 3 multiplicity of infection (MOI) (adsorbption for 1 h). Uninfected cells were used as control. Cells were harvested at different time points and total mRNA was extracted and used to quantify the mRNA levels of the VEGF-A and sVEGFR-1-1.

Degradation assays. Degradation assays were performed as previously described (19). Briefly, 100 ng of rsVEGFR-1-1 (R&D Systems) was incubated with active mouse MMP-2, MMP-7, MMP-8, MMP-9 and MMP-12 (R&D Systems), at 1:1 substrate/enzyme molar ratio at 37°C for 24 hours. Pro-MMPs were activated by p-aminophenylmercuric acetate (Sigma-Aldrich) before use according to manufacturer's protocol. To study the degradation of mouse native sVEGFR-1-1 from cornea, the supernatant from lysed corneal cells was collected and incubated with different activated MMPs [1:1 substrate enzyme molar ratios] at 37°C for 24 hours. MMP activity was inhibited using 20 mM ethylenediaminetetraacetic acid (EDTA). The samples were then analyzed by WB.

Statistics. Student's t test was performed to determine statistical significance and data are expressed as mean ± SEM.

Results

Presence of VEGF-A in ocular tissues of normal mice

Recently, it was demonstrated that VEGF-A is present in normal corneal tissues, but it fails to induce angiogenesis because it is bound to sVEGFR-1-1 (15). Both VEGF-

A and sVEGFR-1-1 are produced continuously by normal ocular tissues. As a prelude to measuring the influence of HSV-1 ocular infection on the balance between VEGF-A and sVEGFR-1-1, we repeated some of the normal mice experiments previously described (15). We were able to confirm many of their observations. Accordingly, as shown in Figure-1, corneal extracts from naïve mice analyzed by WB under reducing conditions revealed a band of 62kDa for sVEGFR-1-1 and two bands for VEGF-A at molecular sizes of 22 and 14 kDa (Figure 3.1A). These bands correspond to two isoforms of VEGF-A. However, under non-reducing conditions, blots revealed only a single band that was far larger than those observed in reducing gels and had an apparent size of between 100-150 kDa (Figure 3.1B). This would be consistent with VEGF-A being bound to another molecule, presumably sVEGFR-1-1. Support for this was obtained performing co-immunoprecipitation that revealed the interaction of VEGF-A and sVEGFR-1-1 (Figure 3.1C).

The fact that normal ocular tissue expressed mRNA for both the VEGF-A and the sVEGFR-1-1 proteins was also demonstrated by RTPCR (Figure 3.1D). The sVEGFR-1-1 molecule was also readily detectable in epithelial and stromal layers of corneal sections by immunohistochemistry (Figure 3.1E). Our findings are consistent with and confirm those reported by the Ambati group and demonstrate that VEGF-A is present in cornea and is mostly bound to sVEGFR-1-1 forming a so called VEGF-A trap (15, 20-21).

Changes in VEGF-A and sVEGFR-1-1 as a consequence of HSV-1 infection

The principal objective of our study was to evaluate if the VEGF-A trap affected the outcome of pathological angiogenesis caused by ocular infection with HSV-1. To do

this, mice were ocularly infected with virus and the expression levels of both VEGF-A and sVEGFR-1-1 mRNA and proteins were measured and compared with controls at various times pi. We focused on initial time points after infection when replicating virus is readily detectable in the cornea (up to 5 day pi) as well as at the stage of clinical SK (day 8 pi) when replicating virus is no longer demonstrable and the stroma is heavily infiltrated by inflammatory cells, particularly neutrophils (4, 22). At each time point, 6 corneas were collected and pooled for analysis from infected and control animals by QPCR. The data expressed in Figure 3.2A records average gene expression values compared with controls for 2 separate experiments. As is evident, increased VEGF-A expression (6.7 fold) was detectable by 24 hours pi and levels peaked in the early phase (average 11.5 fold) in samples tested on days 2 pi. By day 5, VEGF-A mRNA expression levels were at control levels. However, VEGF-A mRNA levels increased in later samples with the highest levels detectable (average 97 fold) in day 11 samples. At day 11, replicating virus and viral mRNA were no longer present in corneal extracts (data not shown) and the VEGF-A that was detected was presumed to be produced mainly by infiltrating inflammatory cells such as neutrophils (described subsequently).

The general pattern observed measuring VEGF-A gene expression was evident with protein levels measured by ELISA and WB. As shown in Figure 3.2B and 3.2C, after an initial peak of VEGF-A protein on days 2 to 3 pi, a second higher peak was observed during the clinical phase. The non-reducing WB of corneal extracts from naïve mice revealed single high molecular weight band for VEGF-A (presumably all bound to sVEGFR-1). However, corneal extracts from day 3 pi showed another low molecular

weight band for VEGF-A suggesting the presence of non sVEGFR-1 associated free VEGF-A after HSV-1 infection (Figure 3.2D).

Quantification of sVEGFR-1-1 gene expression revealed a different response pattern than was noted with VEGF-A (Figure 3.2E). The expression levels were decreased following HSV-1 infection with maximal decreases observed in samples taken at 5 days pi (average 8 fold compared to control). The initial decreased expression of sVEGFR-1-1 could reflect the well known ability of HSV to suppress almost all host gene expression in cells in which it replicates (23, 24). However, VEGF-A gene expression, at least early after infection, may be an exception as are some cytokines (13, 25, 26). To determine if HSV infection could differentially influence the expression of VEGF-A and sVEGFR-1, we studied the outcome of in vitro infection of an eye derived cell line (MK/T-1) that spontaneously expressed both VEGF-A and sVEGFR-1 (Supplemental Figure 3.1A). This cell line was derived from corneal stromal fibroblasts. The results demonstrate that early after HSV-1 infection whereas VEGF-A levels were increased, levels of sVEGFR-1 mRNA were markedly suppressed (Supplemental Figure 3.1B). Although fibroblasts are not the major cell type infected by HSV in vivo, our results imply that a similar outcome could occur in corneal epithelial cells, the primary target cells for HSV infection.

Experiments were also done to quantify protein levels at various time points by ELISA. In corneal extracts of uninfected animals, sVEGFR-1-1 protein was readily detectable, and these levels were far higher than VEGF-A in the same samples (Figure 3.2F). Changes in sVEGFR-1-1 protein levels detectable by ELISA did occur at different time points after infection, and significant reduction in the levels of sVEGFR-1 were

observed on day 1 and from day 5 to 11 pi. Additionally, when the ratio of the number of sVEGFR-1 molecules to VEGF-A molecules from naïve mice was compared with infected animals at various time points pi, there was a decreased ratio of sVEGFR-1 to VEGF-A at all time points pi. Differences were significant on day 1 as well as from day 7 to 14 pi (Figure 3.2G). Furthermore, an interesting situation was revealed by WB analysis under reducing conditions of samples taken at different time point pi (Figure 3.2H). Here it was evident in corneal extracts from uninfected animals that sVEGFR-1-1 protein was represented almost entirely as a single band at approximately 60 kDa size. However, by day 3 pi, there was notable fragmentation of the sVEGFR-1-1 and this situation was also evident in samples collected at other time points after infection. The degradation of sVEGFR-1 could explain why we observed minimal sVEGFR-1 protein at day 11-time point even though sVEGFR-1 mRNA levels peaked at this time. These observations led us to conclude that HSV infection of the cornea diminished the expression of sVEGFR-1-1 and that the intact protein was degraded, at least partially, at different phases of virus infection. Both effects would serve to diminish the inhibitory activity of sVEGFR-1-1 on VEGF-A induced angiogenesis.

An additional series of experiments supported the notion that the activity of sVEGFR-1-1 has a constraining effect on the angiogenic activity of VEGF-A. We anticipated that the provision of an additional exogenous source of sVEGFR-1-1 protein to HSV-1 infected mice might act to diminish the extent of angiogenesis that occurs subsequent to infection. To evaluate this possibility, we obtained recombinant mouse sVEGFR-1-1 (rsVEGFR-1-1) fusion protein that had previously been used by others to counteract VEGF-A activity in a VEGF-A induced micro-pocket assay for angiogenesis

(15). In our pathological system, we chose to administer a higher dose rsVEGFR-1-1, or an isotype fusion protein (Isotype). To evaluate the possible VEGF-A inhibitory effects in vivo, animals were given either rsVEGFR-1-1 or Isotype subconjunctivally to HSV-1 infected animals, either starting at day 1 (Figure 3.3A) or day 7 pi (Figure 3.3E). Animals were followed until day 15 pi to measure the extent of angiogenesis. Results shown in Figure 3.3A-C and Supplemental Figure 3.2A indicated that rsVEGFR-1-1 recipients had significantly diminished angiogenic responses as well as SK lesion severity compared to the isotype group. Corneal cell preparations collected at the end of the experiment revealed diminished frequency and numbers of CD31+ (a marker for blood vessel endothelial cells), neutrophils as well as CD4+ T cells (Figure 3.3D and Supplemental Figure 3.2B). It is of particular interest to note that even when rsVEGFR-1-1 administration was delayed till day 7 pi (Figure 3.3E), a significant level of SK severity and angiogenesis inhibition was still evident. These results further support the concept that sVEGFR-1-1 may limit the angiogenic response to VEGF-A in pathological angiogenesis.

Metalloproteinases could be responsible for sVEGFR-1-1 degradation

The observation that sVEGFR-1-1 protein may be degraded in HSV-1 infected corneas raised the question of how the breakdown was accomplished. Likely enzyme candidates include MMPs, some of which were shown to be present in damaged eyes in other systems (1). Previous reports suggest that MMP-9 could induce neovascularization *in vivo* and inhibition of MMP-9 reduces angiogenesis (27). Moreover, MMP-9 protein is present in the cornea following HSV-1 infection as we have reported previously (28).

Experiments were performed to measure the expression profile by QPCR of several MMP mRNAs at various time points after HSV-1 infection. The results shown in Figure-3.4A demonstrate that compared to uninfected controls, expression levels of several MMPs were elevated following the infection. Peak levels that varied between experiments differed between the MMPs tested, but always occurred between days 5 and days 11 pi. Of the multiple MMP mRNAs examined, expression levels of MMP-9 were the most elevated with its peak evident in day 7 pi samples (Average 249 fold). Another MMP of interest was MMP-7 since this enzyme was shown recently to be uniquely capable degrading human sVEGFR-1-1 (19). Levels of MMP-7 were at their peak on day 11 pi. Additional experiments were done in vitro with the activated form of selected MMPs (MMP-2, MMP-7, MMP-8, MMP-9, and MMP-12) to measure their ability to degrade rsVEGFR-1-1 in vitro as detected by WB. As is evident in Figure 3.4B, MMP-7 was most effective at degrading rsVEGFR-1-1 with MMP-9 also active, but less so. In these assays, MMP-8 and MMP-12 were without activity and MMP-2 had a minimal effect. In additional experiments, MMP-2, MMP-7 and MMP-9 were shown to degrade sVEGFR-1-1 present in naïve corneal extracts (Figure 3.4C).

Experiments were also done to determine if inhibiting the function of MMP enzymes in vivo affected sVEGFR-1-1 degradation, as well the outcome on the extent of angiogenesis and SK severity. To accomplish MMP inhibition, marimastat (29-31) was administered subconjunctivally at different times pi and the results compared to infected mice given subconjunctival injections of mock. In an experiment in which animals received marimastat on days 2,4 and 6 pi, corneal extracts examined by WB on day 7 pi revealed a markedly reduced level of sVEGFR-1-1 degradation compared to controls

(Figure-3.5A). In another experiment, two marimastat injections given on days 2 and 4 also revealed inhibited sVEGFR-1-1 degradation in samples examined on day 5 (Data not shown).

When the outcome of angiogenesis and SK severity was compared in treated and control mice, the marimastat recipients had significantly reduced levels of angiogenesis and SK severity, at least at day 15 pi time point when experiments were terminated (Figure 3.5B). Corneal cell preparations collected at the end of the experiment revealed diminished frequency and numbers of $CD31^+$ endothelial cells, neutrophils and $CD4^+$ T cells (Figure 3.5C and Supplemental Figure 3.3A). Furthermore, in an experiment in which marimastat treatment was begun on day 5 pi and given additional injections on days 7, 9 and 11 there was also a significant reduction of angiogenesis and lesion scores at day 15 pi (Figure 3.5D). Corneal cell preparations collected at the end of the experiment revealed diminished frequency and numbers of $CD31^+$ endothelial cells, neutrophils as well as CD4+ T cells (Figure 3.5E and Supplemental Figure 3.3B). Taken together our results support the concept that metalloproteinases, particularly MMP-2, MMP-7 and MMP-9, are upregulated following HSV-1 infection and these enzymes are responsible for degrading the sVEGFR-1-1 protein that, in turn, constrains the angiogenic activity of VEGF-A.

Neutrophils play multiple roles in ocular angiogenesis

A prominent cell type in the inflammatory response to ocular HSV-1 infection is the neutrophil (8, 13, 22). To investigate the role played by neutrophils in HSV-1 mediated corneal angiogenesis, kinetic studies were carried out for neutrophil infiltration

in the cornea following HSV infection. As shown in Figure 3.6A, neutrophils constitute about 30-80% of total infiltrated leukocytes at all tested time points and infiltrate the cornea in a biphasic manner. An initial wave of infiltration peaked around day 2 pi followed by decline and second wave starting from day 8 till which peaked around day 15 pi (Figure 3.6B). Since, neutrophils studied in other systems are known to be a source of different MMPs as well as VEGF-A (28, 32-34); we anticipated that neutrophils could be a source of MMP enzymes that act to increase angiogenesis by breaking down and releasing bioactive VEGF-A from its bond to sVEGFR-1-1. In support of this, we purified neutrophils from the day 2 infected corneas and WB analysis was carried out to check the presence of protein for MMP-2, MMP-8, MMP-9 and MMP-12. Figure 3.6C shows the presence of MMP-2, MMP-8, MMP-9 and MMP-12. Additionally, depleting neutrophils from day 7 pi (Figure 3.6D) in infected mice led to significantly diminished VEGF-A protein levels and restored levels of sVEGFR-1-1 protein in day 11 samples (Figure 3.6E). QPCR analysis also revealed the decreased expression of VEGF-A and MMP-9 in the depleted mice as compared to isotype antibody treated mice (Figure 3.6F). To further implicate neutrophils as a source of VEGF-A during the clinical phase of SK, neutrophils were purified from pooled corneas at day 11 pi and RTPCR and WB carried out to check for the presence of VEGF-A mRNA message as well as protein. Both VEGF-A mRNA (Figure 3.6G) and protein (Figure 3.6H) could be demonstrated supporting a role for neutrophils in contributing to angiogenesis during the clinical phase of SK when replicating virus is no longer present in the cornea.

To show the influence of neutrophils during HSV-1 induced pathological angiogenesis, experiments were done to compare the extent of angiogenesis and

differences in expression levels of VEGF-A and sVEGFR-1-1 in mice depleted of neutrophils compared to controls. Depletion (with anti-Gr1 MAb) was commenced on day 7 pi. As shown in Figure 3.6I, whereas the extent of angiogenesis and SK lesion severity continued to increase in magnitude in isotype antibody treated animals, by day 15 pi, when the experiment was terminated, the average angiogenic response and SK severity were significantly decreased in animals treated with neutrophil depleting antibody. Although, cell types in inflammatory reaction other than neutrophils can express Gr1, neutrophils are the predominant $Gr1^+$ population in lesion during clinical phase of SK. We interpret Gr-1 depletion experiment where the VEGF-A levels were decreased to mean that neutrophils represent a major source of the VEGF-A that is involved in HSV-1 induced angiogenesis even though a minority of other cell types in inflammatory reaction can also be $Gr1^+$. Taken together these results demonstrate that neutrophils contribute to the severity of the pathological angiogenic response caused by HSV-1 infection. This occurs because neutrophils, can act as one of the sources of VEGF-A as well as the MMP enzymes that degrade sVEGFR-1-1, the molecule that binds to VEGF-A and inhibit its angiogenic activity.

Discussion

In this report, we investigate mechanisms by which HSV-1 infection of the eye results in neovascularization, an essential step in the pathogenesis of SK, an ocular lesion that impairs and can ablate vision (35). We confirm a previous report (15) that VEGF-A, a principal angiogenic factor, is produced by the normal eye, but is constrained from causing angiogenesis by being bound to a soluble form of one of its cellular receptors.

Our results make the novel observation that one consequence of HSV-1 infection is to cause an imbalance in the production of VEGF-A and sVEGFR-1-1 that impedes its activity. Whereas, the infection up-regulates VEGF-A production, the expression of sVEGFR-1-1 is inhibited. Moreover, the sVEGFR-1-1 protein that is made is degraded by the metalloproteinase enzymes MMP-2, -7 and -9 which permits the VEGF-A, initially derived from infected epithelial cells, and later on inflammatory cells, to exert more effective angiogenic activity. Procedures that decrease the breakdown of sVEGFR-1-1, such as the administration of the MMPi, marimastat, or the provision of exogenous rsVEGFR-1-1 protein resulted in lessened angiogenesis. Our results support the notion that the binding of sVEGFR-1-1 to VEGF-A, a so called VEGF-A trap, acts to limit the extent of pathological angiogenesis such as that caused by ocular infection by HSV-1. It is also conceivable that future therapies to control SK could benefit by procedures that influence the production and activity of the sVEGFR-1-1. Our overall results are summarized in Figure-3.7, showing how HSV-1 infection leads to corneal angiogenesis.

The pathogenesis of SK involves multiple events that include neovascularization of the normally transparent tissue anterior to the retina. Thus any new blood vessel development in the anterior tissues damages vision by defracting light and, since new vessels are leaky (4, 11), they readily permit escape of inflammatory cells that further contribute to the loss of transparency. Accordingly, preventing, and ideally reversing, neovascularization is an important objective to retain optimal vision. Numerous mechanisms have been suggested to explain how HSV infection could cause neovascularization (8, 28, 36), but perhaps the most important is the induction of VEGF family members, especially VEGF-A which stimulates corneal angiogenesis by engaging

the receptor VEGFR-2 (8, 10). Supporting this, prior studies have shown that counteracting the VEGF-A made or inhibiting its receptor can significantly reduce HSV induced angiogenesis (8, 10). Others, as well as ourselves, have already reported that HSV infection of the corneal epithelium in the early stages of keratitis results in the expression of VEGF-A protein either in infected or nearby cells (13, 14). What we had not appreciated, until the observations of the Ambati group appeared (15), is that VEGF-A is continually produced by uninfected normal eyes but fails to cause corneal vascularization because the VEGF-A is bound to a soluble form of one of its receptors (15). The important aspect of our study is our observations that the binding of sVEGFR-1-1 to VEGF-A made during a pathological disease process may also act to modulate VEGF-A activity and influence the magnitude of angiogenesis. A series of observations led to this conclusion.

Firstly in the early stages after HSV infection much of the VEGF-A detected by WB under native conditions was of a molecular size consistent to its being bound to another protein that was shown to be sVEGFR-1-1. Of interest, soon after infection one consequence of HSV-1 was to exert a differential effect on gene expression of VEGF-A and sVEGFR-1-1 proteins. Accordingly, whereas infection caused an increased expression of VEGF-A, the production of the sVEGFR-1-1 was inhibited. Additionally, that infection of cells could enhance VEGF-A, but suppress sVEGFR-1-1, gene expression could also be shown by in vitro studies. Thus the initial angiogenesis observed after infection could be the consequence of enhanced VEGF-A activity arising both from increased production as well as diminished inhibition. In support of the latter mechanism, if an additional exogenous source of sVEGFR-1-1 was provided during the early stages

of the disease process, the outcome was diminished angiogenesis. These observations taken together support the idea that a VEGF-A trap operates to limit the extent of pathological angiogenesis at least early after infection.

It is characteristic of HSV-1 ocular infection in the mouse model that the virus is cleared within a few days, but the extent of angiogenesis continues to advance as does the chronic inflammatory process in the corneal stroma that is indicative of SK (4, 8). Our studies show that VEGF-A may also be responsible for the additional angiogenesis but the principal cell source of the VEGF-A is no longer the epithelium (that is no longer infected) but instead derives from invading inflammatory cells, particularly neutrophils. We could show that depleting $Gr1^+$ cells with specific mAb on day 7 pi diminished the extent of the neovascular response compared to non-depleted controls indicating their role in VEGF-A production. Depleted animals also had less VEGF-A protein in corneal extracts when quantified by ELISA. However, we anticipated that at the later phases of the disease process, the activity of VEGF-A was less likely to be impeded by its binding to the sVEGFR-1-1 protein. Thus, in addition to being a source of VEGF-A the invading inflammatory cells are well known to produce many different MMP enzymes (28, 37) some of which could degrade proteins that bind to VEGF-A and limit its activity (34). For example, in some cancer systems where VEGF-A is shown to be bound to a matrix protein, MMP-9 may degrade the matrix protein so releasing VEGF-A to exert angiogenic activity (38). Moreover, VEGF-A processed by different MMPs retains biological activity (39). Also of relevance, MMP-7 was shown very recently to degrade human sVEGFR-1-1 resulting in increased angiogenic activity in an in vitro tube formation assay using human umbilical vein endothelial cells (19). In our present study,

we could demonstrate that the inflammatory exudate cells could express several MMPs and that at least two of them (MMP-7 and MMP-9) were highly effective in vitro at degrading the mouse sVEGFR-1-1 protein, that had not previously been reported. We could show the effect using a recombinant sVEGFR-1-1 protein as well as with sVEGFR-1-1 preparations isolated from normal mouse corneas. However, of special relevance to our viewpoint as the constraining role of sVEGFR-1-1 on VEGF-A activity, we could clearly demonstrate that if we treated animals with marimastat, an inhibitor of MMP enzyme activity, then the extent of the neovascular response was significantly diminished compared to untreated animals. Furthermore**,** WB revealed that sVEGFR-1-1 protein concentrations were higher in marimastat treated corneal samples.

Taken together we contend that our studies have provided novel insight on mechanistic aspects of SK pathogenesis and have revealed a previously unrecognized event that could be targeted for therapeutic manipulation. Accordingly, we show that the important event of ocular angiogenesis mediated by VEGF-A is markedly influenced by the presence and activity of the sVEGFR-1-1 protein. When bound to sVEGFR-1-1, as occurs with all of the VEGF-A made by the normal cornea, VEGF-A is unable to mediate angiogenesis. In a pathological situation this VEGF-A trap is also occurring, but it breaks down when levels of MMPs arrive that can degrade the sVEGFR-1-1 protein (Fig 7). It would seem logical to develop therapies to manage SK that either increase the concentration or retard the breakdown of the sVEGFR-1-1 protein. Further studies are underway to investigate this issue.

LIST OF REFERENCES

1. Azar, D.T. 2006. Corneal angiogenic privilege: angiogenic and antiangiogenic factors in corneal avascularity, vasculogenesis, and wound healing (an American Ophthalmological Society thesis).*Trans. Am. Ophthalmol. Soc.* 104: 264-302
2. Chang, J.H., E.E. Gabiso, T. Kato, and D.T. Azar. 2001. Corneal neovascularization. *Curr Opin Ophthalmol.* 12: 242-249.
3. Deshpande, S. P., S. Lee, M. Zheng, B. Song, D. Knipe, J. A. Kapp, and B. T. Rouse. 2001. Herpes simplex virus-induced keratitis: evaluation of the role of molecular mimicry in lesion pathogenesis. *J. Virol.* 75: 3077-3088.
4. Biswas, P.S, and B. T. Rouse. 2005. Early events in HSV keratitis--setting the stage for a blinding disease. *Microbes Infect.* 7: 799-810.
5. Russell, R. G., M. P. Nasisse, H. S. Larsen, and B. T. Rouse. 1984. Role of T-lymphocytes in the pathogenesis of herpetic stromal keratitis. *Invest. Ophthalmol. Vis. Sci.* 25: 938-944.
6. Sarangi, P.S, and B.T. Rouse. 2010. Herpetic Keratitis. In: Ocular disease mechanisms and management. L.A. Levin, and D. M. Albert, editors. Saunders Elsevier, Philadelphia, PA. 91-97.
7. Zhao, Z.S., F. Granucci, L. Yeh, P. A. Schaffer, and H. Cantor. 1998. Molecular mimicry by herpes simplex virus-type 1: autoimmune disease after viral infection. *Science* 279: 1344-1347.
8. Zheng, M., S. Deshpande, S. Lee, N. Ferrara, and B. T. Rouse. 2001. Contribution of vascular endothelial growth factor in the neovascularization process during the pathogenesis of herpetic stromal keratitis. *J. Virol.* 75: 9828-9835.

9. Kim, B., Q. Tang, P. S. Biswas, J. Xu, R. M. Schiffelers, F. Y. Xie, A. M. Ansari, P. V. Scaria, M. C. Woodle, P. Lu, et al. 2004. Inhibition of ocular angiogenesis by siRNA targeting vascular endothelial growth factor pathway genes: therapeutic strategy for herpetic stromal keratitis. *Am. J. Pathol.* 165: 2177-2185.
10. Kim, B., S. Suvas, P. P Sarangi, S. Lee, R. A. Reisfeld, and B. T. Rouse. 2006. Vascular endothelial growth factor receptor 2-based DNA immunization delays development of herpetic stromal keratitis by antiangiogenic effects. *J. Immunol.* 177: 4122-4131.
11. Nagy, J. A., A. M. Dvorak, and H. F. Dvorak. 2007. VEGF-A and the induction of pathological angiogenesis. *Annu. Rev. Pathol.* 2: 251-275.
12. Ferrara, N., H. P. Gerber, and J. LeCounter. 2003. The biology of VEGF and its receptors. *Nat. Med.* 9: 669-676.
13. Biswas, P. S., K. Banerjee, P. R. Kinchington, and B. T. Rouse. 2006. Involvement of IL-6 in the paracrine production of VEGF in ocular HSV-1 infection. *Exp. Eye Res.* 82: 46-54.
14. Wuest, T. R., and D. J. Carr. 2010. VEGF-A expression by HSV-1-infected cells drives corneal lymphangiogenesis. *J. Exp. Med.* 207: 101-115.
15. Ambati, B. K., M. Nozaki, N. Singh, A. Takeda, P. D. Jain, T. Suthar, R. J. Albuquenrque, E. Richter, E. Sakurai, M. T. Newcomb, et al. 2006. Corneal avascularity is due to soluble VEGF receptor-1. *Nature.* 443: 993-997.
16. Jordan, T., I. Hanson, D. Zaletayev, S. Hodgson, J. Prosser, A. Seawright, N. Hastie, and V. van Heyningen. 1992. The human PAX6 gene is mutated in two patients with aniridia. *Nat. Genet.* 1: 328-32.

17. Dana, M. R., S. N. Zhu, and J. Yamada. 1998. Topical modulation of interleukin-1 activity in corneal neovascularization. *Cornea.* 17: 403-409.

18. Fenton, R. R., S. Molesworth-Kenyon, J. E. Oakes, and R. N. Lausch. 2002. Linkage of IL-6 with neutrophil chemoattractant expression in virus-induced ocular inflammation. *Invest Ophthalmol. Vis. Sci.* 43: 737-743.

19. Ito, T. K., G. Ishii, S. Saito, K. Yano, A. Hoshino, T. Suzuki, and A. Ochiai. 2009. Degradation of soluble VEGF receptor-1 by MMP-7 allows VEGF access to endothelial cells. *Blood*. 113: 2363-2369.

20. Kendall, R.L., and K. A. Thomas. 1993. Inhibition of vascular endothelial cell growth factor activity by an endogenously encoded soluble receptor. *Proc. Natl. Acad. Sci.* U S A. 90: 10705-10709.

21. Goldman, C.K., R. L. Kendall, G. Cabrera, L. Soroceanu, Y. Heike, G. Y. Gillespie, G. P. Siegal, X. Mao, A. J. Bett, W. R. Huckle, et al. 1998. Paracrine expression of a native soluble vascular endothelial growth factor receptor inhibits tumor growth, metastasis, and mortality rate. *Proc. Natl. Acad. Sci.* U S A. 95: 8795-9000.

22. Thomas, J., S. Gangappa, S. Kanangat, and B. T. Rouse. 1997. On the essential involvement of neutrophils in the immunopathologic disease: herpetic stromal keratitis. *J. Immunol.* 158: 1383-1391.

23. Fenwick, M. L., and J. Clark. 1982. Early and delayed shut-off of host protein synthesis in cells infected with herpes simplex virus. *J. Gen. Virol.* 61: 121-125.

24. Fenwick, M.L., and M. J. Walker. 1978. Suppression of the synthesis of cellular macromolecules by herpes simplex virus. *J. Gen. Virol.* 41: 37-51.

25. Kanangat, S. J., S. Babu, D. M. Knipe, and B. T. Rouse. 1996. HSV-1-mediated modulation of cytokine gene expression in a permissive cell line: selective upregulation of IL-6 gene expression. *Virology.* 219: 295-300.

26. Paludan, S. R. 2001. Requirements for the induction of interleukin-6 by herpes simplex virus-infected leukocytes. *J. Virol.* 75: 8008-8015.

27. Ebrahem, Q., S. S. Chaurasia, A. Vasanji, J. H. Qi, P. A. Klenotic, A. Cutler, K. Asosingh, S. Erzurum, and B. A. Apte. 2010. Cross-Talk between Vascular endothelial growth factor and matrix metalloproteinases in the induction of Neovascularization *in Vivo. Am. J. Patho.* 176:496-503.

28. Lee, S., M. Zheng, B. Kim, and B. T. Rouse. 2002. Role of matrix metalloproteinase-9 in angiogenesis caused by ocular infection with herpes simplex virus. *J. Clin. Invest*. 110: 1105-1111.

29. Watson, S. A., T. M. Morris, H. M. Collins, L. J. Bawden, K. Hawkins, and E. A. Bone. 1999. Inhibition of tumour growth by marimastat in a human xenograft model of gastric cancer: relationship with levels of circulating CEA. *Br. J. Cancer.* 81: 19-23.

30. Wada, N., Y. Otani, T. Kubota, M. Kimata, A. Minagawa, N. Yoshimizu, K. Kameyama, Y. Saikawa, M. Yoshida, T. Furukawa, et al. 2003. Reduced angiogenesis in peritoneal dissemination of gastric cancer through gelatinase inhibition. *Clin. Exp. Metastasis.* 20: 431-435.

31. Kimata, M., Y. Otani, T. Kubota, N. Igarashi, T. Yokoyama, N. Wada, N. Yoshimizu, M. Fuzii, K. Kameyama, Y. Okada, et al. 2002. Matrix metalloproteinase inhibitor,

marimastat, decreases peritoneal spread of gastric carcinoma in nude mice. *Jpn. J. Cancer Res.* 93: 834-841.

32. Nozawa, H., C. Chiu, and D. Hanhan. 2006. Infiltrating neutrophils mediate the initial angiogenic switch in a mouse model of multistage carcinogenesis. *Proc. Natl. Acad. Sci.* U S A. 103: 12493-12498.
33. Gong, Y., and D. R. Koh. 2010. Neutrophils promote inflammatory angiogenesis via release of preformed VEGF in an in vivo corneal model. *Cell Tissue Res.* 339: 437-448.
34. Ardi, V. C., T. A. Kupriyanova, E. I. Deryugina, and J. P. Quigley. 2007. Human neutrophils uniquely release TIMP-free MMP-9 to provide a potent catalytic stimulator of angiogenesis. *Proc. Natl. Acad. Sci.* U S A. 104: 20262-20267.
35. Streilein, J.W., M. R. Dana, and B. R. Ksander. 1997. Immunity causing blindness: five different paths to herpes stromal keratitis. *Immunol. Today.* 18: 443-449.
36. Banerjee, K., P. S. Biswas, B. Kim, S. Lee, and B. T. Rouse. 2004. CXCR2-/- mice show enhanced susceptibility to herpetic stromal keratitis: a role for IL-6-induced neovascularization. *J. Immunol.* 172: 1237-1245.
37. Claesson, R., A. Johansson, G. Bebasakis, L. Hanstrom, and S. Kalfas. 2002. Release and activation of matrix metalloproteinase 8 from human neutrophils triggered by the leukotoxin of Actinobacillus actinomycetemcomitans. *J. Periodontal Res.* 37: 353-359.
38. Hawinkels, L. J., K. Zuidwijk, H. W. Verspaget, E. S. de Jonge-Juller, W. van Duijn, V. Ferreira, R. D. Fontijn, G. David, D. W. Hommes, C. B. Lamers, et al. 2008.

VEGF release by MMP-9 mediated heparan sulphate cleavage induces colorectal cancer angiogenesis. Eur. J. Cancer. 44: 1904-1913.

39. Lee, S., S. M. Jilani, G. V. Nikolova, D. Carpizo, and M. L. Iruela-Arispe. 2005. Processing of VEGF-A by matrix metalloproteinases regulates bioavailability and vascular patterning in tumors. *J. Cell Biol.* 169: 681-691.

APPENDIX

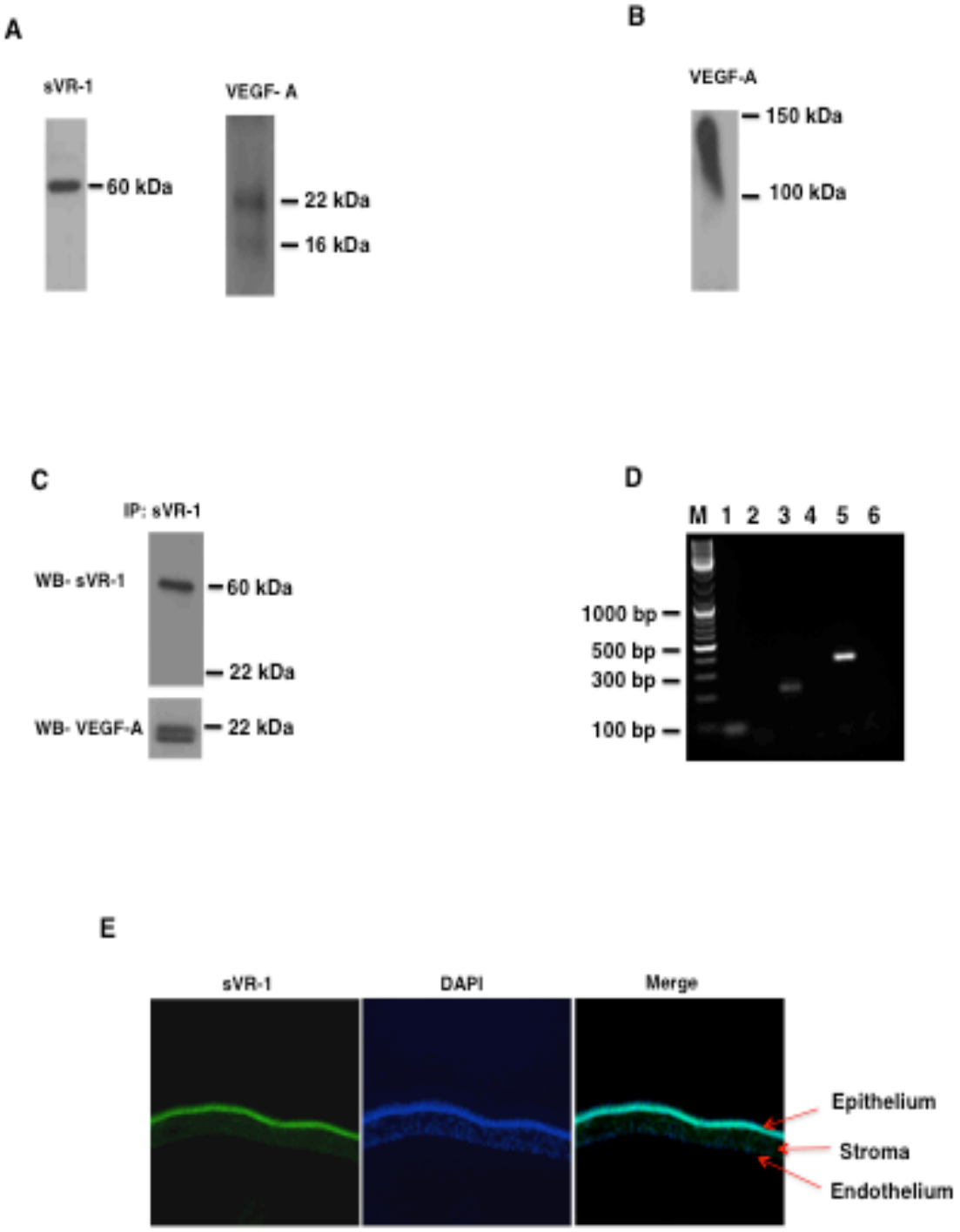
A
sVR-1
60 kDa
VEGF- A
22 kDa
16 kDa
B
VEGF-A
150 kDa
100 kDa
C
IP: sVR-1
WB- sVR-1
60 kDa
22 kDa
WB- VEGF-A
22 kDa
D
M 1 2 3 4 5 6
1000 bp
500 bp
300 bp
100 bp
E
sVR-1
DAPI
Merge
Epithelium
Stroma
Endothelium

FIGURE 3.1. NORMAL CORNEA EXPRESSES VEGF-A BOUND TO SVEGFR-1.

WT mice were sacrificed and 4 to 6 corneas were collected and pooled for WB, Co-immunoprecipitation, and mRNA analysis by RTPCR. Data are representative of two independent experiments. (A) Reducing WB analysis for sVEGFR-1 and VEGF-A reveals presence of sVEGFR-1 at 62 kDa and two isoforms of VEGF-A at 22 and 16 kDa in normal cornea. (B) Non-reducing WB for VEGF-A shows the presence of a much larger band between molecular size of 100 to 150 kDa consistent with its being the bound form. (C) sVEGFR-1 was immunoprecipitated from normal corneal extracts, with anti sVEGFR-1 mAb and the complex was analyzed for the co-immunoprecipitation of VEGF-A by WB. Normal cornea shows the presence of VEGF-A bound to sVEGFR-1. (D) Agarose gel analysis of VEGF-A (214bp) (lane 3) and sVEGFR-1 (358bp) (lane 5) cDNA from normal uninfected cornea. Lane M-marker, lane 1- β-actin (92bp), lane 2, 4 and 6 are reverse transcriptase negative controls for β- actin, VEGF-A and sVEGFR-1. (E) Representative immunofluorescence staining of corneal section for sVEGFR-1 (green, left panel), nuclei (blue, middle panel) reveals the presence of sVEGFR-1 mainly in the corneal epithelial layer and to a lesser extent in the stroma (Merge). Nuclei were stained (blue) with DAPI. Image is representative of two independent experiments. Original magnification × 10.

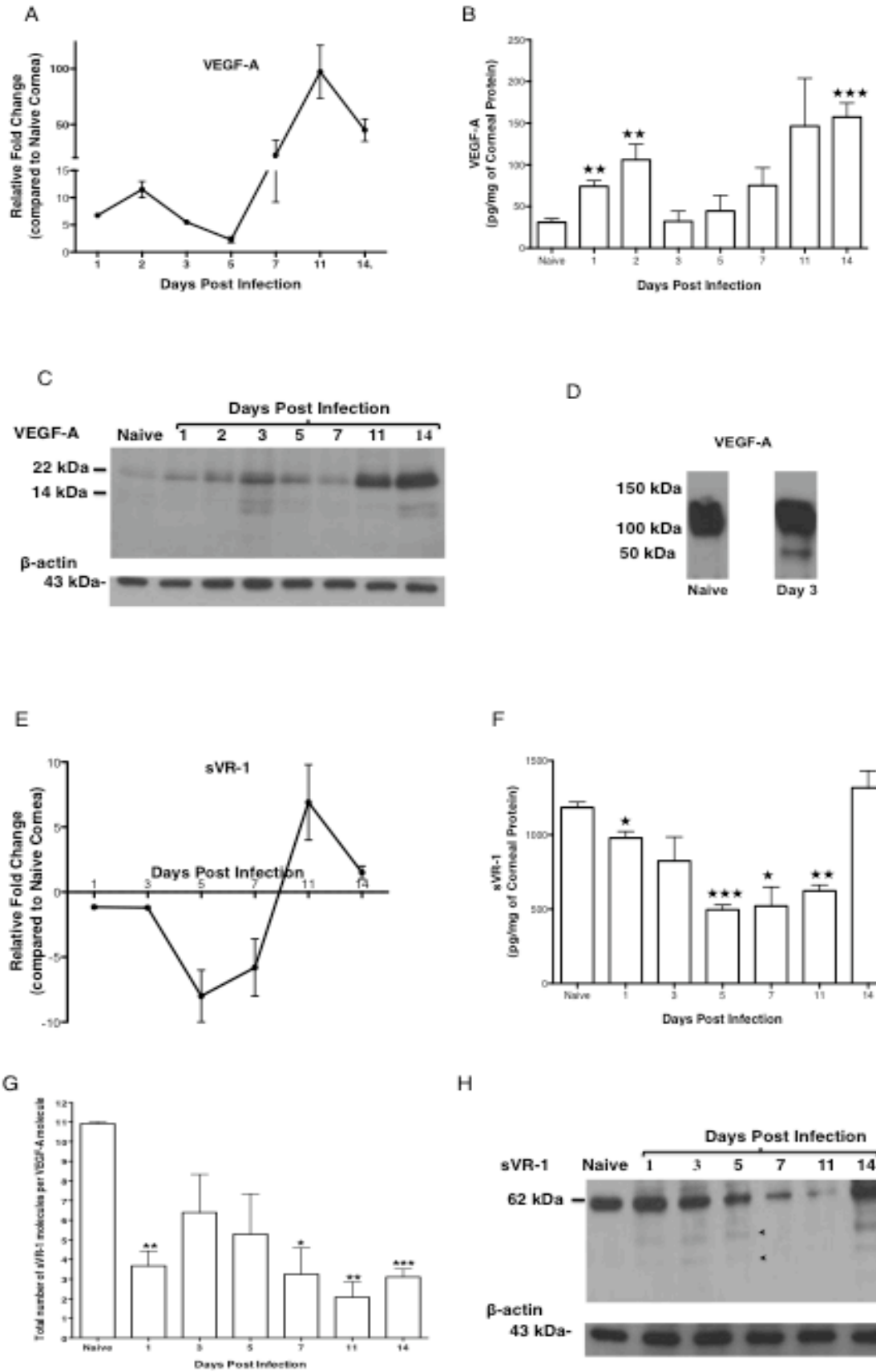
A
VEGF-A
Relative Fold Change (compared to Naive Cornea)
Days Post Infection
B
VEGF-A (pg/mg of Corneal Protein)
Naive
Days Post Infection
C
VEGF-A
Naive
Days Post Infection
22 kDa
14 kDa
β-actin
43 kDa
D
VEGF-A
150 kDa
100 kDa
50 kDa
Naive
Day 3
E
sVR-1
Relative Fold Change (compared to Naive Cornea)
Days Post Infection
F
sVR-1 (pg/mg of Corneal Protein)
Naive
Days Post Infection
G
Days Post Infection
H
sVR-1
Naive
Days Post Infection
62 kDa
β-actin
43 kDa

FIGURE 3.2 CORNEAL HSV-1 INFECTION CAUSES AN IMBALANCE BETWEEN VEGFA AND SVEGFR-1.

WT mice corneas were scarified and infected with 10^4 PFU of HSV in PBS or mock infected with only PBS (naïve control mice). Corneas were harvested from infected mice at indicated time points PI and from naive control mice at 24 hr. (A) At each time point 6 corneas were collected and pooled for mRNA extraction. The expression levels of VEGF-A molecule were normalized to β-actin using ΔCt calculation. Relative expression between control and infected groups were calculated using the $2^{-\Delta\Delta Ct}$ formula. Kinetic analysis for the expression of VEGF-A mRNA by quantitative PCR (QPCR) at different days pi. The expression of VEGF-A shows a biphasic upregulation pattern, early on day 2 pi and then again on day 11 pi as compared to naïve cornea. Figure is a summary of two independent experiments and each experiment represent group of 6 corneas. (B) At each time point 6 corneas were harvested from infected or naïve mice and the levels of VEGF-A were determined by ELISA. Quantification of VEGF-A protein levels in the normal and infected corneas at different days pi reveals similar pattern as that of gene expression. Figure is a summary of at least two independent experiments and each experiment represent group of 6 corneas. $P \leq 0.009$ (**), $P = 0.0004$ (***). (C) At each indicated time points 3-4 corneas were harvested and total protein concentration were measured by BCA protein assay. Samples with equal protein concentration were subjected to SDS-PAGE followed by WB analysis. VEGF-A expression was analyzed by WB analysis showed an increase in the VEGF-A protein levels at different days pi compared to naïve control mice. (D) Three to four corneas were harvested from day 3 pi or naïve control mice at 24 hr pi. Samples with equal protein concentration were subjected to native-

PAGE followed by WB analysis. The left figure shows a band of molecular size between 100 to 150 kDa in naïve corneal sample. The right is from day 3 infected corneas. It shows the large 100-150 kDa band as well as another at 50 kDa indicating the presence of both bound and free VEGF-A. (E) Kinetic analysis for the expression of sVEGFR-1 mRNA by QPCR at different days pi. Relative change in the expression of sVEGFR-1 mRNA at different days pi as compared to the uninfected mice revealed a sharp decrease in the sVEGFR-1 expression from day 3 pi which reached above normal around day 11 pi and back to normal levels at day 14 pi. The figure is a summary of two independent experiments and each experiment represent group of 6 corneas. (F) sVEGFR-1 protein levels analyzed by ELISA from the normal and infected corneas at different days pi shows an early decrease after HSV-1 infection which reaches to level found in normal controls at day 14 pi. The figure is a summary of at least two independent experiments and each experiment represent group of 6 corneas. $P \leq 0.05$ (*), $P = 0.0023$ (**), $P \leq 0.0001$ (***)**.** (G) Quantification of total number of sVEGFR-1 molecules per VEGF-A molecule from naïve and infected corneas at different days pi using protein quantities obtained by ELISA (B & F) shows the significant reduction of total number of sVEGFR-1 molecules per VEGF-A molecule on day 1 and from day 7 to 14 pi. The total number of molecules for sVEGFR-1 and VEGF-A were calculated by multiplying the total quantity of the protein by its molecular weight and Avogadro's number. The figure is a summary of values obtained from figure B and F. $P = 0.0216$ (*), $P \leq 0.0032$ (**), $P \leq 0.0002$ (***)**.** (H) Reducing WB analysis for sVEGFR-1 from uninfected and infected corneas at different time pi shows degradation of sVEGFR-1 after HSV-1 infection. Degraded products are shown by black arrowhead.

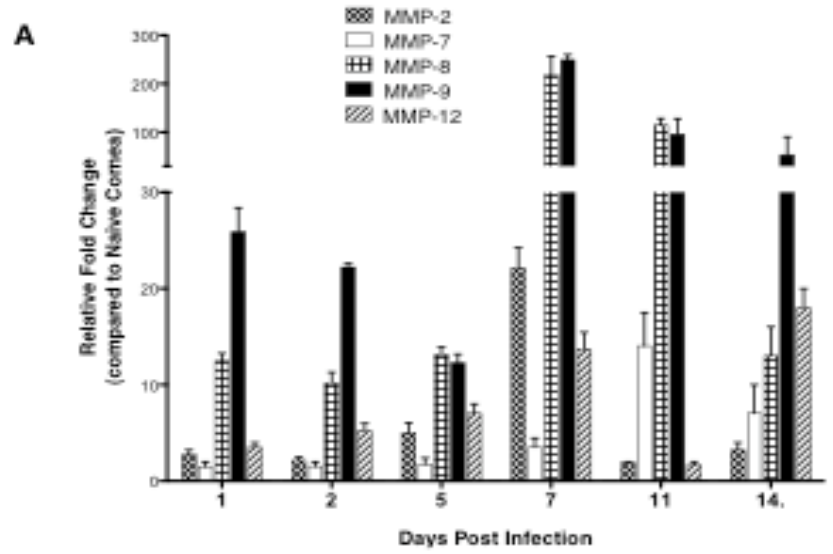
A
MMP-2
MMP-7
MMP-8
MMP-9
MMP-12
Relative Fold Change (compared to Naive Cornea)
300
200
100
30
20
10
0
1
2
5
7
11
14.
Days Post Infection

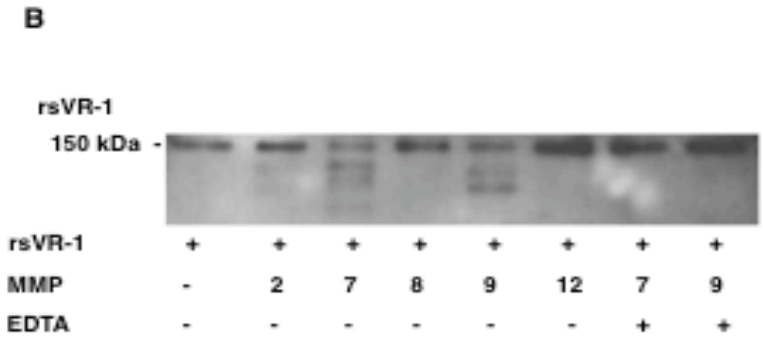
B
rsVR-1
150 kDa -
rsVR-1 + + + + + + + +
MMP - 2 7 8 9 12 7 9
EDTA - - - - - - + +

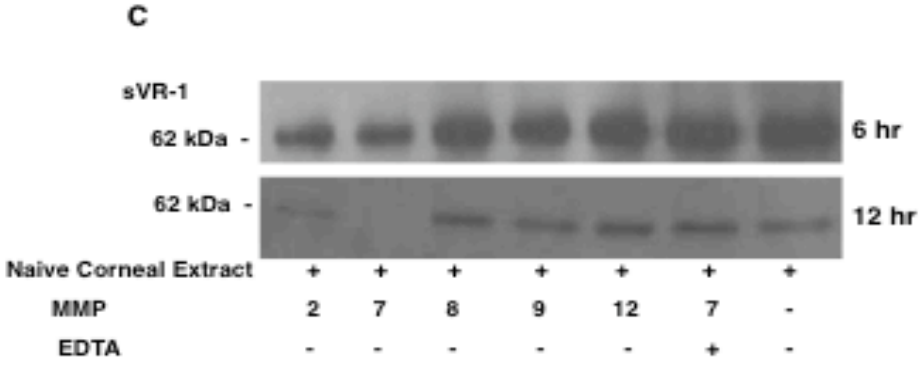
C
sVR-1
62 kDa -
6 hr
62 kDa -
12 hr
Naive Corneal Extract + + + + + + +
MMP 2 7 8 9 12 7 -
EDTA - - - - - + -

FIGURE 3.3. RSVEGFR-1 ADMINISTRATION HINDERS ANGIOGENIC ACTIVITY OF VEGF-A AND INHIBITS CORNEAL ANGIOGENESIS POST HSV-1 INFECTION.

WT mice were ocularly infected by corneal scarification with 10^4 PFU of HSV. (A) rsVEGFR-1 or isotype Fc protein were administered subconjunctivally at 5 μg/eye as shown. The extent of angiogenesis and SK lesion severity in the eyes of HSV infected mice were quantified in a blinded manner using a scale as described in materials and methods. The progression of angiogenesis and SK lesion severity were significantly reduced in the group of mice treated with rsVEGFR-1 as compared to isotype treated mice. Data are representative two independent experiments (n = 10-12 mice/group). $P \leq 0.0007$ (***). (B) Representative whole mount corneas stained for CD31 (lower panel) at day 15 pi shows reduced angiogenic response in rsVEGFR-1 treated mouse. Bars, 100μm. (C) Representative eye photos shows reduced SK lesion severity as well as angiogenesis from rsVEGFR-1 treated mouse compared to isotype treated mouse. (D) rsVEGFR-1 or isotype Fc protein treated mice were sacrifice on day 15 pi and corneas were collected for surface staining of eye infiltrating cells. Total cell numbers per cornea for $CD31^+$ cells, Neutrophils ($CD11b^+$, $Ly6G^+$ cells) gated on total $CD45^+$ cells and $CD4^+$ T cells showed the significant reduction in total numbers of the respective cell population from rsVEGFR-1 treated mice as compared to the isotype treated mice. Data are a representative of two independent experiments (n = 3-5/group). $P = 0.012$ (*), $P \leq 0.0015$ (**). (E) Therapeutic administration of the rsVEGFR-1 was started from day 7 pi when SK becomes visibly evident. Therapeutic administration of rsVEGFR-1 also showed significant reduction in angiogenesis as well as lesion severity further confirming the

inhibitory effect of sVEGFR-1 on the angiogenic activity of VEGF-A. Data are a representative of two independent experiments (n = 8 mice/group). $P \leq 0.012$ (*).

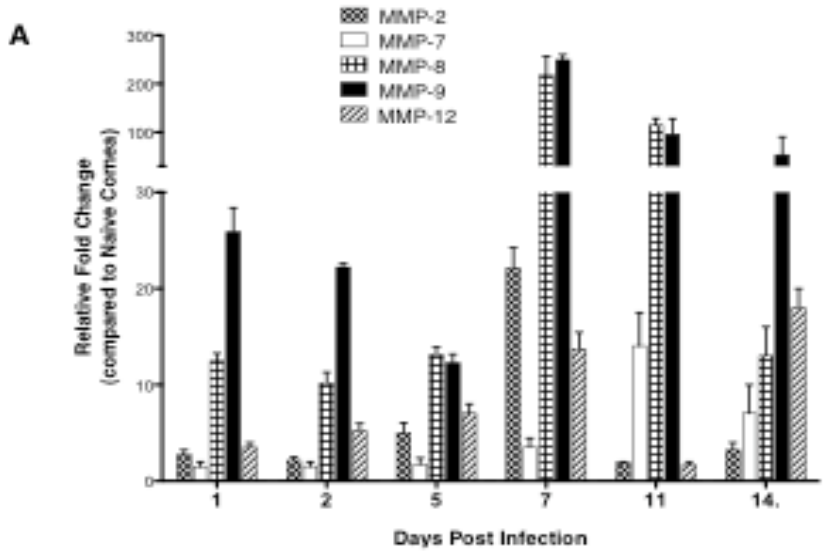
A
MMP-2
MMP-7
MMP-8
MMP-9
MMP-12
Relative Fold Change (compared to Naive Cornea)
300
200
100
30
20
10
0
1
2
5
7
11
14.
Days Post Infection

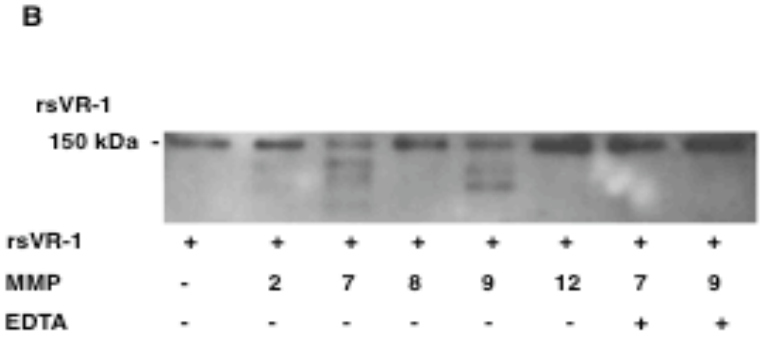
B
rsVR-1
150 kDa -
rsVR-1 + + + + + + + +
MMP - 2 7 8 9 12 7 9
EDTA - - - - - - + +

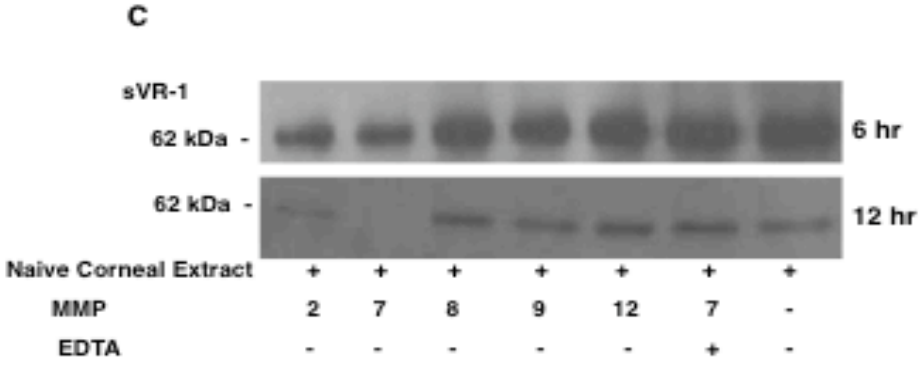
C
sVR-1
62 kDa -
6 hr
62 kDa -
12 hr
Naive Corneal Extract + + + + + + +
MMP 2 7 8 9 12 7 -
EDTA - - - - - + -

FIGURE 3.4. METALLOPROTEINASES ARE UPREGULATED AFTER HSV-1 INFECTION AND MMP-2, 7 AND 9 DEGRADES RSVEGFR-1 AND SVEGFR-1.

(A) WT mice corneas were scarified and infected with 10^4 PFU of HSV in PBS or mock infected with only PBS (naïve control mice). Corneas were harvested from infected mice at indicated time points PI and from naive control mice at 24 hr. At each time point 6 corneas were collected and pooled for mRNA extraction. The expression levels of different MMP molecule were normalized to β-actin using ΔCt calculation. Relative expression between control and infected groups were calculated using the $2^{-\Delta\Delta Ct}$ formula. Kinetic analysis for the relative fold change in the expression levels of MMP- 2, MMP-7, MMP-8, MMP-9 and MMP-12 mRNAs at different days pi. The mRNA expression of all the tested MMPs was upregulated in biphasic manner post HSV-1 infection with the first peak expression at day 1 pi and maximum expression between day 7 and day 11 pi. (B) Mouse rsVEGFR-1 was incubated with activated form of MMP-2, MMP-7, MMP-8, MMP-9 and MMP-12 for 12 hrs at 37^0C and analyzed by WB. MMP-7 (lane 3) showed maximum degradation of rsVEGFR-1 followed by MMP-9 (lane 5) and MMP-2 (lane 2). Addition of the MMP inhibitor, EDTA, inhibited the degradation of rsVEGFR-1 by MMP-7 (lane 7) and MMP-9 (lane 8). Figure is a representative of three independent experiments. (C) Corneal lysates from 4-6 pooled corneas of uninfected WT mice were incubated with activated form MMP-2, MMP-7, MMP-8, MMP-9 and MMP-12 either for 6 hr or 12 hr at 37^0C. The digested corneal lysates were analyzed by WB for sVEGFR-1. MMP-7 showed degradation of corneal sVEGFR-1 even after 6 hrs of incubation (upper panel, lane 2), with complete degradation after 12 hrs of incubation (lower panel, lane 2). MMP-2 (lower panel, lane 1) and MMP-9 (Lower panel lane 4) also showed degradation

of corneal sVEGFR-1 after 12 hrs of incubation. Addition of MMP inhibitor EDTA with MMP-7 (lane 6) showed inhibition of sVEGFR-1 degradation. Figure is a representative of three independent experiments.

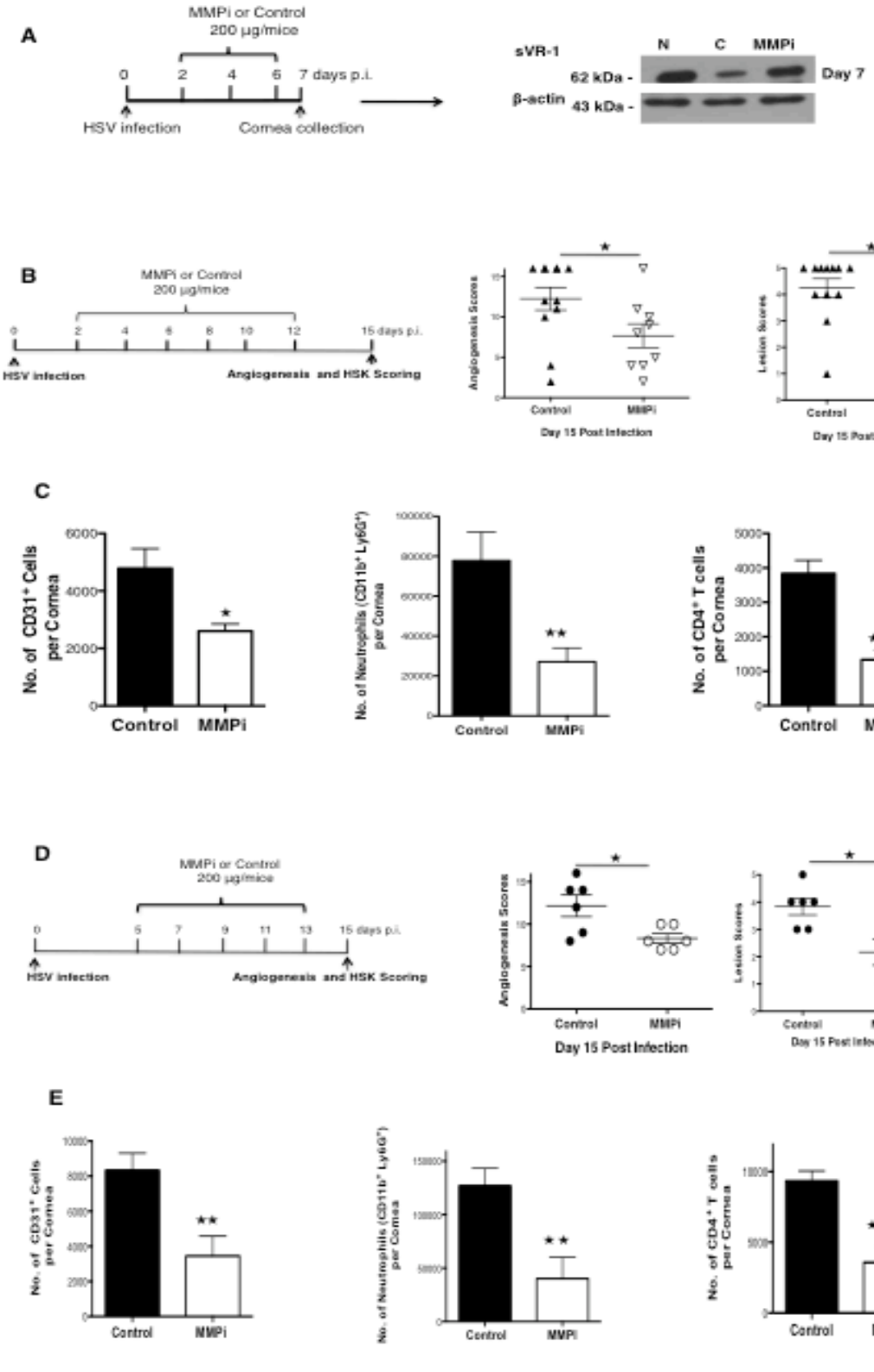
A
MMPi or Control
200 µg/mice
0 2 4 6 7 days p.i.
HSV infection
Cornea collection
sVR-1
N C MMPi
62 kDa -
Day 7
β-actin
43 kDa -
B
MMPi or Control
200 µg/mice
0 2 4 6 8 10 12 15 days p.i.
HSV infection
Angiogenesis and HSK Scoring
Angiogenesis Scores
Control
MMPi
Day 15 Post Infection
Lesion Scores
Control
MMPi
Day 15 Post Infection
C
No. of CD31+ Cells per Cornea
Control
MMPi
No. of Neutrophils (CD11b+ Ly6G+) per Cornea
Control
MMPi
No. of CD4+ T cells per Cornea
Control
MMPi
D
MMPi or Control
200 µg/mice
0 5 7 9 11 13 15 days p.i.
HSV infection
Angiogenesis and HSK Scoring
Angiogenesis Scores
Control
MMPi
Day 15 Post Infection
Lesion Scores
Control
MMPi
Day 15 Post Infection
E
No. of CD31+ Cells per Cornea
Control
MMPi
No. of Neutrophils (CD11b+ Ly6G+) per Cornea
Control
MMPi
No. of CD4+ T cells per Cornea
Control
MMPi

FIGURE 3.5. BLOCKING MMPS ACTIVITY IN VIVO RESCUES SVEGFR-1 DEGRADATION AND DIMINISHES ANGIOGENESIS AND SK SEVERITY.

WT mice corneas were scarified and infected with 10^4 PFU of HSV or mock infected with only PBS (naïve control mice). Marimastat, a broad-spectrum MMP inhibitor (MMPi) was administered subconjunctivally at 200 ug/mouse as shown. Mice in control group received HSV infection with mock treatment. (A) WB analysis of the corneal lysates collected from naïve (N), control treated (C) and MMPi treated mice at day 7 pi shows that MMPi rescues degradation of sVEGFR-1 post HSV-1 infection. The figure is a representative of two independent experiments. (B) Preventive treatment of MMPi in mice infected with HSV-1 was started from day 2 pi as shown. MMPi treatment showed a significant reduction of angiogenesis as well as SK lesion severity at day 15 pi. Data are representative of two independent experiments (n = 9-12 mice/group). $P \leq 0.04$ (*), $P = 0.0065$ (**). (C) MMPi treated or control mice were sacrifice on day 15 pi and corneas were collected for surface staining of eye infiltrating cells. Analysis for total cell numbers per cornea for $CD31^+$ cells, neutrophils ($CD45^+$ $CD11b^+$ $Ly6G^+$ cells) and $CD4^+$ T cells showed significant reduction in frequencies as well as total numbers of the respective cell population in the MMPi treated mice. Data are a representative of two independent experiments (n = 7/group). $P = 0.0115$ (*), $P = 0.0078$ (**), $P = 0.0002$ (***). (D) Therapeutic administration of the MMPi (started from day 5 pi), also showed reduced angiogenesis as well as SK lesion severity at day 15 pi. Data are a summary of two independent experiments (n = 6 mice/group). $P \leq 0.021$ (*). (E) Analysis of total cell numbers per cornea for $CD31^+$ cells, neutrophils ($CD45^+CD11b^+$, $Ly6G^+$ cells) and $CD4^+$ T cells also showed the significant reduction in the total cell numbers per cornea after

preventive MMPi treatment. Data are a representative of two independent experiments (n = 5-6/group). $P \leq 0.0094$ (**).

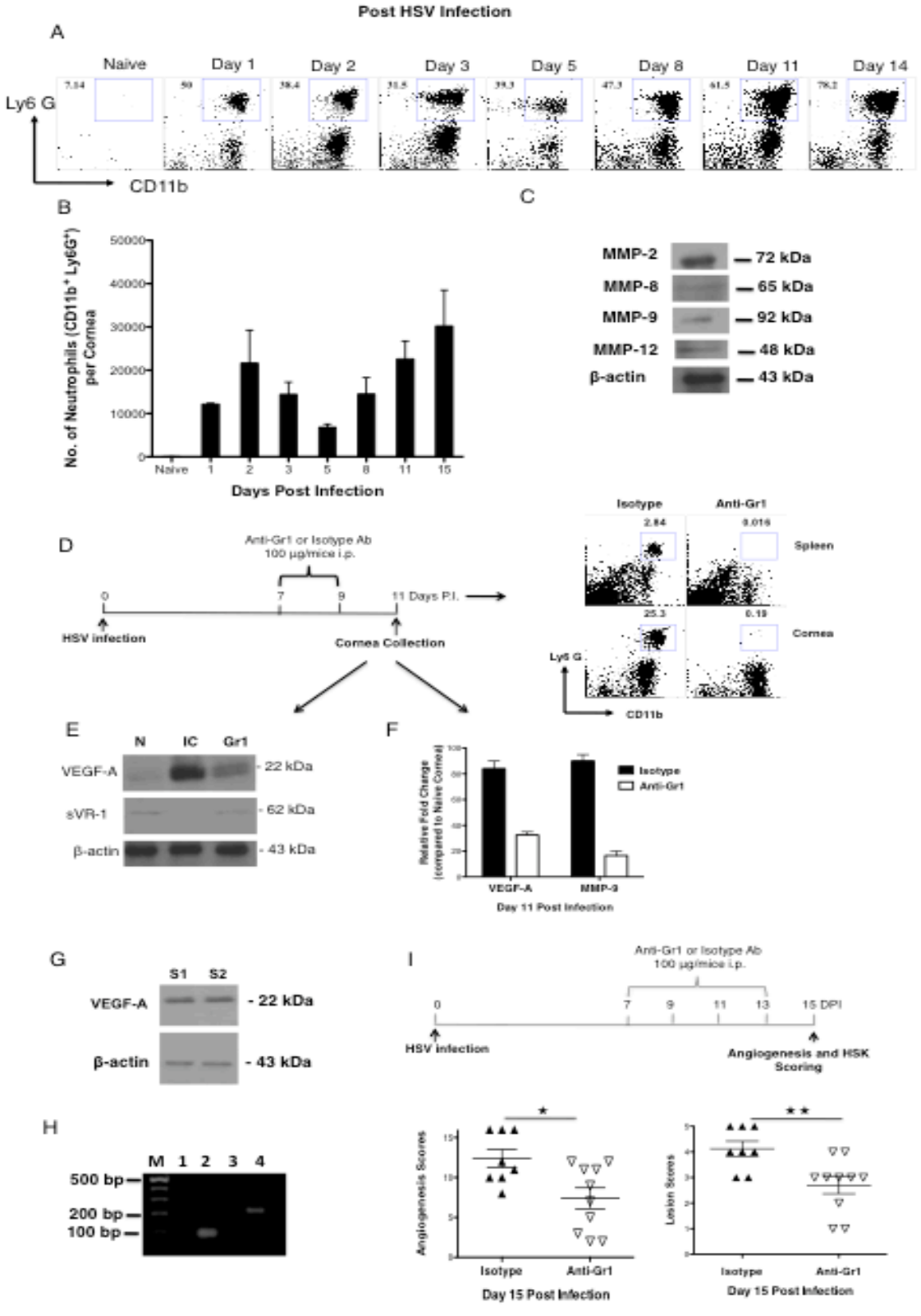
Post HSV Infection
A
Naive
Day 1
Day 2
Day 3
Day 5
Day 8
Day 11
Day 14
Ly6 G
CD11b
B
No. of Neutrophils (CD11b+ Ly6G+) per Cornea
Naive
Days Post Infection
C
MMP-2
MMP-8
MMP-9
MMP-12
β-actin
72 kDa
65 kDa
92 kDa
48 kDa
43 kDa
D
Anti-Gr1 or Isotype Ab
100 µg/mice i.p.
HSV infection
Cornea Collection
11 Days P.I.
Isotype
Anti-Gr1
Spleen
Cornea
E
N
IC
Gr1
VEGF-A
sVR-1
β-actin
22 kDa
62 kDa
43 kDa
F
Relative Fold Change (compared to Naive Cornea)
VEGF-A
MMP-9
Day 11 Post Infection
G
S1
S2
VEGF-A
β-actin
22 kDa
43 kDa
H
M
1
2
3
4
500 bp
200 bp
100 bp
I
Anti-Gr1 or Isotype Ab
100 µg/mice i.p.
HSV infection
Angiogenesis and HSK Scoring
15 DPI
Angiogenesis Scores
Lesion Scores
Isotype
Anti-Gr1
Day 15 Post Infection

FIGURE 3.6. NEUTROPHIL, THE PRINCIPAL CELL IN CORNEA AFTER HSV-1 INFECTION IS SOURCE OF MMPS AND VEGF-A.

WT mice corneas were scarified and infected with 10^4 PFU of HSV or mock infected with only PBS (naïve control mice). At each indicated day pi two mice were sacrificed, corneas were harvested and single cell suspensions were analyzed for surface staining by flow cytometry. (A) Representative FACS plot from each time point shows the percentage of neutrophils ($CD11b^+Ly6G^+$) gated on total $CD45^+$ cells. (B) Total number of neutrophils per cornea at each indicated time point post HSV-1 infection. Data are expressed as mean ± SEM. Figure is a summary of two independent experiments and each experiment represent group of 2 corneas. (C) $Ly6G^+$ neutrophils were purified from day 2 pi corneas using anti-Ly6G beads. Cell suspension from 6-8 pooled corneas was used for neutrophil purification. Western blot analysis for MMP-2, MMP-8, MMP-9 and MMP-12 from purified neutrophils. Data is from single experiment and represent neutrophils from group 6-8 corneas. (D) Neutrophil depletion was carried out from day 7 pi, using anti-Gr-1 mAb (100 μg/mice, intra-peritoneally) as shown. Mice in the control group received isotype control antibody. Representative FACS plot shows complete depletion of neutrophils from spleen (upper panel) and cornea (lower panel) analyzed at day 11 pi. (E) Corneal lysates from normal (N), isotype control antibody treated (IC) and neutrophil depleted (Gr-1) from day 11 pi mice, were analyzed by WB for VEGF-A (upper panel), sVEGFR-1 (middle panel). Figure is a representative of two experiments and each experiment represent at least 3 corneas. (F) Relative fold change in the expression of VEGF-A and MMP-9 mRNA in neutrophil depleted and isotype antibody treated mice at day 11 pi as compared to naïve mock infected mice. Figure is a

representative of two experiments and each experiment represent at least 4 corneas. $Ly6G^+$ neutrophils were sorted from day 11 pi corneas. Cell suspension from 6-8 pooled corneas was used for neutrophil purification. Purified neutrophils were analyzed by either WB or RTPCR for the expression of VEGF-A. (G) Reducing WB analysis for VEGF-A from two different samples S1- Sample 1 and S2-Sample 2 shows the presence of VEGF-A protein from purified neutrophil samples. Data represent two different experiments and each sample represent neutrophils from 6-8 corneas. (H) Agarose gel analysis for β-actin (92bp) (lane 2) and VEGF-A (214bp) (lane 4) of cDNA from purified neutrophils. Lane 1 and 3 are reverse trancriptase negative control for β-actin and VEGF-A respectively. (I) Neutrophil depletion started from day 7 pi and continued until day 13 pi resulted in reduced angiogenesis as well as SK lesion severity. Data are representative of a two independent experiments (n = 8-10 mice/group). P = 0.0131 (*), P = 0.0068 (**).

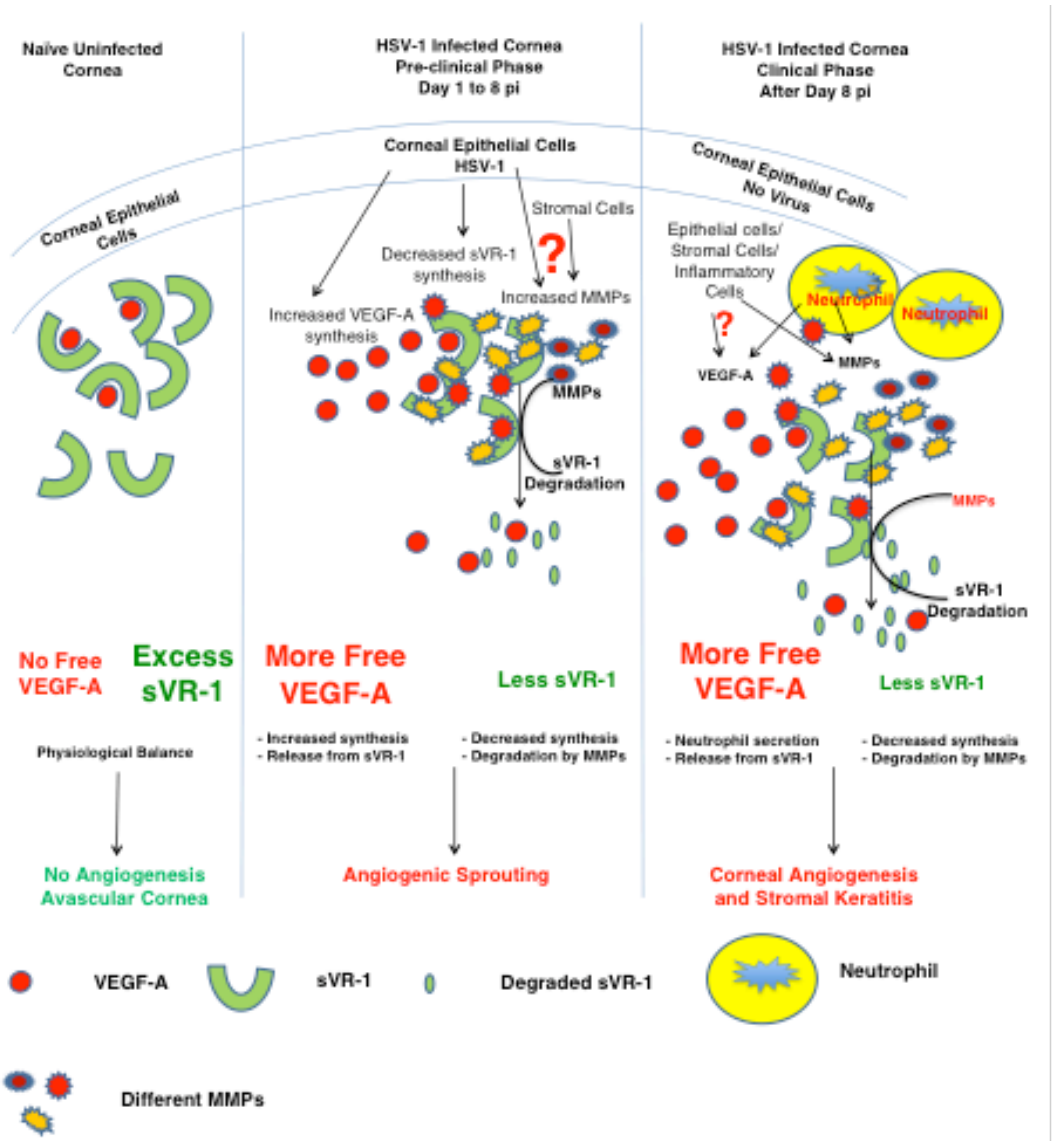
Naïve Uninfected Cornea
HSV-1 Infected Cornea Pre-clinical Phase Day 1 to 8 pi
HSV-1 Infected Cornea Clinical Phase After Day 8 pi
Corneal Epithelial Cells
Corneal Epithelial Cells HSV-1
Stromal Cells
Decreased sVR-1 synthesis
Increased VEGF-A synthesis
Increased MMPs
MMPs
sVR-1 Degradation
Corneal Epithelial Cells No Virus
Epithelial cells/ Stromal Cells/ Inflammatory Cells
Neutrophil
Neutrophil
VEGF-A
MMPs
MMPs
sVR-1 Degradation
No Free VEGF-A
Excess sVR-1
More Free VEGF-A
Less sVR-1
More Free VEGF-A
Less sVR-1
Physiological Balance
- Increased synthesis
- Release from sVR-1
- Decreased synthesis
- Degradation by MMPs
- Neutrophil secretion
- Release from sVR-1
- Decreased synthesis
- Degradation by MMPs
No Angiogenesis Avascular Cornea
Angiogenic Sprouting
Corneal Angiogenesis and Stromal Keratitis
VEGF-A
sVR-1
Degraded sVR-1
Neutrophil
Different MMPs

FIGURE 3.7. SCHEME ILLUSTRATING THE MECHANISM FOR HSV-1 MEDIATED CORNEAL ANGIOGENESIS.

Normal uninfected cornea constitutively secretes large amount of sVEGFR-1 and small amounts of VEGF-A. sVEGFR-1 constrains the physiological effect of VEGF-A by binding it with very high affinity (Left panel). Early after corneal HSV-1 infection, there is sudden increase in the levels of VEGF-A primarily being produced by infected or nearby uninfected corneal epithelial cells. However, levels of sVEGFR-1 go down mainly due to decreased production of sVEGFR-1 by corneal epithelial cells and also due to degradation by MMP-2, MMP7 and MMP9. This in turns leads to more physiologically active VEGF-A, which is now free from inhibitory effect of sVEGFR-1. This active form of VEGF-A drives the initial angiogenic sprouting early after HSV infection (middle panel). During chronic phase of HSK, when HSV-1 is no longer detected in the cornea, inflammatory cells particularly neutrophils act as a source of VEGF-A and different MMPs. This second wave of VEGF-A and MMPs further maintains the angiogenic response by continuous supply of active form of VEGF-A and MMPs, which degrades sVEGFR-1. The development of new leaky blood vessels leads to the release of more plasma and inflammatory cells in the cornea thus setting the stage for chronic SK and blindness (Left Panel).

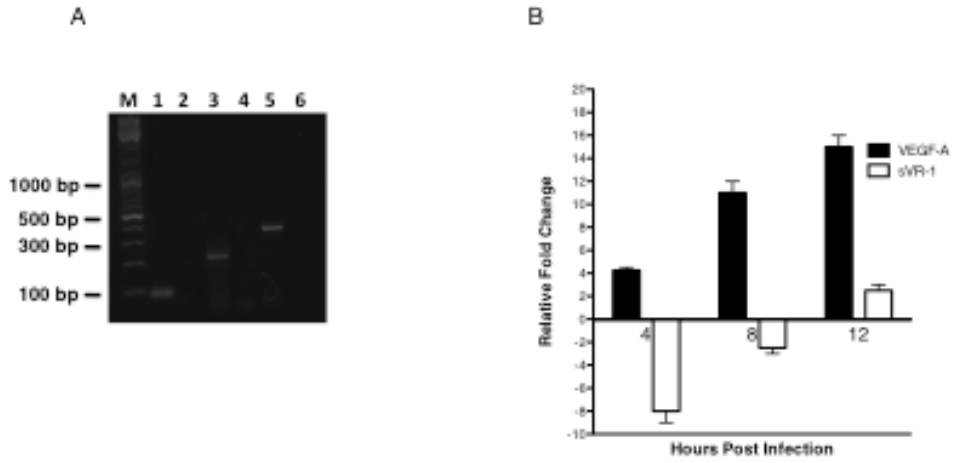

SUPPLEMENTAL FIGURE 3.1: HSV-1 INFECTION OF MK/T-1 CELLS DIFFERENTIALLY REGULATES THE EXPRESSION OF SVEGFR-1 AND VEGF-A.

(A) Uninfected MK/T-1 cells express both VEGF-A (214bp) (lane 3) and sVEGFR-1 (358bp) (lane 5) as shown by agarose gel analysis for cDNA. Lane M- marker, lane 1- β-actin (92bp), lane 2, 4 and 6 are reverse transcriptase negative controls for β- actin, VEGF-A and sVEGFR-1. Figure is representative of two independent experiments. (B) MK/T-1 cells were infected with 3 MOI of HSV-KOS. At each time point cells were harvested for mRNA extraction. The expression levels of VEGF-A and sVEGFR-1 molecule were normalized to β-actin using ΔCt calculation. Quantification of VEGF-A and sVEGFR-1 mRNA at different time point shows differential gene expression post HSV infection as compared to uninfected cells. Data are expressed as mean ± SEM. Figure is a summary of two independent experiments.

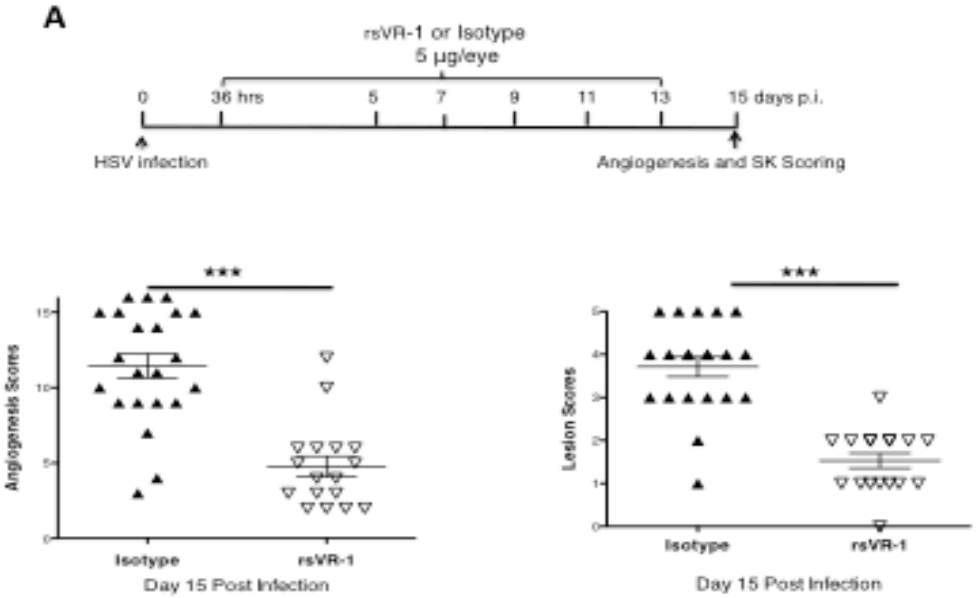
A
rsVR-1 or Isotype
5 µg/eye
0
36 hrs
5
7
9
11
13
15 days p.i.
HSV infection
Angiogenesis and SK Scoring
***
Angiogenesis Scores
Isotype
rsVR-1
Day 15 Post Infection
***
Lesion Scores
Isotype
rsVR-1
Day 15 Post Infection

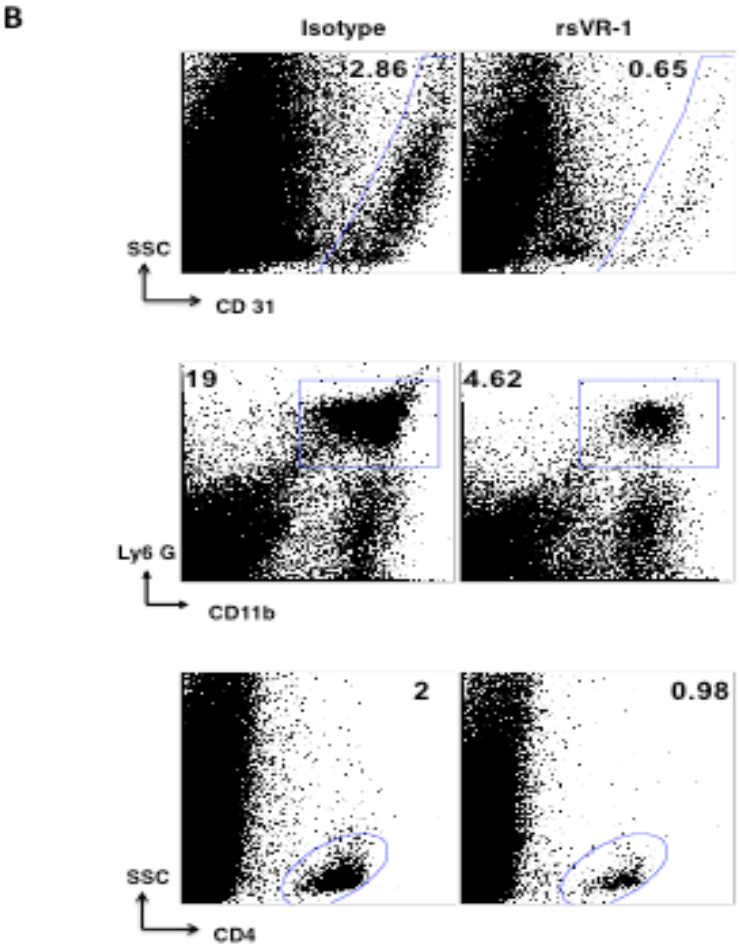
B
Isotype
rsVR-1
2.86
0.65
SSC
CD 31
19
4.62
Ly6 G
CD11b
2
0.98
SSC
CD4

SUPPLEMENTAL FIGURE 3.2. RSVEGFR-1 TREATMENT POST HSV INFECTION DIMINISHES ANGIOGENESIS AND SK LESION SEVERITY.

WT mice were ocularly infected by corneal scarification with 10^4 PFU of HSV. (A) rsVEGFR-1 or isotype Fc protein were administered subconjunctivally at 5 μg/eye as shown. The extent of angiogenesis and SK lesion severity in the eyes of HSV infected mice were quantified in a blinded manner using a scale as described in materials and methods. Cumulative scores for angiogenesis and SK lesion severity at day 15 pi. (n = 17-22 mice/group). Data are a summary of two independent experiments. P = 0.0001 (***). (B) Mice were sacrifice on day 15 pi and corneas were collected for surface staining of eye infiltrating cells. Representative FACS plot for CD31+ cells, Neutrophils ($CD11b^+$, $Ly6G^+$ cells) gated on total CD45+ cells and $CD4^+$ T cells showed reduced frequencies of respective cell population in the rsVEGFR-1 treated mice as compared to the isotype treated mice.

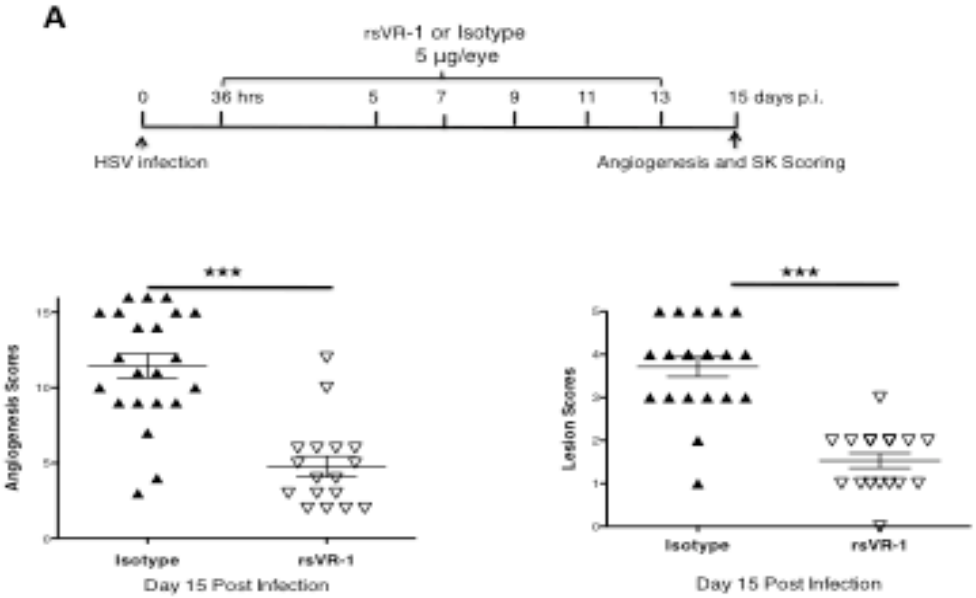
A
rsVR-1 or Isotype
5 µg/eye
0
36 hrs
5
7
9
11
13
15 days p.i.
HSV infection
Angiogenesis and SK Scoring
***
Angiogenesis Scores
Isotype
rsVR-1
Day 15 Post Infection
***
Lesion Scores
Isotype
rsVR-1
Day 15 Post Infection

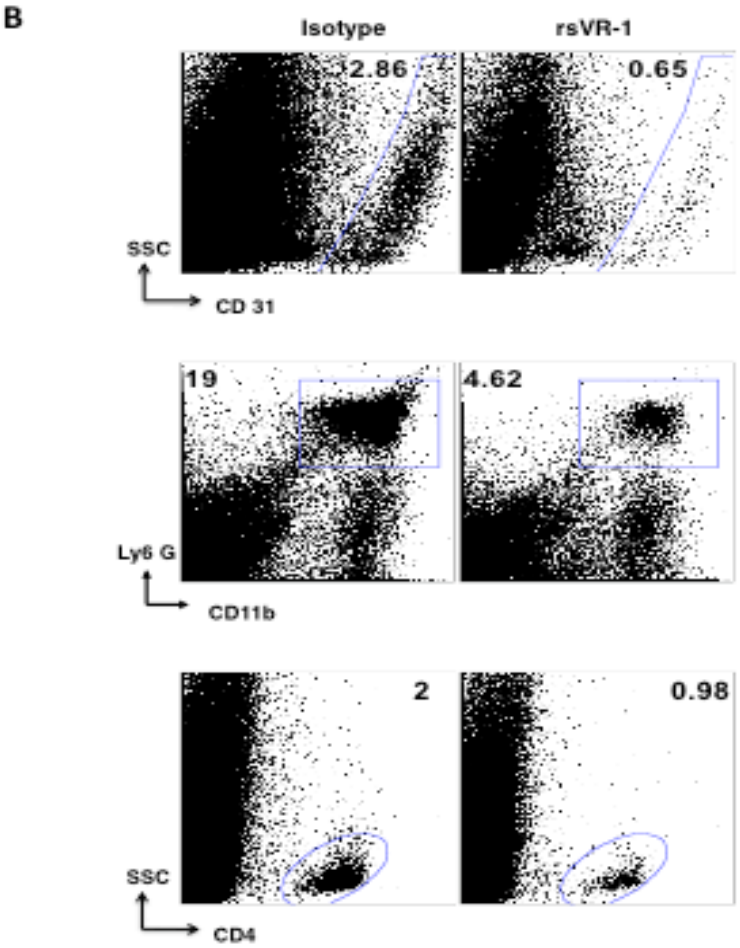
B
Isotype
rsVR-1
2.86
0.65
SSC
CD 31
19
4.62
Ly6 G
CD11b
2
0.98
SSC
CD4

SUPPLEMENTAL FIGURE 3.3. MMPI TREATMENT REDUCES THE FREQUENCIES $CD31^+$ ENDOTHELIAL CELLS, NEUTROPHILS AND $CD4^+$ T CELLS.

WT mice corneas were scarified and infected with 10^4 PFU of HSV or mock infected with only PBS (naïve control mice). Marimastat, a broad-spectrum MMP inhibitor (MMPi) was administered subconjunctivally at 200 ug/mouse preventively (A) or therapeutically (B) as shown. Mice in control group received HSV infection with mock treatment. Representative FACS plot and total cell numbers per cornea for $CD31^+$ cells, Neutrophils ($CD11b^+$, $Ly6G^+$ cells) and $CD4^+$ T cells showed significant reduction in frequencies the respective cell population in the MMPi treated mice.

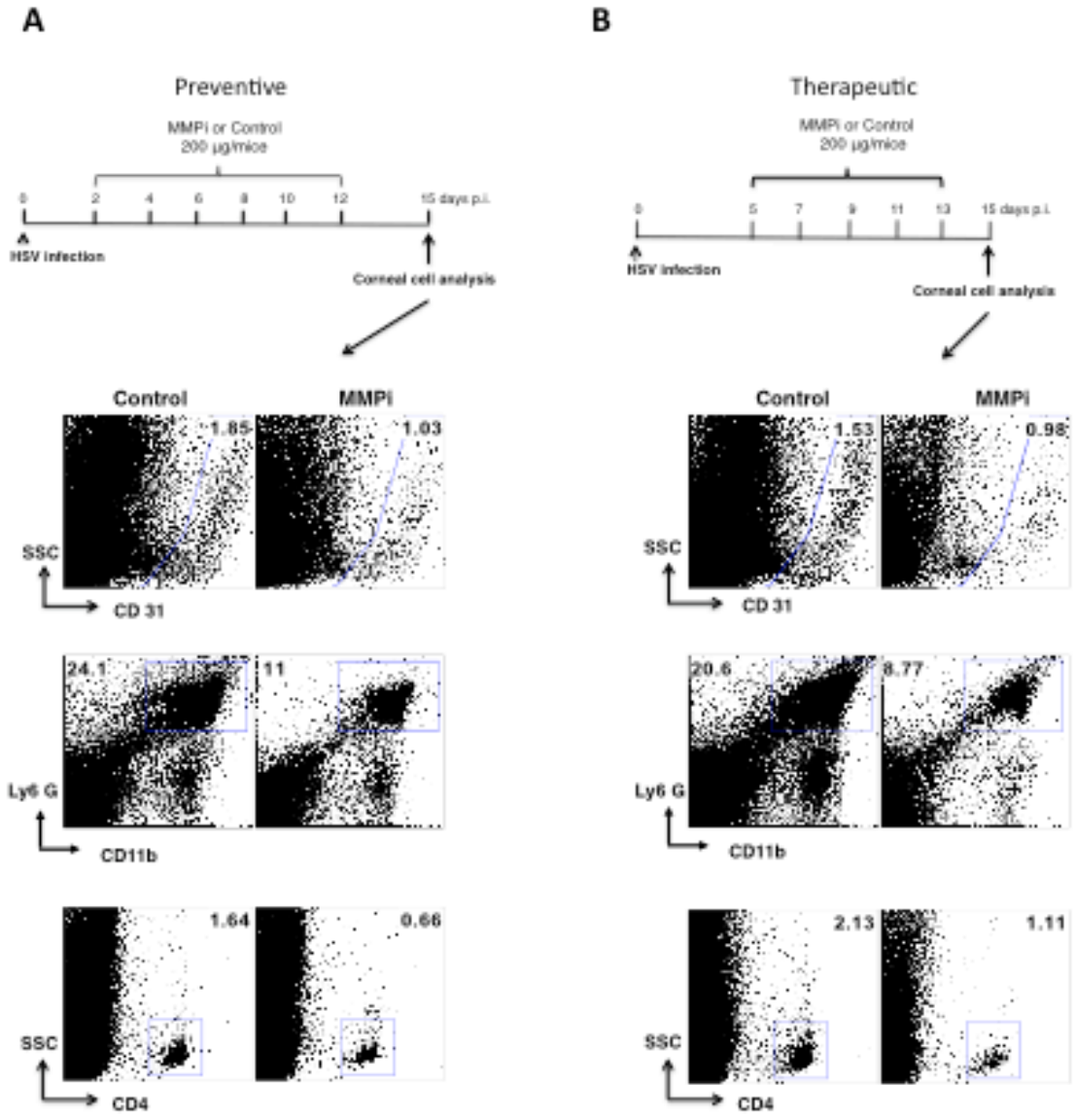
A
Preventive
MMPI or Control
200 µg/mice
0
2
4
6
8
10
12
15 days p.i.
HSV infection
Corneal cell analysis
Control
MMPI
1.85
1.03
SSC
CD 31
24.1
11
Ly6 G
CD11b
1.64
0.66
SSC
CD4
B
Therapeutic
MMPI or Control
200 µg/mice
0
5
7
9
11
13
15 days p.i.
HSV infection
Corneal cell analysis
Control
MMPI
1.53
0.98
SSC
CD 31
20.6
8.77
Ly6 G
CD11b
2.13
1.11
SSC
CD4

PART-IV

ROLE OF IL-17A IN HSV MEDIATED CORNEAL ANGIOGENESIS

In this chapter "our" and "we" refers to me and co-authors. My contribution in the chapter includes (1) Selection of the topic (2) Compiling and interpretation of the literature (3) Designing experiments (4) Understanding the literature and interpretation of the results (5) Providing comprehensible structure to the chapter (6) Preparation of graphs and figures (7) Writing and editing.

Abstract

Corneal herpes simplex virus (HSV) infection leads to the development of angiogenesis by causing an imbalance between vascular endothelial growth factor (VEGF) and its soluble receptor-1 (sVEGFR-1), however the underlying mechanisms are poorly understood. Here we demonstrate that IL-17A, a cytokine induced after HSV infection shifts the balance between VEGF-A and sVEGFR-1 and thereby promotes corneal angiogenesis. Accordingly, HSV infection of mice lacking IL-17 receptor (IL-17RAKO) and IL-17A neutralization in WT HSV infected mice resulted in significantly diminished corneal neovascularization, an outcome of multiple mechanisms. Firstly, IL-17A through direct and indirect actions promoted corneal VEGF-A levels by corneal stromal keratocytes. Secondly, IL-17A enhanced corneal matrix metalloproteinase (MMP) -2, -7 and -9 expression that additionally improved VEGF-A bioavailability through increased sVEGFR-1 degradation. Additionally, IL-17A potentiated the angiogenic response by increased expression of CXCL1/KC and subsequent migration of neutrophils in the cornea. Moreover, neutrophils contribute to the imbalance between VEGF-A and sVEGFR-1 by acting as a source of VEGF-A as well as MMPs that degrade sVEGFR-1. Collectively, the multiple actions of IL-17A acted to increase VEGF-A and

diminish the anti-angiogenic action of the sVEGFR-1. This could mean that targeting IL-17A mediated effects represent a useful therapeutic approach to manage ocular angiogenesis.

Introduction

Optimal vision demands corneal transparency so that light transmission proceeds to the retina without interruption. Several mechanisms are employed to achieve transparency. These include events that suppress angiogenesis and tissue damaging inflammatory and immune reactions in the pre-retinal tissues (*1-3*). The control system lacks perfection and breaks down in response to some injurious events. Infection of the cornea with herpes simplex virus-1 (HSV) is one such event and this can result in corneal blindness (stromal keratitis- SK) after frequent recrudescences from latent infection in the trigeminal ganglion (*3, 4*). The SK lesions, which largely represent T cell orchestrated inflammatory reactions set off by the virus (*5-7*), are one of the commonest infectious causes of vision loss in developed countries (*3*). One prominent feature of SK lesions is the establishment of new blood vessels in the normally avascular cornea (*3, 8, 9*). Most of our understanding of the pathogenesis of SK, particularly the role of neovascularization, comes from studies of animal models where SK is a regular outcome of primary HSV infection of the cornea (*5-7*). Although several molecules may participate in corneal neovascularization, the principal mediator is VEGF-A signaling through the VEGFR-2 receptor (*8, 10*). Curiously, VEGF-A is synthesized by the normal cornea, but its angiogenic activity is constrained by its binding to an excess of the soluble form of the VEGF receptor 1 (sVEGFR-1) that is produced by corneal epithelial cells (*2*). This

situation is often referred as the VEGF trap (*2, 11-13*). The consequence of HSV ocular infection is a change in the concentration balance between VEGF-A and the soluble receptor (*14*), but how this is achieved is not fully understood.

Previous studies have established that HSV infection, either directly or indirectly, causes the increased production of VEGF-A, but reduces the synthesis sVEGFR-1 (*8, 14-17*). Additionally, the inflammatory reaction induced by HSV includes the infiltration of cells that produce enzymes such as MMP-2, -7 and -9 that degrades sVEGFR-1, into inactive fragments (*14, 18*). Since regulation of VEGF levels and molecules that influence its signaling represent valuable approach to control pathological angiogenesis (*3, 8-10, 14, 19*), it is important to understand how the multiple molecules generated in the inflamed cornea after HSV infection impact on VEGF function. In the present report, we focus on the cytokine IL-17A which, as we showed recently (unpublished data), is rapidly upregulated in the eye after HSV infection. Moreover, past studies had demonstrated that fibroblasts and monocytes exposed in vitro to IL-17 may produce VEGF-A (*20-25*). Additionally, IL-17 was shown to play a role in mediating tumor angiogenesis by causing the proliferation and migration of vascular endothelial cells into tissue (*26*). Little is currently known about the participation of IL-17 in ocular angiogenesis, particularly how it might impact on the efficiency of the VEGF-A trap.

In the present report, we demonstrate that HSV induced IL-17A expression in the cornea is a critical factor responsible for changing the balance between VEGF-A and sVEGFR-1. HSV infection of mice lacking IL-17A signaling or neutralization of IL-17A in WT HSV infected mice showed reduced corneal angiogenic responses. The mechanisms for diminished angiogenesis were multiple and included reduced corneal

expression of VEGF-A but no effects on sVEGFR-1 levels by HSV infected IL-17RA-/- mice when compared to WT counterparts. Additionally, IL-17A induced IL-6 production by corneal stromal fibroblasts, and IL-6 in combination with IL-17A acted in concert to further up-regulate VEGF-A production. Furthermore, IL-17A directly enhanced MMP-9 production by corneal fibroblast cells as well as indirectly affected the corneal MMP-2 and MMP-9 expression after HSV infection. Theses MMPs further increased VEGF-A bioavailability through increased sVEGFR-1 degradation. Moreover, IL-17A also induced the expression of a neutrophil chemoattractant, CXCL1/KC in the cornea after HSV infection. The increased levels of CXCL1/KC in the cornea promoted the migration of neutrophils at the site of inflammation, which further affected the balance between VEGF-A and sVEGFR-1 by providing an additional source of pre-formed VEGF-A as well as sVEGFR-1 degrading MMPs. Taken together our data shows that IL-17A plays a central role in regulating ocular angiogenesis and does so at least in part by limiting the efficacy of the VEGF trap.

Material and Methods

Mice, Virus and cell lines. IL-17RA-/- mice on a C57BL/6 background were obtained from Amgen (Thousand Oaks, CA). C57BL/6 mice were purchased from Harlan Sprague Dawley, Indianapolis, IN. Animals were housed in the animal facilities approved by the Association for Assessment and Accreditation of Laboratory Animal Care (AAALAC) at The University of Tennessee and all experimental procedures were in complete agreement with the Association for research in Vision and Ophthalmology resolution on the use of animals in research. HSV-1 RE Tumpey viruse was grown in Vero Cell

monolayers (ATCC no. CCL81, American Type Culture Collection). The virus was concentrated, titrated, and stored in aliquots at -80^0 C until use. MK/T-1 cell line (Immortalised keratocytes from C57/BL6 mouse corneal stroma) was kindly gifted by Dr. Reza Dana, Schepens Eye Research Institute and Department of Ophthalmology, Harvard Medical School, Boston MA.

Corneal HSV Infection and Clinical Scoring. Corneal infections of mice were conducted under deep anaesthesia induced by i.p. injection of avertin as previously described (*8*). Mice were scarified on their corneas with 27-gauge needle, and a 3-µl drop containing 1×10^4 PFU of virus was applied to the eye. The eyes were examined on different days pi for the development and progression of clinical lesion by slit-lamp biomicroscope (Kowa Company, Nagoya, Japan). The progression of SK lesion severity and angiogenesis of individually scored mice was recorded. The scoring system was as follows: 0, normal cornea; +1, mild corneal haze; +2, moderate corneal opacity or scarring; +3, severe corneal opacity but iris visible; +4, opaque cornea and corneal ulcer; +5, corneal rupture and necrotizing keratitis. The severity of angiogenesis was recorded as described previously (*27*). According to this system, a grade of 4 for a given quadrant of the circle represents a centripetal growth of 1.5 cm towards the corneal center. The score of the four quadrants of the eye were then summed to derive the neo vessel index (range 0–16) for each eye at a given time point.

Sub-conjunctival Injection. Subconjunctival injections of anti-IL-17 were performed as described previously (*28*). Briefly, subconjunctival injections were done using a 2-cm, 32-gauge needle and syringe (Hamilton, Reno, NV) to penetrate the perivascular region

of conjunctiva, and the required dose of anti-IL-17 mAb was delivered into subconjunctival space. Control mice received isotype mAb.

IL-17 Neutralization. C57BL/6 mice were ocularly infected and 0.05 mg of anti-IL-17 was given intraperitoneally (ip) starting from day 7 followed by day 10 and 13 pi. For local depletion, 5 μg anti-IL-17 mAb was administered by sub-conjunctival injection either startind from day 1 pi followed by day 3 and day 5 pi for earl y depletion or starting from day 7 pi followed by day 9, day 11 and day 13 pi for late depletion.

γδ T cell Depletion. C57BL/6 mice were injected 2 days before infection with 500 μg per mouse of anti-mouse γδ TCR mAb (clone UC3-10A6) followed by 250 μg per mouse on day of infection.

Flow Cytometry. Corneas were excised, pooled group wise, and digested with 60 U/ml Liberase for 35 minutes at 37^0C in a humified atmosphere of 5% CO_2. After incubation, the corneas were disrupted by grinding with a syringe plunger on a cell strainer and a single-cell suspension was made in complete RPMI 1640 medium. The single cell suspensions obtained from corneas were stained for different cell surface molecules for FACS. All steps performed at 4^0C. Briefly, cell suspension was first blocked with an unconjugated anti□CD32/CD16 mAb for 30 min in FACS buffer. After washing with FACS buffer, samples were incubated with CD45-allophycocyanin (30-F11), CD11b-PerCP (M1/79), Ly6G-PE (1A8) and CD31-PE (MEC13.3) (All from BD Biosciences-Pharmingen) for 30 min on ice. Finally, the cells were washed three times and re-suspended in 1% *para*-formaldehyde. The stained samples were acquired with a FACS Calibur (BD Biosciences) and the data were analyzed using the FlowJo software.

Quantitative Real-Time PCR (qRT-PCR). Corneal cells were lysed and total mRNA was extracted using TRIzol LS reagent (Invitrogen). Total cDNA was made with 500 ng of RNA using oligo(dT) primer. Quantitative PCR was performed using SYBR Green PCR Master Mix (Applied Biosystem, Foster City, CA) with iQ5 real-time PCR detection ssystme (Bio Rad, Hercules, CA). The expression levels of different molecules were normalized to β-actin using ΔCt calculation. Relative expression between control and experimental groups were calculated using the $2^{-\Delta\Delta Ct}$ formula. The PCR primers used were as follows

β ACTIN- For 5'-TCCGTAAAGAATCTCATGCC-3', Rev 5'-ATCTTCATCCTCCTAGGAGC-3'; IFN-Ɣ For 5'-GGATGCATTCATGAGTATTGC-3', Rev 5'-GCTTCCTGAGGCTGGATTC-3'; IL17A For 5'- GCTCCAGAAGGCCCTCAG-3', Rev 5'- CTTTCCCTCCGCATTGACA-3'; IL6- For 5'- CGTGGAAATGAGAAAAGAGTTGTGC-3', Rev 5'-ATGCTTAGGCATAACGCACTAGGT-3' TGFβ-For 5'- TTGCTTCAGCTCCACAGAGA-3', Rev 5'- TGGTTGTAGAGGGCAAGGAC-3'; CCL20 - For 5'-GCCTCTCGTACATACAGACGC-3', Rev5'-CCAGTTCTGCTTTGGATCAGC-3'.

Western blot analysis. The supernatants from lysed corneal cells were quantified using BCA protein Assay kit (Thermo scientific, Waltham, MA) using BSA as a standard and samples with equal protein concentrations were denatured by boiling in Laemmli buffer. Polypeptides were resolved by SDS-PAGE and transferred onto a PVDF membrane. The membrane was blocked with 5% BSA in Tris-buffered saline with Tween20 (20 mM Tris [pH 7.4], 137 mM NaCl, and 0.1% Tween20) overnight at 4^0C and probed with specific primary and secondary antibodies. Proteins were detected using chemiluminiscent HRP

substrate (Millipore, Billerica, MA). The membrane was kept in stripping buffer for 10 min and re-probed using anti-β-actin antibody. The antibodies used were rat anti sVEGFR-1 (141515; R&D Systems), mouse anti-VEGF-A (EE02; Santa Cruz Biotechnology, Santa Cruz, CA), mouse anti-β-actin (AC74; Sigma-Aldrich, St Louis MO), goat anti rat IgG-HRP (R & D Systems), goat anti-mouse IgG-HRP (Santa Cruz Biotechnology) and donkey anti goat IgG-HRP (Santa Cruz Biotechnology).

Immunofluorescence staining. For immunofluorescence staining, the eyes from naïve uninfected mice were enucleated, and snap frozen in OCT compound. Six-micron thick sections were cut, air dried, and fixed in acetone-methanol (1:1) at room -20 ^{0}C for 10 min. Sections were blocked with 10% goat serum containing 0.05% Tween20 and 1:200 dilution of Fc block (Clone 2.42G2; BD Biosciences Pharmingen, San Diego, CA). Rat anti-Ly6G (Clone RB6-8C5; eBioscience) was diluted in 1% BSA containing 0.1% Triton-X and incubated at room temp for 1 hr. After incubations sections were washed several times with PBST and then stained with rabbit anti rat Alexa-488 for 45 min. The corneal sections were repeatedly washed with PBST and mounted with mounting media containing propidium iodide as a nuclear stain (Vector Laboratories) and visualized under a Immunofluorescence microscope.

ELISA. The pooled corneal samples were homogenized using a tissue homogenizer and supernatant was used for analysis. The concentrations of VEGF-A, sVEGFR-1, CXCXL-1/KC (R & D Systmes) and IL-6 (eBioscience) were measured by using sandwich ELISA kits as per the manufacturer's instructions.

Statistics. Student's t test was performed to determine statistical significance and data are expressed as mean ± SEM.

Results

Lack of IL-17A receptor signaling diminishes severity of HSV induced corneal angiogenesis

To study the role of IL-17A and IL-17A receptor signaling effects on HSV induced corneal angiogenesis, IL-17RA-/- mice were ocularly infected with HSV and the severity of angiogenesis was compared with infected control WT mice. At all time points, IL-17RA-/- mice showed significantly lesser angiogenesis than WT animals (Fig 4.1A-B). The onset of visible angiogenic sprouting was delayed, angiogenesis scores were lower and more mice had diminished angiogenesis scores in IL-17RA-/- mice as compared to their WT counterparts (Fig 4.1A). Additionally, not only the frequency but also the severity of angiogenesis (scores of $\geq$8) was reduced in mice in the IL-17RA-/- group (2 of 8 eyes at day 21) compared to WT counterparts (9 of 11 eyes at day 21) (Fig 4.1B). Analysis by FACS of pooled corneas from IL-17RA-/- and WT mice in each group at day15 pi revealed reduced frequencies as well as total numbers of $CD31^+$ cells (a marker for blood vessel endothelium) in IL-17RA-/- as compared to WT animals (Fig 4.1C-E).

Further evidence that IL-17A signaling was involved in HSV induced corneal angiogenesis came from measuring the outcome of neutralizing anti-IL-17 mAb treatment of HSV infected WT mice over a period of 15 days. IL-17 neutralization was started from day 7 pi when angiogenic sprouting became evident, followed by additional treatment on days 10 and 13 pi (Fig 4.2A). Animals that received the mAb showed a significant reduction in peak angiogenesis scores as compared to control isotype treated

mice (Fig 4.2B). Moreover, the frequency of severe angiogenesis (scores of ≥8) was significantly reduced in animals from the mAb recipients (3 of 8 eyes) as compared to isotype Ab recipients (7 of 8 eyes) (Fig 4.2C).

Interestingly, local sub-conjunctival administration of anti-ILA mAb showed an even more profound inhibitory effect on the onset as well as severity of HSV induced corneal angiogenesis (Fig 4.2D-G). Corneal samples collected at the end of the experiment revealed reduced frequency as well numbers of $CD31^+$ cells in the IL-17A neutralized group as compared to isotype mAb recipients (Fig 4.2H-J). Taken together these data indicate that mice lacking signaling for IL-17A were more resistant to HSV induced corneal angiogenesis indicating that IL-17A plays a critical role in driving the neovascularization resulting from HSV infection.

A. IL-17A differentially regulates VEGF-A and sVEGFR-1 expression after HSV infection

To further study the role of IL-17A in HSV induced corneal angiogenesis, the levels of VEGF-A and sVEGFR-1 produced by HSV infected corneas was measured by ELISA, RT-PCR and WB in both WT and IL-17RA-/- mice at various time points pi. As already described, compared to WT, IL-17RA-/- mice showed diminished levels of VEGF-A (Fig 4.3A-B), but the level of sVEGFR-1was not reduced and remained approximately the same as in uninfected control animals (Fig 4.3 C, D). Additionally, when the ratio of total number of sVEGFR-1 molecules per VEGF-A molecule from naïve mice was compared with infected animals at varios time points pi, the ratio was significantly decreased in WT animals at all days pi, but not in IL-17RAKO mice (Fig

4.3E). Furthermore, depletion of γδ T cells, which act as an early source of IL-17A, resulted into diminished levels of VEGF-A further confirming the role of IL-17A in VEGF-A production (Fig 4.3F-G). To further confirm the role of IL-17A in VEGF-A up-regulation, IL-17A neutralization was carried out either starting from day 1 until day 7 pi (Fig 4.3H), or starting from day 7 pi until day 15 pi (Fig 4.3I). Both the depletion strategies resulted into reduced VEGF-A mRNA expression (Fig 4.3J) as well as reduced VEGF-A protein production (Fig 4.3K).

Additional *in-vitro* experiments were performed with an immortalized murine corneal stromal fibroblast cell line (MK/T-1 cells) to measure the effect of IL-17A stimulation on the production of both VEGF-A and sVEGFR-1. Stimulation with IL-17A caused a dose dependent increase of VEGF-A secretion, but had minimal and insignificant effects on sVEGFR-1 levels as measured by ELISA (Fig 4.3L-N). Taken together, these in vitro studies also support the idea that the presence of IL-17A could shift the balance between VEGF-A to its inhibitory sVEGFR-1, making the VEGF-A trap less efficacious.

B. IL-17A induces IL-6 expression and in combination expands production of VEGF-A by corneal stromal fibroblasts.

One potential mechanism by which IL-17A acts could be to influence the expression of other cytokines known to be indirectly involved in angiogenesis such as IL-6 and IL-1β (*3, 16, 20, 23, 24*). To evaluate the possibility, levels of corneal IL-6 were compared between HSV infected IL-17RA-/- and WT counterparts at various days pi by RT-PCR. Corneal samples from IL-17RA-/- mice showed diminished expression of IL-6

at all tested days pi (Fig 4.4A). Moreover, local neutralization of IL-17A during early as well as late phase of HSV infection (Fig 4.4B) resulted into reduced mRNA expression of IL-6 on day 7 and day 15 pi (Fig 4.4C). Further *in-vitro* studies were done to study the effect of IL-17A on the expression of IL-6/IL-1β and their combined role in the induction of VEGF-A by corneal stromal fibroblasts (MK/T-1) cells. IL-17A increased the production by MK/T-1 cells of IL-6 in a dose dependent manner, and addition of anti-IL-17A mAb completely blocked IL-17A induced production of IL-6 (Fig 4.4D-E). Interestingly, IL-17A in combination with IL-6 and IL-1β potentiated VEGF-A production by corneal stromal fibroblast cells (Fig 4.4 F-H). Taken together, these data indicated that IL-17A indirectly promoted the expression of VEGF-A through increased expression of pro-angiogenic cytokines such as IL-6. These cytokines independently as well as in combination with IL-17A increased the expression of VEGF-A, further deviating the balance between VEGF-A and sVEGFR-1.

C. IL-17A drives increased expression of various MMPs responsible for sVEGFR-1 degradation

Another mechanism by which IL-17A signaling could influences angiogenesis was via its effect on the expression of different MMP enzymes that degrade sVEGFR-1, but not VEGF-A (*14, 29, 30*), into non-functional fragments. Comparing the corneal samples from HSV infected IL-17RAKO and WT mice taken at various days pi, levels of MMP-2, MMP-7 and MMP-9 were reduced in IL-17RAKO mice as compared to WT (Fig 4.5A-C). Furthermore, neutralization of IL-17A in WT HSV infected mice resulted into diminished expression of MMP-2, MMP-7 and MMP-9 when compared to isotype

treated animals (Fig 4.5 D-G). Additionally, in vitro experiments with IL-17A stimulated MK/T-1 cells also revealed dose dependent increase in MMP-9 mRNA expression as measured by RT-PCR (Fig 4.5H). This effect was inhibited by the addition of anti-IL-17A mAb indicating that it was IL-17A specific. Collectively, these results indicate that IL-17A could influence the efficacy of the VEGF-A trap by increasing the synthesis of some MMPs that can cause sVEGFR-1 degradation, making more VEGF-A available to induce angiogenesis.

C. Additional mechanisms caused by IL-17A affecting efficiency of the VEGF-A trap

Additional consequences of IL-17A induction following HSV infection might also contribute indirectly to angiogenesis by increased the synthesis of CXCL1/KC, a chemoattractant for neutrophils (*22, 23, 25, 31-33*). The consequent higher infiltration of neutrophils ($CD45^+CD11b^+$ $Ly6^+$ cells), act as a source of VEGF-A as well as sVEGFR-1 degrading MMPs (*14, 18, 34*). To test this possibility, we measured the levels of CXCL1/KC between WT and IL-17RAKO mice at various time points. At all times tested, significantly reduced CXCL1/KC levels were observed in corneas of IL-17RAKO mice as compared to WT control mice (Fig 4. 6A-B). The role of IL-17A in CXCL1/KC production was further confirmed by the in-vitro stimulation of MK/T-1 cells with different concentrations of IL-17A for 24 hr. Unstimulated MK/T-1 cells produced basal amounts of CXCL1/KC, but the addition of IL-17A even at very low concentrations to the culture media, increased CXCL1/KC production by 4.5 fold (Fig 4.6 C-D). Neutralization of IL-17A completely inhibited the CXCL1/KC production by stromal

fibroblasts indicating a direct role of IL-17A in the upregulation of CXCL1/KC. Moreover, IL-17A was a more potent inducer of CXCL1/KC, when compared to IL-6 (Fig 4.6 E).

Further evidence for the role of IL-17A in corneal migration of neutrophils post HSV infection came from comparing the corneal infiltrating neutrophils between HSV infected WT and IL-17RAKO mice. Accordingly, IL-17RAKO mice had significantly reduced frequencies and total cell numbers of neutrophils when compared to WT counterparts (Fig 4.6 F-G). Moreover, *in-vivo* neutralization of IL-17A in WT HSV infected mice showed diminished infiltration of neutrophils, further confirming the critical role of IL-17A in the migration of these cells to the site of inflammation (Fig 4.6 H-M). Collectively, these results indicated that the reduced degradation of sVEGFR-1 and diminished levels of VEGF-A in IL-17RAKO mice as well as post IL-17A neutralization in WT mice could be the result of diminished expression of CXCL1/KC and consequent reduced infiltration of neutrophils, which indirectly contribute to the source of VEGF-A and sVEGFR-1 degrading MMPs.

Discussion

The normal eye employs numerous strategies to maintain the corneal transparency that is essential for optimal vision. One such inhibitory interaction is between VEGF-A and sVEGFR-1. With this VEGF-A trap preventing corneal vascularity reaction. However, conditions such as HSV infection of the cornea disrupts the VEGF-A trap resulting in corneal neovascularization an essential step in the pathogenesis of SK and subsequent vision loss (*3, 8, 9*). In this report, we investigated how IL-17A induced

following HSV infection of the cornea influences the efficacy of the VEGF-A trap. We show that IL-17A contributes to changing the balance between VEGF-A and sVEGFR-1 through multiple mechanisms. Accordingly, animals lacking response to IL-17A signaling because of IL-17 receptor knock out or treatment with neutralizing mAb to IL-17A resulted into significant diminished angiogenesis as compared to WT counterparts. The reduced angiogenesis was the consequence of reduced VEGF-A production, but retention in levels of sVEGFR-1. Lesser amounts of sVEGFR-1 degrading MMP enzymes were produced in the absence of IL-17A signaling as were the production of chemokine and cytokines that contributes indirectly to angiogenesis. In vitro results too demonstrated that IL-17A stimulated ocular fibroblast produced VEGF-A, but not sVEGFR-1 along with neutrophil chemokine, CXCL1/KC, sVEGFR-1 degrading enzyme, MMP-9 and proinflammatory cytokine IL-6 and IL-1β, which are indirectly involved in angiogenesis. Collectively, our results demonstrated that IL-17A could influence the HSV induced corneal angiogenesis by targeting multiple pathways leading to the reduce efficacy of the VEGF-A trap. It is conceivable that targeting IL-17A mediated effects could prove a better therapeutic option to control of HSV induced corneal angiogenesis and lesions of SK. Our overall results are summarized in Fig 4.7, showing how HSV induced IL-17A expression orchestrates various critical events involved in corneal angiogenesis.

Since neovascularization is a critical step in the pathogenesis of SK, understanding how it is induced in response to HSV infection could reveal new approaches for its control. The clue that IL-17A could represent a key event in neovascularization came from studies in tumor angiogenesis where IL-17A was shown to

act as an inducer of VEGF-A from fibroblast cells (*20, 22, 25, 26*). Recently, we demonstrated that IL-17A is induced early after ocular infection with HSV arising initially from γδ T cells that are early invaders of the corneal stroma and spontaneous producers of IL-17A (Unpublished data). However, conceivably the earliest source of IL-17A after HSV infection could be the epithelium itself responding to products released by virus infected cells. Virus infected cells may also be the initial source of VEGF-A the principal mediator of angiogenesis. However, subsequently the production of VEGF-A would seem to depend on stimulation of producer cells by IL-17A. Two lines of evidence supported this notion. Firstly we could show a marked reduction in angiogenesis in animals unable to respond IL-17A because they lack the IL-17A receptor. Furthermore, angiogenesis levels were diminished if infected animals were suppressed with anti-IL-17A neutralizing mAb. The effect was most evident when the mAb treatment was given locally starting on day 7 pi a time when angiogenesis had already begun indicating that IL-17A may exerts its predominant influence after the initial phase of neovascularization. The overall effect of IL-17A in ocular angiogenesis appeared to be the consequence of multiple events. These included the stimulation of VEGF-A production from cells in the stroma, as we could model in vitro, as well as the production by stimulated cells of a cytokine that attracts neutrophils to the corneal stroma. A second ongoing issue was that IL-17 had no stimulatory effect on sVEGFR-1 production, a molecule that can bind to VEGF-A and limits its angiogenic activity. More of relevance, IL-17A induced the production of MMP-9 from stromal fibroblasts and caused the production of a cytokine s that recruits neutrophils into the stroma. Neutrophils also act as a source of VEGF-A as

well as several MMP enzymes that could degrade sVEGFR-1. The overall outcome was a marked reduction in the efficacy of the VEGF-A trap and enhanced angiogenesis.

Newly developed blood vessels during pathological angiogenesis are often abnormal, lack normal architecture and are leaky thus permitting the escape of pro-inflammatory cells/molecules into the corneal stroma (*3, 19*). Prior studies have shown the critical role of VEGF-A/VEGFR-2 in mediating HSV induced corneal angiogenesis (*8-10, 14, 16, 17*). However, molecular mechanisms responsible for the VEGF-A induction post HSV infection are still unclear. One important aspect of HSV induced corneal angiogenesis is the loss of the VEGF-A trap efficacy mainly through increased synthesis of VEGF-A and reduced expression of sVEGFR-1 along with its degradation by various MMPs (*14*). Past studies have shown that early after HSV infection, infected corneal epithelial or nearby uninfected cells predominantly contribute to the early source of VEGF-A (*16, 17*). Additionally, once virus is cleared from the cornea around day 7 pi (*3*), innate cells such as neutrophils act as an additional source of VEGF-A during the clinical stage of SK pathogenesis (*3, 14, 18, 34*). Although, HSV infection of corneal epithelial cells have been shown to induce the expression of VEGF-A, various other factors such as IL-6, CpG oligonucleotide could also induce the VEGF-A expression by corneal epithelial or stromal fibroblast cells (*15, 16*). Numerous studies in arthritis and tumor systems have indicated the pro-angiogenic role of IL-17A, mainly through induction of VEGF-A, MMP-9, IL-1B and IL-6 (*20-23, 25, 26*). Since we observed increased expression of IL-17A early after HSV infection (unpublished data, Part II), it is conceivable that IL-17A could be modulating the expression of VEGF-A in the cornea post HSV infection. In consequence, the reduced levels of VEGF-A in IL-17RA-/- mice

and post IL-17 neutralization in WT mice indicated that IL-17A plays a similar role in the induction of VEGF-A post corneal HSV infection. Consistent with the findings, in-vitro data indicated that corneal stromal fibroblasts could also provide a supplementary source of VEGF-A through IL-17A mediated signaling. Since epithelial cells also express IL-17RA, increased VEGF-A expression post HSV infection could be the combined result of IL-17A mediated paracrine expression of VEGF-A by corneal epithelial as well as stromal fibroblast cells. However, currently we lack evidence for the IL-17A mediated effects on corneal epithelial cell expression of VEGF-A. Further studies using corneal epithelial cell line would shed more light on role of IL-17A and the relative contribution of epithelial cells to the source of VEGF-A.

In addition to increased VEGF-A expression, reduced levels of sVEGFR-1, mainly through reduced synthesis along with MMP mediated increased degradation, potentiate the VEGF-A mediated effects and subsequent corneal angiogenesis post HSV infection (*14, 29*). Furthermore, increased degradation of sVEGFR-1 post HSV infection could also contribute to the source of VEGF-A by releasing pre-formed VEGF-A bound to sVEGFR-1 (*2, 14*). HSV infection drives the increased expression of various MMPs, which selectively degrade sVEGFR-1 into biologically non-active form (*14, 18*), contributing to the inefficacy of the VEGF-A trap. Although earlier studies showed that HSV infection upregulated the expression of MMPs (*14, 18*), underlying mechanisms for MMPs upregulation are poorly understood. Our study showed that IL-17A orchestrated various events following HSV infection. In addition to increased expression of VEGF-A, IL-17A also upregulated the expression of MMP-9 by corneal stromal fibroblast cells, which through degradation of sVEGFR-1 enhanced the biological activity of VEGF-A.

Support for this finding came by observing the levels of various MMPs in the corneas of HSV infected IL-17RA-/- mice, which showed significantly diminished expression of MMP-7 and -9. Additionally, reduced degradation of sVEGFR-1 from corneal samples of IL-17RA-/- mice suggested that IL-17 directly affects the efficacy of the VEGF-A trap through the expression of various sVEGFR-1 degrading MMPs. Our findings are in accord with the previously published reports where lack of MMP activity post HSV infection as observed in MMP-9-/- mice or treatment of HSV infected WT mice with broad spectrum MMP inhibitor showed diminished angiogenesis (*14, 18*). Thus our data indicates that increased expression of IL-17A post HSV infection perturbs the balance between VEGF-A by directly increasing the expression of VEGF-A as well as MMPs, which participate in the degradation of sVEGFR-1.

Another important aspect of IL-17A mediated signaling is the upregulation of CXCL1/KC, a chemoattractant for neutrophils and subsequent neutrophil mediated effects in the promotion of corneal angiogenesis (*22, 23, 25, 31-33*). Neutrophils are the predominant cells that infiltrate the cornea during all stages of SK pathogenesis (*14*). Although, neutrophils initially play a protective role in virus clearance (*35*), subsequently they contribute to the corneal tissue damage and angiogenesis by providing an additional source of VEGF-A, various oxy-radicals as well as MMPs (*3, 14, 18*). IL-17A through its myriad effects on epithelial and stromal fibroblast cells were also shown to increase the expression of neutrophil chemoattractant CXCL1/KC and subsequent infiltration of neutrophils at the site of inflammation (*22, 23, 25, 31-33*). Since, earlier reports from our lab showed that HSV infection induces IL-17A expression (unpublished data) as well as migration of the neutrophils in the cornea (*3, 14, 36*), it is conceivable that IL-17A may

contribute to the neutrophil influx by increasing the expression of CXCL1/KC by stromal fibroblasts. Although, this initial innate immune response early after HSV infection is essential for viral clearance, subsequent continued migration of neutrophils could set up a stage for the development of complex SK pathogenesis. Indeed our data showing the reduced levels of CXCL1/KC, subsequent diminished infiltration of neutrophils along with reduced angiogenesis in mice lacking IL-17RA signaling and after IL-17 neutralization in WT mice confirmed the previous findings as well as supported the notion that neutrophil infiltration during clinical stages of SK could promote corneal angiogenesis. Furthermore, our data also indicated the critical link between HSV infection and migration of neutrophils through IL-17A mediated increased expression of CXCL1/KC by corneal stromal fibroblast cells. The diminished levels of CXCL1/KC in HSV infected IL-17RA-/- mice as well as post IL-17 neutralization indicated the important role of IL-17A signaling in promoting neutrophil infiltration at the site of inflammation. Additionally, stimulation of corneal stromal fibroblast with IL-17A showed significant upregulation of CXCL1/KC even at very low concentration confirming the role of IL-17A in the induction of CXCL1/KC. Moreover, IL-17A was found to be a more potent inducer of CXCL1/KC as compared to other known factors such as IL-6 (*16, 37*). An important aspect of this finding is the effect of IL-17A on the efficacy of the VEGF-A trap. It is important to note that IL-17A through increased expression of CXCL1/KC contributes indirectly to the source of VEGF-A and sVEGFR-1 degrading enzymes by promoting the migration of neutrophils (*3, 14, 18*). In addition, IL-17A also promoted the expression of other pro-inflammatory cytokines such as IL-1B and IL-6, which were shown to exert angiogenic effects in HSV induced corneal

angiogenesis (*16, 38-40*). Previous studies have shown the important role of IL-17A signaling in the stabilization and increased mRNA expression of various pro-inflammatory cytokines and chemokines (*22, 23, 33*). Accordingly, we found significantly diminished expression of IL-1B, IL-6 and TNF-A in mice lacking IL-17A signaling, so confirming earlier findings. Furthermore, IL-6 has been shown to play an important role in HSV induced corneal angiogenesis, as it promotes the paracrine expression of VEGF-A by corneal epithelial cells (*16*). In accord with previously published reports, our in vitro data showed that IL-17A stimulation of MK/T-1 cells upregulated the expression of IL-6 and IL-1B. Interestingly, we observed the increased expression of VEGF-A by MK/T-1 cells when cells were stimulated with IL-17A in the presence of IL-6 and IL-1B. These results demonstrated that IL-17A could serve as a critical mediator of various key events responsible for HSV induced corneal neovascularization.

In summary, this study identifies new functions of IL-17A responsible for HSV induced corneal angiogenesis. It is conceivable that IL-17A through multiple mechanisms shifts the balance between VEGF-A and sVEGFR-1 affecting the efficacy of VEGF-A trap. Mechanisms for this imbalance were numerous which included direct increased expression of VEGF-A, sVEGFR-1 degrading MMPs, IL-6, IL-1B and neutrophil chemoattractant. The net effect of IL-17A mediated signals was to increase the levels of VEGF-A and reduce the synthesis of sVEGFR-1 along with increased MMP mediated degradation of pre-formed sVEGFR-1 molecules. This degradation of sVEGFR-1 might also contribute to the source of VEGF-A by being released from its bond to sVEGFR-1 in the VEGF-A trap. In addition to direct increased expression of VEGF-A, IL-17 mediated

increased expression of IL-6 and IL-1B potentiated the expression of VEGF-A by corneal fibroblasts through combined action of all three cytokines. Moreover, IL-17A also indirectly contributed to the source of VEGF-A through the increased expression of CXCL1/KC followed by increased migration of neutrophils, which further bring the pre-formed VEGF-A as well as various sVEGFR-1 degrading MMPs at the site of inflammation. Since IL-17A signaling controls almost all events in affecting the efficacy of the VEGF-A trap, it would seem logical to develop therapies targeting IL-17A mediated effects to control corneal angiogenesis and SK immunopathology, an important cause of human blindness.

LIST OF REFERENCES

1. Azar, D. T. (2006) Corneal angiogenic privilege: angiogenic and antiangiogenic factors in corneal avascularity, vasculogenesis, and wound healing (an American Ophthalmological Society thesis), *Trans Am Ophthalmol Soc 104*, 264-302.
2. Ambati, B. K., Nozaki, M., Singh, N., Takeda, A., Jani, P. D., Suthar, T., Albuquerque, R. J., Richter, E., Sakurai, E., Newcomb, M. T., Kleinman, M. E., Caldwell, R. B., Lin, Q., Ogura, Y., Orecchia, A., Samuelson, D. A., Agnew, D. W., St Leger, J., Green, W. R., Mahasreshti, P. J., Curiel, D. T., Kwan, D., Marsh, H., Ikeda, S., Leiper, L. J., Collinson, J. M., Bogdanovich, S., Khurana, T. S., Shibuya, M., Baldwin, M. E., Ferrara, N., Gerber, H. P., De Falco, S., Witta, J., Baffi, J. Z., Raisler, B. J., and Ambati, J. (2006) Corneal avascularity is due to soluble VEGF receptor-1, *Nature 443*, 993-997.
3. Biswas, P. S., and Rouse, B. T. (2005) Early events in HSV keratitis--setting the stage for a blinding disease, *Microbes Infect 7*, 799-810.
4. Streilein, J. W., Dana, M. R., and Ksander, B. R. (1997) Immunity causing blindness: five different paths to herpes stromal keratitis, *Immunol Today 18*, 443-449.
5. Niemialtowski, M. G., and Rouse, B. T. (1992) Phenotypic and functional studies on ocular T cells during herpetic infections of the eye, *J Immunol 148*, 1864-1870.
6. Niemialtowski, M. G., and Rouse, B. T. (1992) Predominance of Th1 cells in ocular tissues during herpetic stromal keratitis, *J Immunol 149*, 3035-3039.

7. Russell, R. G., Nasisse, M. P., Larsen, H. S., and Rouse, B. T. (1984) Role of T-lymphocytes in the pathogenesis of herpetic stromal keratitis, *Invest Ophthalmol Vis Sci 25*, 938-944.

8. Zheng, M., Deshpande, S., Lee, S., Ferrara, N., and Rouse, B. T. (2001) Contribution of vascular endothelial growth factor in the neovascularization process during the pathogenesis of herpetic stromal keratitis, *J Virol 75*, 9828-9835.

9. Zheng, M., Schwarz, M. A., Lee, S., Kumaraguru, U., and Rouse, B. T. (2001) Control of stromal keratitis by inhibition of neovascularization, *Am J Pathol 159*, 1021-1029.

10. Kim, B., Tang, Q., Biswas, P. S., Xu, J., Schiffelers, R. M., Xie, F. Y., Ansari, A. M., Scaria, P. V., Woodle, M. C., Lu, P., and Rouse, B. T. (2004) Inhibition of ocular angiogenesis by siRNA targeting vascular endothelial growth factor pathway genes: therapeutic strategy for herpetic stromal keratitis, *Am J Pathol 165*, 2177-2185.

11. Kendall, R. L., and Thomas, K. A. (1993) Inhibition of vascular endothelial cell growth factor activity by an endogenously encoded soluble receptor, *Proc Natl Acad Sci U S A 90*, 10705-10709.

12. Banks, R. E., Forbes, M. A., Searles, J., Pappin, D., Canas, B., Rahman, D., Kaufmann, S., Walters, C. E., Jackson, A., Eves, P., Linton, G., Keen, J., Walker, J. J., and Selby, P. J. (1998) Evidence for the existence of a novel pregnancy-

associated soluble variant of the vascular endothelial growth factor receptor, Flt-1, *Mol Hum Reprod 4*, 377-386.

13. Hornig, C., Barleon, B., Ahmad, S., Vuorela, P., Ahmed, A., and Weich, H. A. (2000) Release and complex formation of soluble VEGFR-1 from endothelial cells and biological fluids, *Lab Invest 80*, 443-454.
14. Suryawanshi, A., Mulik, S., Sharma, S., Reddy, P. B., Sehrawat, S., and Rouse, B. T. (2011) Ocular neovascularization caused by herpes simplex virus type 1 infection results from breakdown of binding between vascular endothelial growth factor A and its soluble receptor, *J Immunol 186*, 3653-3665.
15. Zheng, M., Klinman, D. M., Gierynska, M., and Rouse, B. T. (2002) DNA containing CpG motifs induces angiogenesis, *Proc Natl Acad Sci U S A 99*, 8944-8949.
16. Biswas, P. S., Banerjee, K., Kinchington, P. R., and Rouse, B. T. (2006) Involvement of IL-6 in the paracrine production of VEGF in ocular HSV-1 infection, *Exp Eye Res 82*, 46-54.
17. Wuest, T. R., and Carr, D. J. (2010) VEGF-A expression by HSV-1-infected cells drives corneal lymphangiogenesis, *J Exp Med 207*, 101-115.
18. Lee, S., Zheng, M., Kim, B., and Rouse, B. T. (2002) Role of matrix metalloproteinase-9 in angiogenesis caused by ocular infection with herpes simplex virus, *J Clin Invest 110*, 1105-1111.
19. Nagy, J. A., Dvorak, A. M., and Dvorak, H. F. (2007) VEGF-A and the induction of pathological angiogenesis, *Annu Rev Pathol 2*, 251-275.

20. Numasaki, M., Lotze, M. T., and Sasaki, H. (2004) Interleukin-17 augments tumor necrosis factor-alpha-induced elaboration of proangiogenic factors from fibroblasts, *Immunol Lett 93*, 39-43.

21. Takahashi, H., Numasaki, M., Lotze, M. T., and Sasaki, H. (2005) Interleukin-17 enhances bFGF-, HGF- and VEGF-induced growth of vascular endothelial cells, *Immunol Lett 98*, 189-193.

22. Gaffen, S. L. (2009) Structure and signalling in the IL-17 receptor family, *Nat Rev Immunol 9*, 556-567.

23. Shen, F., and Gaffen, S. L. (2008) Structure-function relationships in the IL-17 receptor: implications for signal transduction and therapy, *Cytokine 41*, 92-104.

24. Ryu, S., Lee, J. H., and Kim, S. I. (2006) IL-17 increased the production of vascular endothelial growth factor in rheumatoid arthritis synoviocytes, *Clin Rheumatol 25*, 16-20.

25. Numasaki, M., Watanabe, M., Suzuki, T., Takahashi, H., Nakamura, A., McAllister, F., Hishinuma, T., Goto, J., Lotze, M. T., Kolls, J. K., and Sasaki, H. (2005) IL-17 enhances the net angiogenic activity and in vivo growth of human non-small cell lung cancer in SCID mice through promoting CXCR-2-dependent angiogenesis, *J Immunol 175*, 6177-6189.

26. Numasaki, M., Fukushi, J., Ono, M., Narula, S. K., Zavodny, P. J., Kudo, T., Robbins, P. D., Tahara, H., and Lotze, M. T. (2003) Interleukin-17 promotes angiogenesis and tumor growth, *Blood 101*, 2620-2627.

27. Dana, M. R., Zhu, S. N., and Yamada, J. (1998) Topical modulation of interleukin-1 activity in corneal neovascularization, *Cornea 17*, 403-409.

28. Fenton, R. R., Molesworth-Kenyon, S., Oakes, J. E., and Lausch, R. N. (2002) Linkage of IL-6 with neutrophil chemoattractant expression in virus-induced ocular inflammation, *Invest Ophthalmol Vis Sci 43*, 737-743.

29. Ito, T. K., Ishii, G., Saito, S., Yano, K., Hoshino, A., Suzuki, T., and Ochiai, A. (2009) Degradation of soluble VEGF receptor-1 by MMP-7 allows VEGF access to endothelial cells, *Blood 113*, 2363-2369.

30. Lee, S., Jilani, S. M., Nikolova, G. V., Carpizo, D., and Iruela-Arispe, M. L. (2005) Processing of VEGF-A by matrix metalloproteinases regulates bioavailability and vascular patterning in tumors, *J Cell Biol 169*, 681-691.

31. Hoshino, H., Lotvall, J., Skoogh, B. E., and Linden, A. (1999) Neutrophil recruitment by interleukin-17 into rat airways in vivo. Role of tachykinins, *Am J Respir Crit Care Med 159*, 1423-1428.

32. Laan, M., Cui, Z. H., Hoshino, H., Lotvall, J., Sjostrand, M., Gruenert, D. C., Skoogh, B. E., and Linden, A. (1999) Neutrophil recruitment by human IL-17 via C-X-C chemokine release in the airways, *J Immunol 162*, 2347-2352.

33. Datta, S., Novotny, M., Pavicic, P. G., Jr., Zhao, C., Herjan, T., Hartupee, J., and Hamilton, T. (2010) IL-17 regulates CXCL1 mRNA stability via an AUUUA/tristetraprolin-independent sequence, *J Immunol 184*, 1484-1491.

34. Ardi, V. C., Kupriyanova, T. A., Deryugina, E. I., and Quigley, J. P. (2007) Human neutrophils uniquely release TIMP-free MMP-9 to provide a potent

catalytic stimulator of angiogenesis, *Proc Natl Acad Sci U S A 104*, 20262-20267.

35. Tumpey, T. M., Chen, S. H., Oakes, J. E., and Lausch, R. N. (1996) Neutrophil-mediated suppression of virus replication after herpes simplex virus type 1 infection of the murine cornea, *J Virol 70*, 898-904.

36. Thomas, J., Gangappa, S., Kanangat, S., and Rouse, B. T. (1997) On the essential involvement of neutrophils in the immunopathologic disease: herpetic stromal keratitis, *J Immunol 158*, 1383-1391.

37. Rajasagi, N. K., Reddy, P. B., Suryawanshi, A., Mulik, S., Gjorstrup, P., and Rouse, B. T. (2011) Controlling herpes simplex virus-induced ocular inflammatory lesions with the lipid-derived mediator resolvin E1, *J Immunol 186*, 1735-1746.

38. Banerjee, K., Biswas, P. S., Kim, B., Lee, S., and Rouse, B. T. (2004) CXCR2-/- mice show enhanced susceptibility to herpetic stromal keratitis: a role for IL-6-induced neovascularization, *J Immunol 172*, 1237-1245.

39. Biswas, P. S., Banerjee, K., Kim, B., and Rouse, B. T. (2004) Mice transgenic for IL-1 receptor antagonist protein are resistant to herpetic stromal keratitis: possible role for IL-1 in herpetic stromal keratitis pathogenesis, *J Immunol 172*, 3736-3744.

40. Biswas, P. S., Banerjee, K., Zheng, M., and Rouse, B. T. (2004) Counteracting corneal immunoinflammatory lesion with interleukin-1 receptor antagonist protein, *J Leukoc Biol 76*, 868-875.

APPENDIX

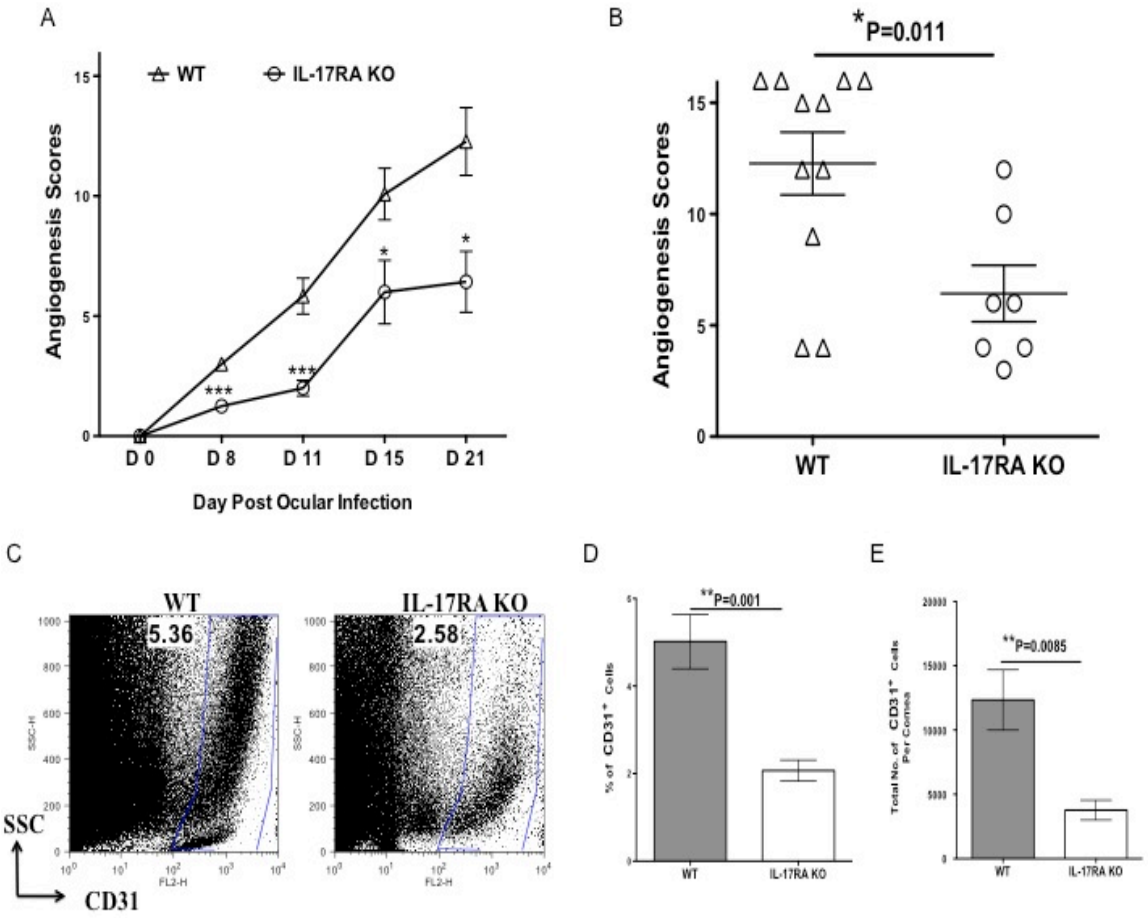
A
WT
IL-17RA KO
Angiogenesis Scores
Day Post Ocular Infection
D 0
D 8
D 11
D 15
D 21
B
*P=0.011
Angiogenesis Scores
WT
IL-17RA KO
C
WT
IL-17RA KO
5.36
2.58
SSC
CD31
FL2-H
D
**P=0.001
% of CD31+ Cells
E
**P=0.0085
Total No. of CD31+ Cells Per Cornea

FIGURE 4.1. IL-17RA KO DISPLAY DIMINISHED HSV INDUCED CORNEAL ANGIOGENESIS.

To compare the development and progression of corneal angiogenesis, WT and IL-17RA KO mice were infected with 1×10^4 PFU of HSV by corneal scarification. (A) The development of new blood vessels in normally avascular cornea was assessed on day 8, 11, 15 and 21 PI. (B) Corneal Angiogenesis score of individual mice on day 21 PI. Data represents means ± SEM (n= 8 to 12 mice per group from two independent experiments; *P<0.03, ***P=0.0003). (C-E) Mice were sacrificed on day 15 PI and corneas were pooled group wise for flow cytometry analysis. (C) Representative FACS plots for corneal $CD31^+$ endothelial cells between WT and IL-17RA KO mice. (D-E) Bar graphs show reduced $CD31^+$ endothelial cell frequencies (D) as well as reduced total cell numbers per cornea (E) from IL-17RA KO mice group as compared to WT. Data represents mean ± SEM from two independent experiments (n= 5 for WT and 6 for IL-17RA KO mice. Each sample is representative of two corneas).

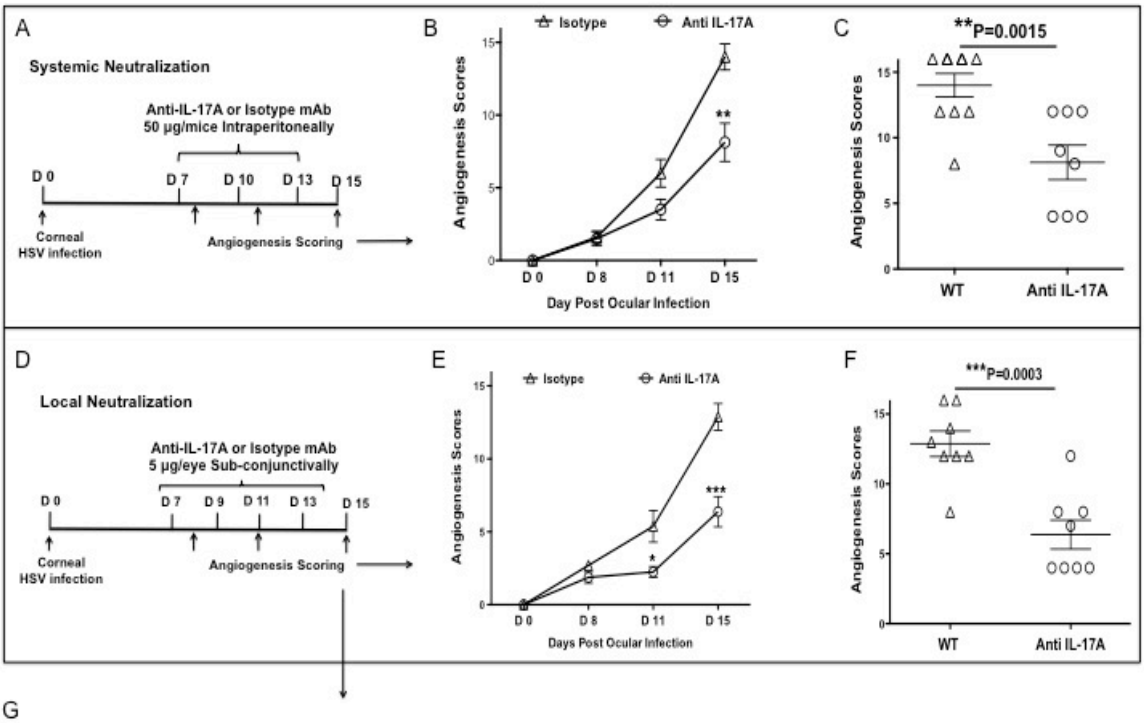
A
Systemic Neutralization
Anti-IL-17A or Isotype mAb
50 µg/mice Intraperitoneally
D 0
D 7
D 10
D 13
D 15
Corneal HSV infection
Angiogenesis Scoring
B
Isotype
Anti IL-17A
Angiogenesis Scores
D 0
D 8
D 11
D 15
Day Post Ocular Infection
C
**P=0.0015
Angiogenesis Scores
WT
Anti IL-17A
D
Local Neutralization
Anti-IL-17A or Isotype mAb
5 µg/eye Sub-conjunctivally
D 0
D 7
D 9
D 11
D 13
D 15
Corneal HSV infection
Angiogenesis Scoring
E
Isotype
Anti IL-17A
Angiogenesis Scores
D 0
D 8
D 11
D 15
Days Post Ocular Infection
F
***P=0.0003
Angiogenesis Scores
WT
Anti IL-17A

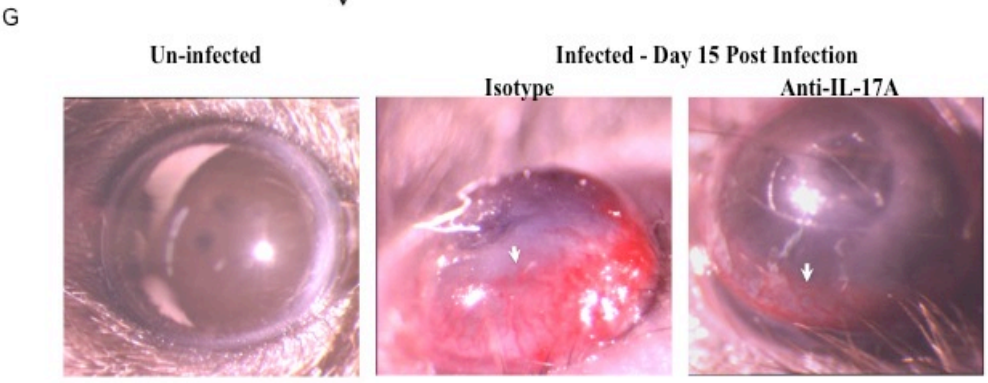
G
Un-infected
Infected - Day 15 Post Infection
Isotype
Anti-IL-17A

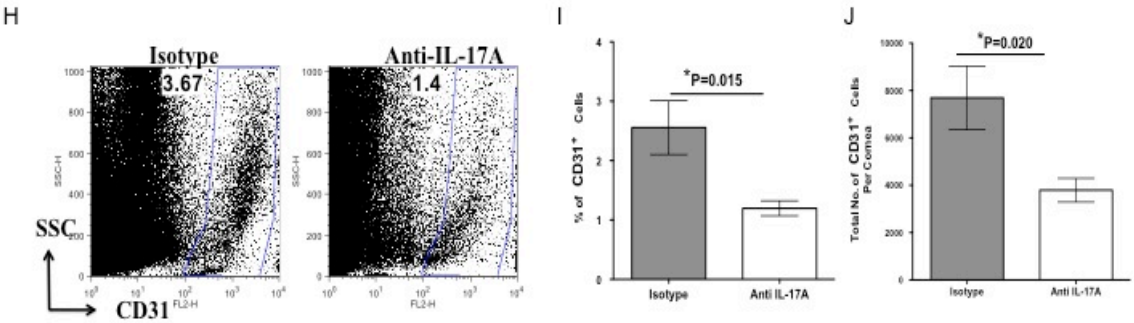
H
Isotype
3.67
Anti-IL-17A
1.4
SSC
CD31
I
*P=0.015
% of CD31+ Cells
Isotype
Anti IL-17A
J
*P=0.020
Total No. of CD31+ Cells Per Cornea
Isotype
Anti IL-17A

FIGURE 4.2. SYSTEMIC AND LOCAL IL-17A NEUTRALIZATION REDUCES SEVERITY OF HSV INDUCED CORNEAL NEOVASCULARIAZTION.

WT mice were infected with 1×10^4 PFU of HSV by corneal scarification. (A) For systemic IL-17A neutralization, animals were injected intraperitoneally with 50 μg anti-IL-17A or control IgG1 mAb as indicated. (B) The development of new blood vessels in normally avascular cornea was assessed on day 8, 11 and 15 PI. (C) Corneal Angiogenesis score of individual mice on day 15 PI. Data represents means ± SEM (n= 8 corneas per group from two independent experiments; **P=0.0015). (D) For local IL-17A neutralization, mice were injected sub-conjunctivally with 5 μg of anti-IL-17A or control IgG1 mAb as indicated. (E) The development of response in normally avascular cornea was assessed on day 8, 11 and 15 PI. (F) Corneal angiogenesis score of individual mice on day 15 PI. Data represents means ± SEM (n= 8 corneas per group from two independent experiments; **P=0.0003). (G) Representative eye photograph of naïve uninfected, local isotype mAb or anti-IL-17A mAb treated mice on day 15 PI. In uninfected mice, cornea is clear and devoid of any blood vessels (left panel). By day 15 PI, new blood vessel development reaches to the center of the cornea in isotype mAb treated mice (middle panel), but only halfway in anti-IL-17A treated mice (right panel) as indicated by white arrows. This panel is representative of two independent experiments with 8 eyes per group. (H-J) Mice from local IL-17A neutralization groups were sacrificed on day 15 PI and corneas were pooled group wise for flow cytometry analysis. (H) Representative FACS plots for corneal $CD31^+$ endothelial cells between isotype mAb and anti-IL-17A mAb treated mice. (I-J) Bar graphs show reduced $CD31^+$ endothelial cell frequencies (I) as well as reduced total cell numbers per cornea (J) from anti-IL-17A

treated group as compared to isotype treated group. Data represents mean ± SEM from two independent experiments (n= 4 and each sample is representative of two corneas).

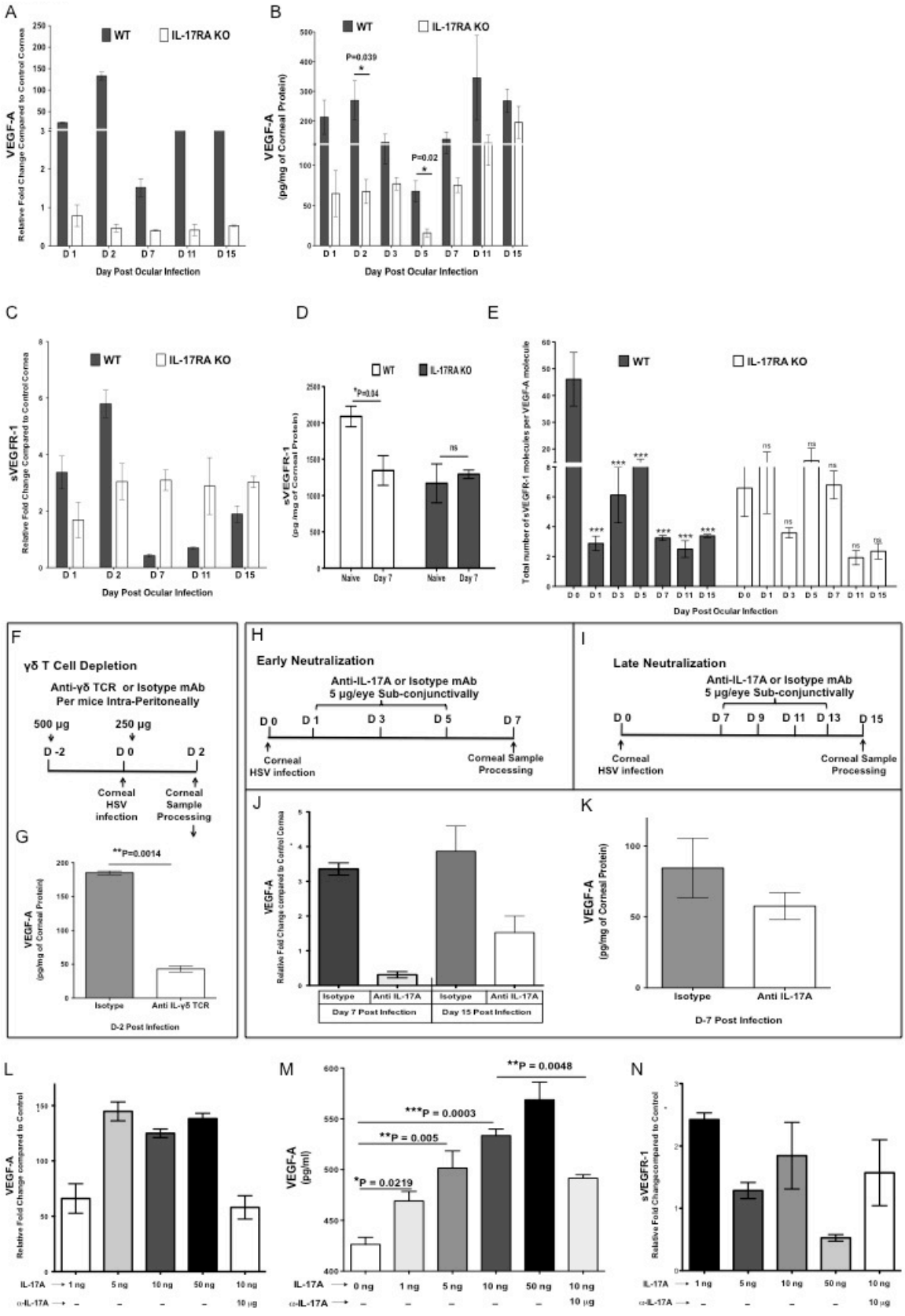
A
WT
IL-17RA KO
VEGF-A
Relative Fold Change Compared to Control Cornea
Day Post Ocular Infection
B
WT
IL-17RA KO
P=0.039
P=0.02
VEGF-A
(pg/mg of Corneal Protein)
Day Post Ocular Infection
C
WT
IL-17RA KO
sVEGFR-1
Relative Fold Change Compared to Control Cornea
Day Post Ocular Infection
D
WT
IL-17RA KO
*P=0.04
ns
sVEGFR-1
(pg /mg of Corneal Protein)
Naive
Day 7
E
WT
IL-17RA KO
Total number of sVEGFR-1 molecules per VEGF-A molecule
Day Post Ocular Infection
F
γδ T Cell Depletion
Anti-γδ TCR or Isotype mAb
Per mice Intra-Peritoneally
500 µg
250 µg
D -2
D 0
D 2
Corneal HSV infection
Corneal Sample Processing
G
**P=0.0014
VEGF-A
(pg/mg of Corneal Protein)
Isotype
Anti IL-γδ TCR
D-2 Post Infection
H
Early Neutralization
Anti-IL-17A or Isotype mAb
5 µg/eye Sub-conjunctivally
D 0
D 1
D 3
D 5
D 7
Corneal HSV infection
Corneal Sample Processing
I
Late Neutralization
Anti-IL-17A or Isotype mAb
5 µg/eye Sub-conjunctivally
D 0
D 7
D 9
D 11
D 13
D 15
Corneal HSV infection
Corneal Sample Processing
J
VEGF-A
Relative Fold Change compared to Control Cornea
Isotype
Anti IL-17A
Isotype
Anti IL-17A
Day 7 Post Infection
Day 15 Post Infection
K
VEGF-A
(pg/mg of Corneal Protein)
Isotype
Anti IL-17A
D-7 Post Infection
L
VEGF-A
Relative Fold Change compared to Control
IL-17A → 1 ng 5 ng 10 ng 50 ng 10 ng
α-IL-17A → – – – – 10 µg
M
**P = 0.0048
***P = 0.0003
**P = 0.005
*P = 0.0219
VEGF-A
(pg/ml)
IL-17A → 0 ng 1 ng 5 ng 10 ng 50 ng 10 ng
α-IL-17A → – – – – – 10 µg
N
sVEGFR-1
Relative Fold Change compared to Control
IL-17A → 1 ng 5 ng 10 ng 50 ng 10 ng
α-IL-17A → – – – – 10 µg

FIGURE 4.3. IL-17A DIFFERENTIALLY REGULATES THE CORNEAL VEGF-A AND SVEGFR-1 EXPRESSION.

WT and IL-17RA KO mice were infected with 1X104 PFU of HSV in PBS or mock infected with only PBS by corneal scarification. (A) VEGF-A mRNA expression was examined and compared between WT and IL-17RAKO mice by quantitative real-time PCR (qRT-PCR). VEGF-A mRNA levels in mock-infected mice were set to 1 and used for relative fold up-regulation at various days PI. Data represents means + SEM from two independent experiments (n=2 and each sample is representative of 8 corneas). (B) Corneal VEGF-A protein levels were analyzed from WT and IL-17RAKO mice at indicated time points. Data show mean values + SEM from three different independent experiments (n=3 and each sample is representative of 8 corneas). (C) sVEGFR-1 mRNA expression was examined and compared between WT and IL-17RAKO mice by quantitative real-time PCR (qRT-PCR). sVEGFR-1 mRNA levels in mock-infected mice were set to 1 and used for relative fold change at various days PI. Data represents means + SEM from two independent experiments (n=2 and each sample is representative of 8 corneas). (D) Corneal sVEGFR-1 protein levels were analyzed from WT and IL-17RAKO mice at day 7 PI. Data show mean values + SEM from three different independent experiments (n=3 and each sample is representative of 8 corneas). (E) Ratio of total number of sVEGFR-1 molecules per VEGF-A molecule from naïve (D0) and infected corneas at different days PI were compared between WT and IL-17RAKO mice. Ratios were calculated. The total number of molecules for sVEGFR-1 and VEGF-A were calculated using protein quantities obtained by ELISA and multiplying it with molecular weight respective protein and Avogadro's number. Data show mean values + SEM from

three different independent experiments (n=3 and each sample is representative of 8 corneas). (F) gamma delta T cell depletion was carried out using anti-gamma delta TCR antibody (500 ug per mice) as indicated. (G) Corneal VEGF-A protein levels were analyzed and compared between isotype and anti-gamma delta TCR mAb treated mice at day 2 PI. Data show mean values + SEM from two different independent experiments (n=2 and each sample is representative of 8 corneas). Local neutralization of IL-17A was carried out using anti-IL-17A mAb by sub-conjunctival injection during early (H) and late (I) stages of HSV infection as indicated. (J) VEGF-A mRNA expression was examined and compared between isotype and anti-IL-17A mAb treated mice by quantitative real-time PCR (qRT-PCR). VEGF-A mRNA levels in mock-infected mice were set to 1 and used for relative fold up-regulation at day 7 PI. Data represents means + SEM from two independent experiments (n=2 and each sample is representative of 8 corneas). (K) Corneal VEGF-A protein levels were analyzed and compared between isotype and anti-IL-17A mAb treated mice at day 7 PI. Data show mean values + SEM from two different independent experiments (n=2. Each sample consisted of 8-pooled corneas). (M-O) MK/T-1 cells (Corneal stromal keratocytes) were stimulated under different concentrations of IL-17 in the presence or absence of anti-IL-17A mAb for 24 hrs. Supernatants were collected for VEGF-A protein estimation by ELISA and cells were collected and pooled for analysis of VEGF-A and sVEGFR-1 mRNA expression by qRT-PCR. The mRNA levels in control media were set to 1 and used for relative fold up-regulation at various days PI. (L) IL-17A stimulated VEGF-A production by MK/T-1 cells in a dose dependent manner. Data represents means + SEM from two independent experiments (n=6). Relative fold change in VEGF-A (M) and sVEGFR-1 (N) mRNA

expression as compared to control media. Data represents means + SEM from two independent experiments (n=2 and each sample is representative of pooled cells from 3 different wells).

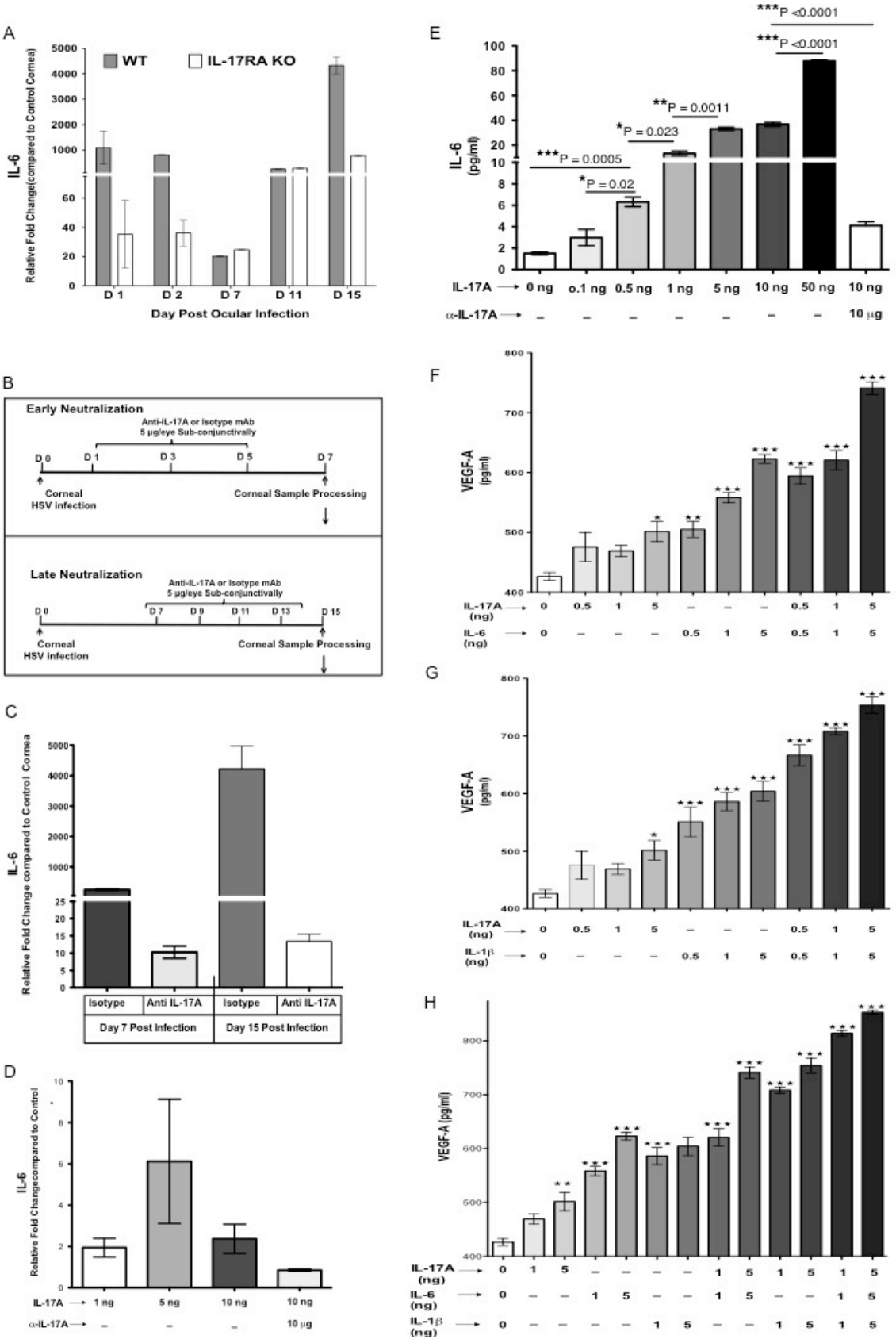
A
WT
IL-17RA KO
IL-6
Relative Fold Change(compared to Control Cornea)
D 1
D 2
D 7
D 11
D 15
Day Post Ocular Infection
B
Early Neutralization
Anti-IL-17A or Isotype mAb
5 µg/eye Sub-conjunctivally
Corneal HSV infection
Corneal Sample Processing
Late Neutralization
C
Relative Fold Change compared to Control Cornea
Isotype
Anti IL-17A
Day 7 Post Infection
Day 15 Post Infection
D
Relative Fold Changecompared to Control
IL-17A
α-IL-17A
E
IL-6 (pg/ml)
P = 0.0005
P = 0.02
P = 0.023
P = 0.0011
P <0.0001
F
VEGF-A (pg/ml)
G
H

FIGURE 4.4. IL-17A STIMULATES IL-6 PRODUCTION BY CORNEAL STROMAL FIBROBLAST CELLS AND BOTH THE CYTOKINES FURTHER STIMULATE VEGF-A PRODUCTION.

WT and IL-17RA KO mice were infected with 1X104 PFU of HSV in PBS or mock infected with only PBS by corneal scarification. (A) IL-6 mRNA expression was examined and compared between WT and IL-17RAKO mice by qRT-PCR. (B) Local neutralization of IL-17A was carried out using anti-IL-17A mAb by sub-conjunctival injection during early () and late () stages of HSV infection as indicated. (C) IL-6 mRNA expression was examined and compared between isotype and anti-IL-17A mAb treated mice by quantitative real-time PCR (qRT-PCR). IL-6 mRNA levels in mock-infected mice were set to 1 and used for relative fold up-regulation at various days PI. Data represents means + SEM from two independent experiments (n=2 and each sample is representative of 8 corneas). MK/T-1 cells (Corneal stromal keratocytes) were stimulated under different concentrations of IL-17 in the presence or absence of anti-IL-17A mAb for 24 hrs. Supernatants were collected for IL-6 protein estimation by ELISA and cells were collected and pooled for analysis of IL-6 mRNA expression by qRT-PCR. () Relative fold change in IL-6 mRNA expression as compared to control media. Data represents means + SEM from two independent experiments (n=2 and each sample is representative of pooled cells from 3 different wells). The mRNA levels in control media were set to 1 and used to relative fold change in mRNA expression. () IL-17A stimulated IL-6 production by MK/T-1 cells in a dose dependent manner. Data represents means + SEM from two independent experiments (n=6). (N) MK/T-1 cells (Corneal stromal keratocytes) were stimulated under different concentrations of IL-17A and IL-6 for 24

hrs. Supernatants were collected for VEGF-A protein estimation by ELISA. VEGF-A production by MK/T-1 cells under different concentrations of IL-17A and IL-6 as indicated.

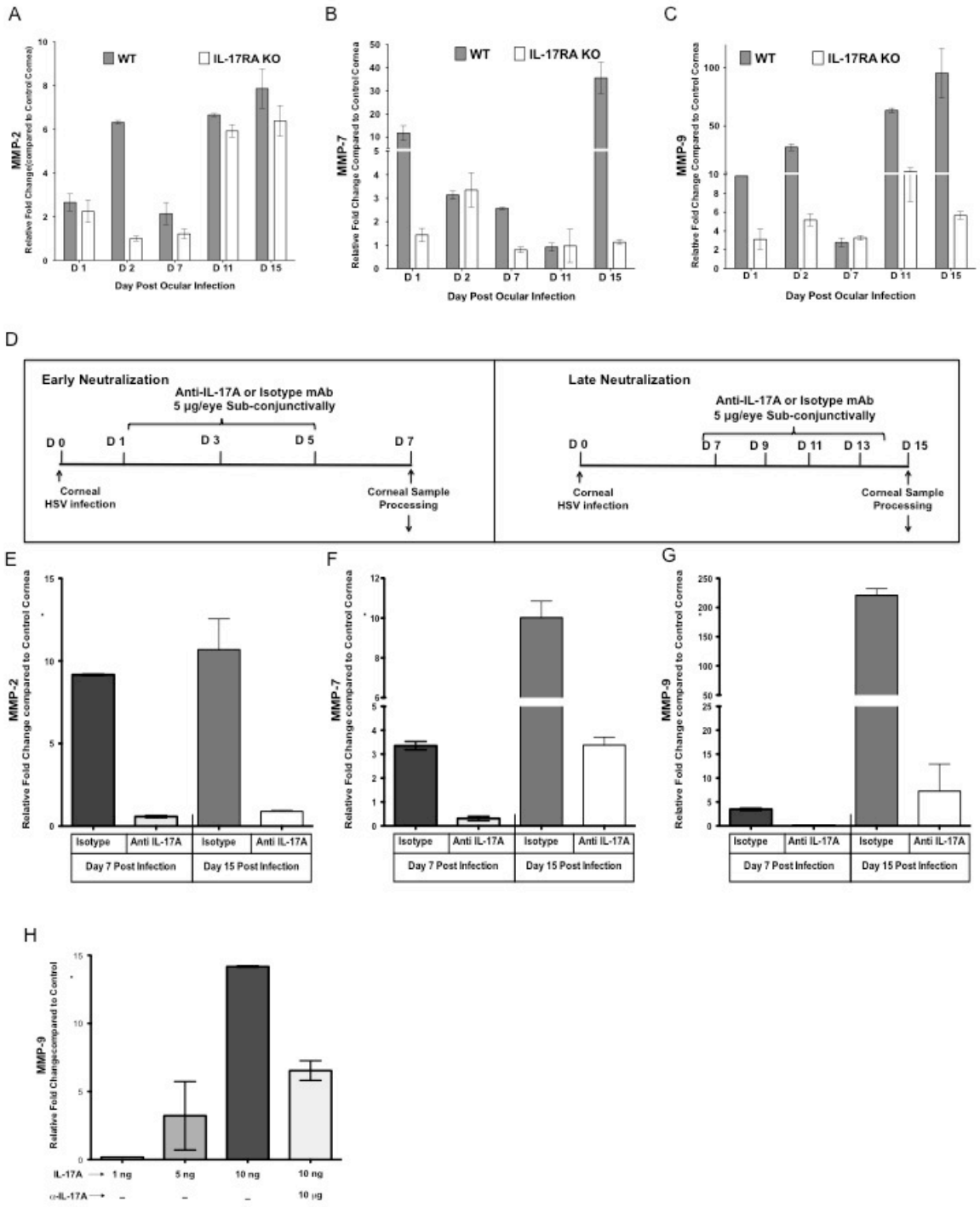
A
B
C
WT
IL-17RA KO
MMP-2
MMP-7
MMP-9
Relative Fold Change(compared to Control Cornea)
Relative Fold Change Compared to Control Cornea
D 1
D 2
D 7
D 11
D 15
Day Post Ocular Infection
D
Early Neutralization
Anti-IL-17A or Isotype mAb
5 µg/eye Sub-conjunctivally
D 0
D 1
D 3
D 5
D 7
Corneal
HSV infection
Corneal Sample
Processing
Late Neutralization
D 9
D 11
D 13
E
F
G
Relative Fold Change compared to Control Cornea
Isotype
Anti IL-17A
Day 7 Post Infection
Day 15 Post Infection
H
Relative Fold Changecompared to Control
IL-17A
1 ng
5 ng
10 ng
α-IL-17A
10 µg

FIGURE 4.5. IL-17A PROMOTES MMP-2, -7 AND -9 EXPRESSION AND AFFECTS VEGF-A BIOAVAILABILITY THROUGH SVEGFR-1 DEGRADATION.

WT and IL-17RA KO mice were infected with 1X104 PFU of HSV in PBS or mock infected with only PBS by corneal scarification. (A) MMP-2, (B) MMP-7 and (C) MMP-9 mRNA expression were examined and compared between WT and IL-17RAKO mice by qRT-PCR. (D) Local neutralization of IL-17A was carried out using anti-IL-17A mAb by sub-conjunctival injection during early and later stages of HSV infection as indicated. (E) MMP-2, (F) MMP-7 and (G) MMP-9 mRNA expression were examined and compared between isotype and anti-IL-17A mAb treated mice by quantitative real-time PCR (qRT-PCR). MMP-2, -7 and -9 mRNA levels in mock-infected mice were set to 1 and used for relative fold up-regulation at various days PI. Data represents means + SEM from two independent experiments (n=2 and each sample is representative of 8 corneas). (H) MK/T-1 cells were stimulated under different concentrations of IL-17 in the presence or absence of anti-IL-17A mAb for 24 hrs. Cells were collected and pooled for analysis of MMP-9 mRNA expression by qRT-PCR. () Relative fold change in MMP-9 mRNA expression as compared to control media. Data represents means + SEM from two independent experiments (n=2 and each sample is representative of pooled cells from 3 different wells). The mRNA levels in control media were set to 1 and used to relative fold change in mRNA expression.

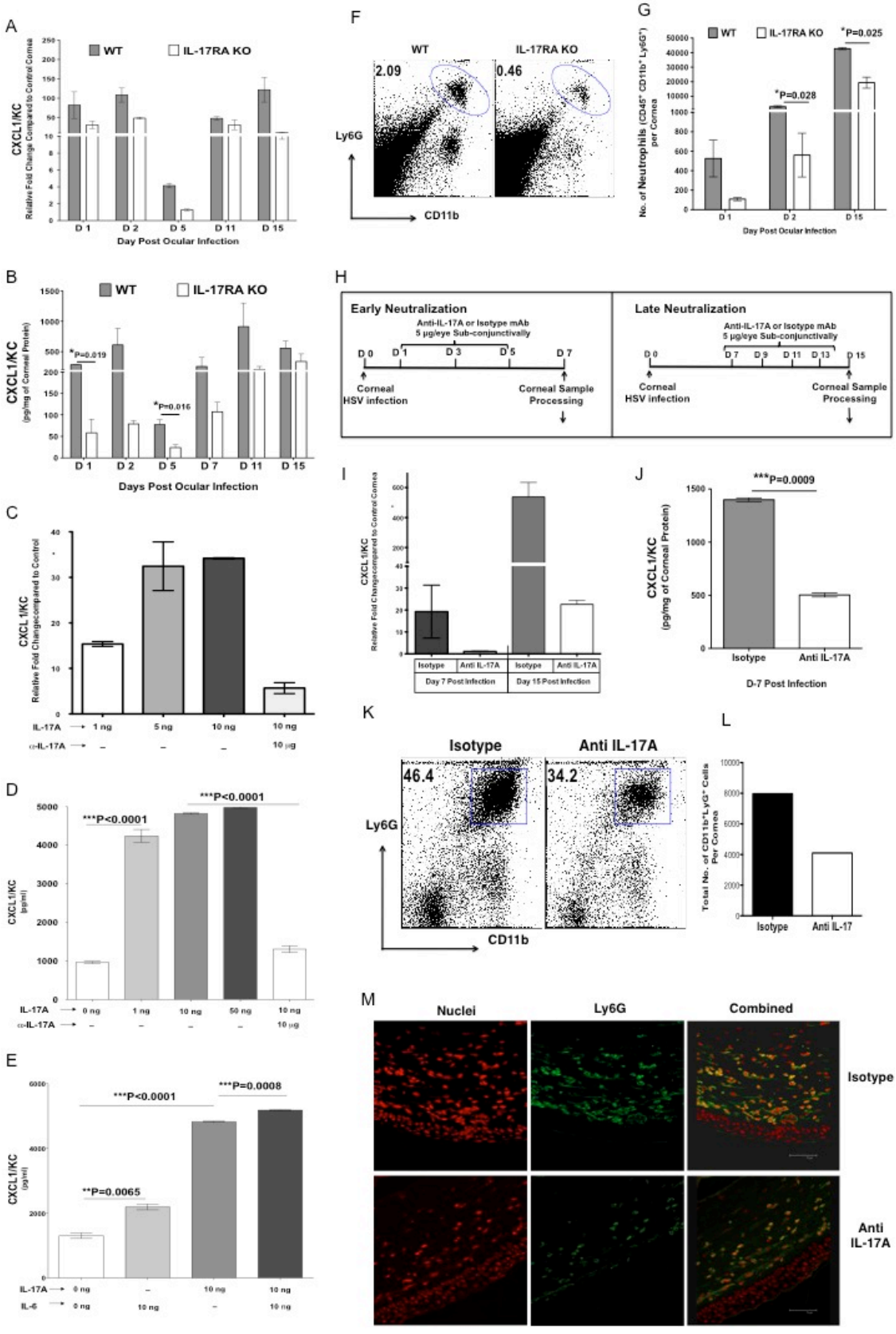
A
WT
IL-17RA KO
CXCL1/KC
Relative Fold Change Compared to Control Cornea
D 1
D 2
D 5
D 11
D 15
Day Post Ocular Infection
B
WT
IL-17RA KO
CXCL1/KC
(pg/mg of Corneal Protein)
*P=0.019
*P=0.016
D 1
D 2
D 5
D 7
D 11
D 15
Days Post Ocular Infection
C
CXCL 1/KC
Relative Fold Changecompared to Control
IL-17A
1 ng
5 ng
10 ng
10 ng
α-IL-17A
10 µg
D
***P<0.0001
***P<0.0001
CXCL1/KC
(pg/ml)
IL-17A
0 ng
1 ng
10 ng
50 ng
10 ng
α-IL-17A
10 µg
E
***P<0.0001
***P=0.0008
**P=0.0065
CXCL1/KC
(pg/ml)
IL-17A
0 ng
10 ng
10 ng
IL-6
0 ng
10 ng
10 ng
F
WT
IL-17RA KO
2.09
0.46
Ly6G
CD11b
G
WT
IL-17RA KO
*P=0.025
*P=0.028
No. of Neutrophils (CD45+ CD11b+ Ly6G+) per Cornea
D 1
D 2
D 15
Day Post Ocular Infection
H
Early Neutralization
Anti-IL-17A or Isotype mAb
5 µg/eye Sub-conjunctivally
D 0
D 1
D 3
D 5
D 7
Corneal HSV infection
Corneal Sample Processing
Late Neutralization
Anti-IL-17A or Isotype mAb
5 µg/eye Sub-conjunctivally
D 0
D 7
D 9
D 11
D 13
D 15
Corneal HSV infection
Corneal Sample Processing
I
CXCL1/KC
Relative Fold Changecompared to Control Cornea
Isotype
Anti IL-17A
Isotype
Anti IL-17A
Day 7 Post Infection
Day 15 Post Infection
J
***P=0.0009
CXCL1/KC
(pg/mg of Corneal Protein)
Isotype
Anti IL-17A
D-7 Post Infection
K
Isotype
Anti IL-17A
46.4
34.2
Ly6G
CD11b
L
Total No. of CD11b+Ly6+ Cells Per Cornea
Isotype
Anti IL-17
M
Nuclei
Ly6G
Combined
Isotype
Anti IL-17A

FIGURE 4.6. IL-17A PROMOTES NEUTROPHIL INFILTRATION IN THE CORNEA AFTER HSV INFECTION THROUGH CXCL1/KC INDUCTION.

WT and IL-17RA KO mice were infected with 1X104 PFU of HSV in PBS or mock infected with only PBS by corneal scarification. (A) CXCL1/KC mRNA expression was examined and compared between WT and IL-17RAKO mice by quantitative real-time PCR (qRT-PCR). CXCL1/KC mRNA levels in mock-infected mice were set to 1 and used for relative fold up-regulation at various days PI. Data represents means + SEM from two independent experiments (n=2 and each sample is representative of 8 corneas). (B) Corneal CXCL1/KC protein levels were analyzed from WT and IL-17RAKO mice at indicated time points. Data show mean values + SEM from three different independent experiments (n=3 and each sample is representative of 8 corneas). MK/T-1 cells (Corneal stromal keratocytes) were stimulated under different concentrations of IL-17 in the presence or absence of anti-IL-17A mAb for 24 hrs. Supernatants were collected for VEGF-A protein estimation by ELISA and cells were collected and pooled for analysis of VEGF-A and sVEGFR-1 mRNA expression by qRT-PCR. The mRNA levels in control media were set to 1 and used for relative fold up-regulation at various days PI. (C) IL-17A stimulated CXCL1/KC production by MK/T-1 cells in a dose dependent manner as analyzed by qRT-PCR (top) and ELISA (bottom). (D) IL-17A was more potent inducer of CXCL1/KC as compared to IL-6. Data represents means + SEM from two independent experiments (n=6). (N) HSV infected WT and IL-17RAKO Mice were sacrificed on day 1, 2 and 15 PI and corneas were pooled group wise for flow cytometry analysis. (E) Representative FACS plots for corneal $CD45^+$ $CD11b^+$ $Ly6G^+$ neutrophils between WT and IL-17RA KO mice. (F) Bar graphs show

reduced $CD45^+$ $CD11b^+$ $Ly6G^+$ neutrophil numbers per cornea from IL-17RA KO mice group as compared to WT. (G) Local neutralization of IL-17A was carried out using anti-IL-17A mAb by sub-conjunctival injection during early (left panel) and late (right panel) stages of HSV infection as indicated. (H) CXCL1/KC mRNA expression was examined and compared between isotype and anti-IL-17A mAb treated mice by quantitative real-time PCR (qRT-PCR). CXCL1/KC mRNA levels in mock-infected mice were set to 1 and used for relative fold up-regulation at various days PI. Data represents means + SEM from two independent experiments (n=2 and each sample is representative of 8 corneas). Mice from local IL-17A neutralization groups were sacrificed on day 15 PI and corneas were pooled group wise for flow cytometry analysis. (I) Representative FACS plots for corneal $CD45^+$ $CD11b^+$ $Ly6G^+$ neutrophils between isotype mAb and anti-IL-17A mAb treated mice. (J) Bar graphs show reduced total $CD45^+$ $CD11b^+$ $Ly6G^+$ neutrophils numbers per cornea from anti-IL-17A treated group as compared to isotype treated group. (Data is representative of one experiment from 4-pooled corneas). Corneal sections from HSV infected corneas of isotype and anti-IL-17A mAb treated mice were analyzed by immunofluorescence microscopy with antibody specific for Ly6G (green). Sections were counterstained with propidium idodide (red) for nuclear staining. Images are representative of 6 corneas from two independent experiments. Bars, um.

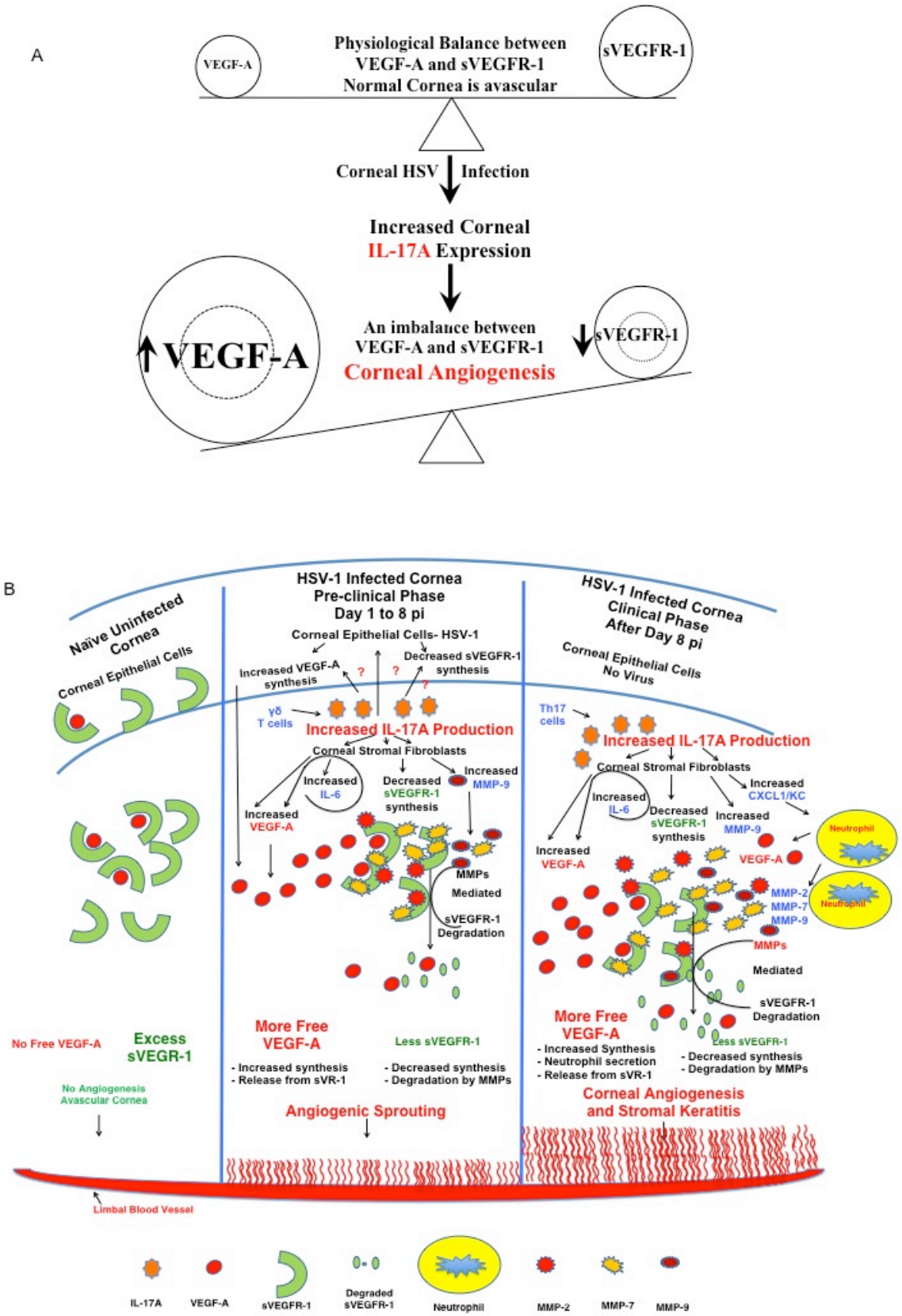
A
VEGF-A
Physiological Balance between
VEGF-A and sVEGFR-1
Normal Cornea is avascular
sVEGFR-1
Corneal HSV Infection
Increased Corneal
IL-17A Expression
VEGF-A
An imbalance between
VEGF-A and sVEGFR-1
Corneal Angiogenesis
sVEGFR-1
B
Naïve Uninfected Cornea
Corneal Epithelial Cells
HSV-1 Infected Cornea
Pre-clinical Phase
Day 1 to 8 pi
Corneal Epithelial Cells- HSV-1
Increased VEGF-A synthesis
Decreased sVEGFR-1 synthesis
γδ T cells
Increased IL-17A Production
Corneal Stromal Fibroblasts
Increased IL-6
Decreased sVEGFR-1 synthesis
Increased MMP-9
Increased VEGF-A
MMPs Mediated sVEGFR-1 Degradation
HSV-1 Infected Cornea
Clinical Phase
After Day 8 pi
Corneal Epithelial Cells
No Virus
Th17 cells
Increased IL-17A Production
Corneal Stromal Fibroblasts
Increased CXCL1/KC
Increased IL-6
Decreased sVEGFR-1 synthesis
Increased MMP-9
Neutrophil
Increased VEGF-A
VEGF-A
MMP-2
MMP-7
MMP-9
Neutrophil
MMPs Mediated sVEGFR-1 Degradation
No Free VEGF-A
Excess sVEGR-1
No Angiogenesis
Avascular Cornea
More Free VEGF-A
- Increased synthesis
- Release from sVR-1
Less sVEGFR-1
- Decreased synthesis
- Degradation by MMPs
Angiogenic Sprouting
More Free VEGF-A
- Increased Synthesis
- Neutrophil secretion
- Release from sVR-1
Less sVEGFR-1
- Decreased synthesis
- Degradation by MMPs
Corneal Angiogenesis and Stromal Keratitis
Limbal Blood Vessel
IL-17A
VEGF-A
sVEGFR-1
Degraded sVEGFR-1
Neutrophil
MMP-2
MMP-7
MMP-9

FIGURE 4.7. SCHEME DEPICTING VARIOUS CRITICAL EVENTS ORCHESTRATED BY IL-17A AFTER HSV INFECTION IN CAUSING CORNEAL ANGIOGENESIS.

(A) Model proposing the critical role of IL-17A in the deviation of physiological balance between VEGF-A and sVEGFR-1 after HSV infection. (B) Mechanisms by which IL-17A promotes corneal angiogenesis after HSV infection. Normally, naïve uninfected cornea constitutively secretes large amounts of sVEGFR-1 and small amounts of VEGF-A. This leads to a perfect physiological balance between these two molecules, sVEGFR-1 counteracting angiogenic properties of VEGF-A. The net result is the absence of any blood vessels in normally uninfected corneas (left panel). However, early after HSV infection there is increased expression of IL-17A in the cornea, which is mainly contributed by early innate cells such as γδ T cells. The increased levels of IL-17A then further contributes to the increased VEGF-A expression by direct stimulation of corneal stromal fibroblast cells as well as indirectly through increased production of IL-6 which in turn in combination with IL-17A further promotes VEGF-A production. Moreover, HSV infection of corneal epithelial cells as well as IL-17A mediated signaling also downregulates sVEGFR-1 expression in the cornea. In addition to reduced expression of sVEGFR-1, IL-17A also promotes expression of MMP-9, which further affects the VEGF-A bioavailability by increased sVEGFR-1 degradation. This in turn leads to more physiologically active VEGF-A, which is free from inhibitory actions of sVEGFR-1. This free VEGF-A drives the initial angiogenic sprouting early after HSV infection (middle panel). During later stages of SK, when replicating virus is cleared off from the cornea, IL-17A also promotes the CXCL1/KC expression, which promotes the migration of neutrophils in the inflamed cornea. These neutrophils act as an additional source of pre-

formed VEGF-A as well as MMPs that contribute to sVEGFR-1 degradation. These events in addition to direct stimulatory effects of IL-17A on VEGF-A, IL-6 and MMP-9 production, further deviates the balance between VEGF-A and sVEGF-1 and leads to the development of corneal angiogenesis as observed during late stages of SK (Right Panel).

VITA

Amol Suryawanshi was born on March 25, 1983, in Maharashtra, India. After his primary education in a village school, he attended Jawahar Navodaya Vidyalaya, Sakegaon (Jalgaon) and completed high school and secondary education in 1998 and 2000 respectively. He was then admitted to Mumbai Veterinary College, Mumbai in 2000 and received his Bachelor in Veterinary Sciences and Animal Husbandry (B.V. Sc. & A. H.) in 2005. He obtained his Master of Veterinary Science (M.V.Sc.) in Biochemistry from the Department of Biochemistry, Indian Veterinary Research Institute, Barilly (UP).

He joined the University of Tennessee, Knoxville in August 2007 and received a Doctor of Philosophy (Ph.D.) from the graduate program of Comparative and Experimental Medicine, Department of Pathobiology, College of Veterinary Medicine in July 2011. He is going to pursue his post-doctoral training at Emory Vaccine Center with Dr. Bali Pulendran.